GIS-based Analysis and Assessment of Urban Noise Exposure and Adverse Health Effects

Dissertation
with the aim of achieving a doctoral degree
at the Faculty of Mathematics, Informatics and Natural Sciences
Department of Earth Sciences at
Universität Hamburg

submitted by
Myriam Kristin Albrecht, Arlesheim, Swiss

Hamburg, 2022

Accepted as a dissertation at the Department of Earth Science.

Date of Oral Defense:	08.09.2022
Reviewers:	Prof. Dr. Jürgen Böhner Dr. Christoph Lechner
Members of the examination commission:	Chair Prof. Dr. Jürgen Böhner Dr. Christoph Lechner Prof. Dr. Jürgen Oßenbrügge Prof Dr. Uwe Schneider Dr. Olaf Conrad
Chair of the Subject Doctoral Committee Earth System Sciences:	Prof. Dr. Hermann Held
Dean of Faculty MIN:	Prof. Dr. Heinrich Graener

Acknowledgements

This dissertation was written at the Institute of Geography at the University of Hamburg as part of the research project *"UrbMod - Cities in Transition: Development of a Multisectoral Urban Development Impact Model"*. This interdisciplinary project of the University of Hamburg, the Hamburg University of Technology, the University Medical Center Hamburg-Eppendorf, the Institute for Coastal Research at the Helmholtz Centre Geesthacht, the Max Planck Institute for Meteorology and HafenCity University was founded by the he Free and Hanseatic City of Hamburg (Landesforschungsförderung) from 2015 to 2017 (state research funding). The overall aim of the project work was to investigate effects of the city on the health of its residents. In total, three doctoral and three post-doctoral positions were funded as part of the project.

My special thanks go to my supervisor Prof. Böhner and to second supervisor, Dr. Lechner who always gave me the time I needed. They gave me an open ear and a wide range of advice and supported me whenever needed to implement my ideas and complete my dissertation. Their experience and criticism improved this work considerably.

The survey in particular would not have been possible without the intensive cooperation with my colleague Malte von Szombathely: Thanks to his experience in quantitative surveys, good data could be obtained. I would like to thank Olaf Conrad for his support on all GIS issues. Thanks to him, SAGA-GIS is my best friend today. Helpful and important was also the always inspiring exchange with Katharina Peterknecht. I would also like to thank the student assistants who supported me during the measurement campaign 2016 and 2017.

For the proofreading, my special thanks go to Jack Harris, not only did your comments contribute significantly to improving the thesis, your humorous remarks always cheered me up, especially in the final stages. But I also like to thank Katharina Peterknecht, Michael Cziebalski, Douglas Tommasi and my mother Gundula Albrecht, due to their expertise, this thesis has become a readable work.

Finally, I would also like to thank my parents and my whole of my family, who always supported and motivated me to keep on going, even when times weren’t easy.

ZUSAMMENFASSUNG

Hintergrund: Durch die zunehmende Urbanisierung und die damit einhergehende Steigerung des Verkehrsaufkommens steigt auch die Lärmbelastung in Städten. Hohe und andauernde Schallbelastung kann die Ursache für verschiedene Krankheitsbilder sein, zudem kann zu starker Lärmbelästigung nach aktuellen Erkenntnissen eine Vorstufe ernsterer Krankheitsbilder sein. Folglich steigt die Relevanz, Brennpunkte zu identifizieren die von hohem Verkehrslärm betroffen sind, um gezielt Maßnahmen zur Reduzierung ergreifen zu können. Die für die Berechnung notwenigen Vorgaben zur Bestimmung des absoluten Risikos belästigt zu sein, sowie die dafür benötigten Berechnungsvorschriften für die Exposition [L_{den}], sind in der Direktive 2002/49/EC verankert. Die Berechnungen des L_{den}, ist jedoch gerade im urbanen Raum aufwendig und geht oft mit Lizenzgebühren einher. In Folge dessen wird derzeit vermehrt nach alternativen Instrumenten zur Bestimmung der Exposition gesucht. Dabei steht der Einfluss verschiedener urbaner Bebauungsstrukturen auf die Schallausbreitung im Fokus. So konnte in den letzten Jahren gezeigt werden, dass Bebauungsstrukturen, die sich hinsichtlich verschiedener Oberflächenparameter unterscheiden, unterschiedlich stark durch Lärm belastet sind. Andere Forschungsgebiete verwenden ähnliche Oberflächenparameter, um generalisierte Strukturkarten zu erstellen, die Im Fall von Urbanen Hitze Inseln und Local Climate Zones auch zur Lokalisation von Brennpunkten verwendet werden können.

Ziele: Es wird in dieser Arbeit die Fragestellung untersucht, ob es möglich ist, auf der Basis von Oberflächenparametern eine generalisierte Strukturkarte zu erstellen, die die unterschiedliche hohe Belastung, in Abhängigkeit von den unterschiedlichen Bebauungsstrukturen wiederspiegelt. Daran schließt sich die Frage an, ob darüber hinaus, durch diese generalisierte Strukturkarte die räumliche Verteilung der damit einhergehenden möglichen gesundheitlichen Beeinträchtigungen durch hohe Verkehrsbelastung (absolutes Belästigungsrisiko), abgebildet wird.

Methoden: Zunächst werden geeignete Oberflächenparameter identifiziert, die sowohl in bekannten Kartierungsverfahren zum Einsatz kommen, als auch im Zusammenhang mit der Schallausbreitung im urbanen Raum untersucht werden. Im Anschluss werden diese oder ähnliche Oberflächenparameter mittels einer Open-Source-Software berechnet. Es folgt eine Random Forest Klassifikation von ausgewählten Baublöcken der Stadt Hamburg. Es werden Karten auf Basis verschiedener Eingangsparameter berechnet, welche dann an Hand drei verschiedener Schallausbreitungsszenarien validiert werden. So kann zum einen überprüft werden, ob sich die ermittelten Klassen signifikant bezüglich der Exposition [L_{den}] unterscheiden und ob nur den Einfluss der Stadtstruktur auf die Schallausbreitung, oder auch das damit verbundene Verkehrsaufkommen abgebildet werden. Die Validierung erfolgt mittels Kruskal-Wallis-Tests, paarweisem Vergleich und der Effektstärke. Das durch die finale Klassifikation am besten abgebildeten Scenario wird dahingehend untersucht, ob die

modellierte Werte Aussagen über die messbare Exposition zulassen. Hierfür werden in ausgesuchten Gebieten Messungen durchgeführt und die Korrelation der modellierten und der gemessenen Werte berechnet. Im nächsten Schritt wird untersucht ob sich das absolute Belästigungsrisiko ebenfalls signifikant zwischen den Klassen unterscheidet. Auch hier werden ein Kruskal-Wallis-Test und ein paarweiser Vergleich durchgeführt sowie die Effektstärke berechnet. Abschließend wird mittels Umfragedaten zur verkehrsbedingten Lärmbelästigung überprüft, ob das auf Grundlage der modellierten L_{den} Werte absolute Belästigungsrisiko der empfundenen Belästigung entspricht.

Ergebnisse: Es kann gezeigt werden, dass mittels einer Random Forest Klassifikation, basierend auf geometrischen, strukturellen und Dichteparametern, die sowohl auf Vektor- und Rasterdaten in SAGA-GIS berechnet wurden, eine Strukturkarte generiert werden kann, deren Klassen sich sowohl hinsichtlich der Expositionshöhe als auch hinsichtlich des absoluten Belästigungsrisikos signifikant unterscheiden. Zudem konnte gezeigt werden, dass die auf diesem Ansatz basierende Klassifizierung nicht nur den Einfluss der urbanen Oberfläche berücksichtigt, sondern ebenso das damit verbundene Verkehrsaufkommen sowie die zulässigen Höchstgeschwindigkeiten. Zudem fällt die empfundene Belästigung durch Verkehrslärm in Hamburg höher aus, als das nach der Direktive 2002/49/EC berechnete absolute Risiko belästigt zu sein.

ABSTRACT

Background: Due to increasing urbanization and the associated increase in traffic volume, noise pollution is on the rise. High and continuous sound exposure can be the cause of various diseases directly, but also indirectly though annoyance, which is known to be a precursor of more serious diseases. Thus, it is of pressing importance to identify noise pollution hot spots in urban areas where traffic noise reducing activities should be undertaken. The assessment of the population affected through the exposure level [L_{den}] is a key calculation here, which is anchored in the Directive 2002/49/EC, and there are numerous approaches in the literature to determine exposure level based on the surface parameters of different morphological urban structures. However, as the calculation of the L_{den}, especially in urban areas, is computationally and financially expensive, there is a need to find more simplified ways to understand the relationship between sound propagation and urban structures. There are different research fields, that use similar surface parameters to create generalized structure maps. In the case of Urban Heat Island and Local Climate Zone mapping these maps are used to identify hot spots.

Objectives: Based on this background, this thesis investigates the question of whether it is possible to create a generalised structural map on the basis of surface parameters that documents the different levels of traffic related noise exposure, depending on the building structures. Furthermore, the question of whether this generalised structural map also represents the spatial distribution of the associated possible adverse health effects, in the form of annoyance caused by traffic noise, will be examined.

Methods: First, suitable surface parameters, which are used in known mapping approaches as well as investigated in the context of sound propagation in urban areas are identified. These and similar surface parameters where next calculated using open source software. Based on different input parameters (vector- and grid-based, as well as combined), the building blocks where classified for selected regions in Hamburg using a random forest algorithm. For the validation, three different sound propagation scenarios where generated. Thus, it could be analysed whether the determined classes differ significantly with regard to the exposure [L_{den}] and whether only the influence of the urban structure on the sound propagation or additionally the associated traffic volume are represented. The validation was carried out by means of a Kruskal-Wallis tests, a pairwise comparison and by calculating the effect size. The scenario which is best represented by the final classification was then examined to determine whether the modelled values permit statements about the actual measurable exposure. For this purpose, measurements were carried out in selected areas and examined for their correlation with the measured values. In the next step, it was investigated whether the absolute annoyance risk also differs significantly between the classes. Again, a Kruskal-Wallis test and a pairwise comparison is performed and the effect sizes were calculated. Finally, survey data on traffic-related noise annoyance was used to see

whether the absolute risk of being highly annoyed calculated in acc. Directive 2002/49/EC based scenario L_{den} values, corresponds to the self-reported traffic related noise annoyance.

Results: By applying a classifying approach based on geometric, statistical and density surface parameters, which were calculated on vector and grid data in SAGA-GIS, it was possible to generate a structure map which offers classes that differ significantly with regard to exposure level and the risk of being highly annoyed. Additionally, it was proven that the classification based on this approach not only considers the influence of the urban surface, but also the related traffic volume, as well as the maximum speeds allowed. Furthermore, the absolute risk of being highly annoyed, calculated in acc. with the END seems to underestimate the self-reported traffic related noise annoyance for Hamburg’s population.

TABLE OF CONTENT

LIST OF FIGURES

LIST OF TABLES

List of Important Acronyms

%HA	Highly Annoyed
BB	Building Block
BMZ	Bundesentwicklungsministerium
BST	Building Structure Type
BSU	(ehemalige) Behörde für Stadtentwicklung und Umwelt (Hamburg)
BSW	Behörde für Stadtentwicklung und Wohnen (Hamburg)
BUE	Behörde für Umwelt und Energie (Hamburg)
CM	Compact Midrise
DALYs	Disability Adjusted Life Years
DLR	German Aerospace Center
EEA	European Environment Agency
END	Directive 2002/49/EC of the European Parliament and of the Council.
EU	European Union
GBD	Global Burden of Disease
ISO	International Organization for Standardization
LCZ	Local Climate Zone
Lden	Day-Evening-Night Level
Lden75	Scenario considering average traffic volume and speed
LdenDTV	Scenario considering modelled traffic volume and max. speed
LdenHH	Scenario considering the Noise Map of Hamburg
LoD-DE1	Level of Detail 1
LR	Lowrise
MR	Midrise
UBA	Umweltbundesamt
UHI	Urban Heat Island
UN	United Nations
UrbWellth	Health related Urban Well-Being
USSZ	Urban Sound Sensitive Zones
UVCZ	Urban Vulnerability Climate Zones
VBUS	Vorläufige Berechnungsmethode für den Umgebungslärm an Straßen
WHO	World Health Organization
WUDAP	World Urban Database and Access Portal Tools

1 INTRODUCTION

Everyone has the right to access conditions that promote healthy living and well-being. This is granted by the first principle of the Stockholm Declaration from 1972 where it is stated that: "*Man has the fundamental right to freedom, equality and adequate conditions of life, in an environment of a quality that permits a life of dignity and well-being, […]"* (UN GENERAL ASSEMBLY, 1972, p. 2). However, it also states: *"[…] he bears a solemn responsibility to protect and improve the environment for present and future generations"* (UN GENERAL ASSEMBLY, 1972, p. 2). Thus, as human health and well-being are influenced not only by personal characteristics but also by the human environment, a safe and health-promoting environment is a prerequisite for this claim (UN GENERAL ASSEMBLY, 1972, p. 2; WHO 2019). In particular, access to health-promoting resources is one of a multitude of influencing factors that differs clearly for everyone (WHO, 2010). Access to resources and the influence of hazardous environmental stressors varies greatly from continent to continent, from country to country, and from city to city (WHO, 2019). Many studies have addressed this issue of Environmental Justice and it is indisputable that these conditions are not evenly distributed across the world and thus across the world's population. These differences exist at diverse scales. Thus, there are remarkable differences between the urban and the rural population. But even within a city, environmental stressors are unevenly distributed (SZOMBATHELY et al., 2018). In 2018, more than half of the world´s population already lived in cities, and the number is expected to continue to rise up to 60 % by 2030 and about 75 % by 2050. Therefore, urban space and its liveable design are becoming more and more important (BMZ, 2014; UN, 2018).

This trend of urbanisation, which has accelerated since the beginning of industria-lization, is accompanied by an increasing economic importance of cities. Today up to 80 % of gross domestic product is generated in cities (BMZ, 2014; UN, 2018). With this rising economic importance and the need for people to live in or near the cities, major conflicts arise. The growing industrialization and the intensifying need and use of the transportation system leads both not only to a sharp increase in carbon dioxide emissions and other air pollutants, but also to a rapid increase of the traffic and industrial induced noise levels (WHO,2011). As a result, the most relevant urban stressors are air quality and noise pollution, followed by heat and cold stress, depending on the region (EEA,2009).

Hazardous environmental stressors are intensively researched across different fields of science. Most studies are focused on health consequences and the unequal degree by which groups of different socio-economic status are affected by stressors (SCHLOSBERG, 2007; SZOMBATHELY et al., 2018). Many of these studies are limited to a relatively coarse aggregation with a minimum at city-, but mostly not on neighbourhood-level (SZOMBATHELY et al., 2018). Especially in the case of noise pollution, this coarse aggregation bears the risk of misinterpretation (UBA,2010b), for example, due to the ecological fallacy (BAHRENBERG, G., GIESE, E., MEVENKAMP, N., & NIPPER, J.,2010). Additionally, recent studies have shown that for

Hamburg there are already significant differences within cities on neighbourhood levels in terms of access to resources and the negative influence of noise as stressors (BRAUN, OßENBRÜGGE, & SCHULZ, 2018; SZOMBATHELY et al., 2018). Understanding the interactions and connections between city structure and noise propagation, as well as their influence on well-being and health, is thus becoming more and more important. This knowledge is important for the sustainable (re)design and development of cities. It is therefore necessary to carry out investigations on urban health at the most detailed level possible (EEA,2009; WHO,2019).

The conceptual approach of SZOMBATHELY et al (2017) focuses precisely on these small-scale effects and thus includes the possible interconnections of urban morphology and sound propagation as well as the resulting exposure and adverse health effects. In order to determine this relationship, and thus the adverse health effects, accurate noise exposure data are needed (SZOMBATHELY et al.,2018; SZOMBATHELY et al.,2018). But the small-scale and high-resolution calculation of sound exposure is limited by computationally intensive software which is in addition often expensive due to corresponding license fees (GARG & MAJI, 2014; STEELE, 2001).

Therefore, a pressing interest is developing more inexpensive alternatives to determine sound exposure, so that studies can be easily replicated anywhere. An approach that has received increasing attention in recent years is studying the influence of building structure on sound propagation and the correlation between certain structural parameters and the level of sound exposure (KANG, 2001). But all these analyses and models are likewise based either on costly and time-consuming calculations and/or measurement campaigns. The question therefore arises whether it is possible, on the basis of the already known link between the built environment and the noise exposure level, to generate generalized maps from which adverse noise effects can be derived, as is done, for example, in the case of the research field on Urban Heat Islands (UHIs). Against this background, the main questions that motivate this thesis are:

1. ***Does a generalized map based on surface parameters reflect the noise sensitivity of urban areas?***
2. ***What conclusions about adverse health effects can be drawn from the final generalized map?***

Thus, this research aims to generate “structure maps” of Urban Sound Sensitivity Zones (USSZ) based on the urban morphology and the corresponding surface parameters. These maps will be analysed with regard to the possibility to draw conclusions about the spatial distribution of the high L_{den} that can cause adverse health effects. These findings could be fundamental for developing new traffic concepts in order to reduce the percentage of Highly Annoyed ($\%HA$), where necessary, and thus to increase the overall health level.

The study is conducted for the city of Hamburg, which is the second largest city in Germany, located in northern of the country. Due to the size and the different sub-centers found in the city, which differ in the development patterns (BSU, 2007; STATISTIKAMT NORD, 2016), a variety of different urban structures can be studied here. Additionally, it is a metropolitan region that is currently characterized by strong commuter flows, and a high share of heavy vehicles and private cars, which leads to irregularly distributed, sometimes heavy traffic flows, across the city (FOLLMER & GRUSCHWITZ, 2020). This makes it possible to study different urban structures as well as traffic loads of varying intensity.

To outline the need of this research for an inexpensive and easy to calculate approach to determine noise exposure and the related adverse health effect on a small-scale, the most common theories in the field of urban health and urban stressors (in particular noise) are presented, starting with Health-related Urban Well-Being. This is followed by a more detailed discussion of the contemporary state of research on noise induced adverse health effects, including the current approaches of assessing environmental noise and noise annoyance. This outlines the need for assessing methods for recording these effects, particularly the need for noise maps, to determine the dose responds relation, that indicates the relationship of exposure level and adverse health effects, and shows how complex these approaches are. Next current approaches to understanding the relation between urban structures and their influence on sound propagation are reviewed, and thus enabling the determination of which surface parameters and settings are used to understand exposure. This is followed by a brief insight into other research fields which are already dealing with generalized structure maps; to outlines the commonalities regarding the surface parameters used for the classification with those investigated in the research on sound propagation in urban areas. The chapter closes with the subsequent research objectives.

The State of Research is followed by theoretical considerations, in which the research communities of mapping approaches and the research on urban structure and sound propagation are outlined in more detail. This illustrates which surface parameters could be suitable for a classification due to being used in both fields. The case study will be conducted for Hamburg and the selection of the final Focus Areas will be based on different variables, to ensure, that the heterogeneity (especial in terms of the urban morphology) is reflected. The first research question focuses on the choice of suitable surface parameters which can be applied for a supervised automatically classification to identify areas differ with regard to their influence on sound propagation, the so-called Sound Sensitivity Urban Zones (USSZ). The final maps will be validated by analysing their aptness to reproduced zones that differ with regard to the sound exposure level. To proof if it’s only the influence of the urban structure, or maybe likewise the traffic volume, which is related to that urban structure, different sound propagation scenarios will be calculated. Based on these findings, and the final USSZ map, which represents the differences in sound exposure best, the second research question will be investigated. Based on three different health related variables it will be analysed, to see if the generalized map, additionally to statements about the distribution of L_{den}, allows to draw conclusions about the related adverse health effects. A rapid and easy identification of such hot spots could be used to get an overview of where it is most urgent to undertake actions to reduce the noise exposure.

2 State of Research

This chapter starts by outlining the research on urban health where the focus will be particularly set on noise as a stressor in section 2.1 *Health-Related Urban Well-Being*[1]. This is followed by section 2.2 *Noise induced Adverse Health Effects,* which gives a more detailed look on noise induced adverse health effects and current approaches followed by the assessment of noise induced annoyance in sub-section 2.2.1 *Assessment of Noise Annoyance* and the assessments for the determination of noise exposure in section 2.2.2. The state of research on the interconnections of urban morphology and sound exposure are presented in section 2.3 *Urban Morphology as an Indicator of Noise Exposure*, which shows alternative ways to determine exposure and provides information on which methods of parameterization have already been tried and tested. The overview of the concept of Urban Heat Islands (UHIs) and thus the current methods of mapping Local Climate Zones (LCZs) as well as the mapping techniques for Building Structure Types (BSTs) presented in section 2.4 *Generalized Structure Maps*, offers the possibility to show common aspects of these fields of research and provides the opportunity to prove the transferability of these concepts to determine the exposure level with a generalized map in section 2.4. This chapter closes with the conclusions that can be drawn and the resulting research objectives in section 2.5.

2.1 Health-Related Urban Well-Being

In 1946 the WHO defined health as *"[...] a state of complete physical, mental and social well-being and not merely the absence of disease or infirmity"* (WHO, 1946, p. 1). This very broad definition clarifies that not only physical integrity, but also the personal physical condition and behaviour as well as the personal environment effects health. Hence, today it is unquestioned that the environment in which one lives has as great impact on personal health and well-being. This is also stated in an EEA Report from 2009: *"The urban environment influences human physical, social and mental well-being, therefore, a healthy, supportive environment is indispensable to quality of life in cities [...]"* (EEA, 2009, p. 13). This is particularly important because if one considers that the number of people living in cities is constantly rising, it becomes evident that urban health and the associated influencing urban variables are getting increasingly relevant. This explains the growing interest in the interaction of urban environment, health and well-being, which is reflected in the remarkable amount of research across several disciplines, including public health, urban planning, natural sciences and epidemiology, on the potential associations between urban areas and health or well-being (Krefis et al., 2018). The following provides a brief presentation of the most important concepts on urban health.

[1] The state of research presented in the chapters 2.1 Health-Related Urban Well-Being, 2 is based on papers, prepared within the framework of the UrbMod project on which the author of this thesis has collaborated. For more detailed information see Szombathely et al. (2017), A. C. Krefis et al. (2017); A. Krefis, Augustin, Schlünzen, Oßenbrügge, and Augustin (2018) and Szombathely et al. (2018).

HANCOCK was one of the first researchers who included aspects of both the definitions provided by the WHO and the EEA. His model, *The mandala of health: a model of the human ecosystem* describes the human being as an individual consisting of the three parts: body, mind and spirit. These parts of the individual are influenced by four factors, namely personal behaviour, biological physical condition, psycho-socio-economic condition, and importantly by the physical environment. These factors are embedded in the built environment and society, which in turn are shaped by the biosphere and cultures influences (HANCOCK, 1985).

EVANS and STODDART (1990) followed Hancock, distinguishing between three different environmental aspects, namely genetic, physical and social environments. In addition, they introduced well-being as a target variable. According to their model, there is no direct interdependency between well-being and disease. Even tough, there is a drawback from the outcome well-being on individual behaviour and thus on disease in their model (EVANS & STODDART,1990), the exact components of the physical environment remain unclear.

Introduced ten years later, the model by NORTHRIDGE, SCLAR, and BISWAS considers the links between health and well-being as well. While they do not consider direct links between environment, health and well-being, they divide the influence variables into different levels, similar to HANCOCK, but with more specific information on the interaction of the various groups and subgroups (NORTHRIDGE, SCLAR, & BISWAS, 2003).

In 2005 GALEA, FREUDENBERG, and VLAHOV also distinguished between different levels of influence and inserted a division between social and physical environments. The model focuses on the impact of policy alternatives at various levels on migration and immigration processes and their influence on typical urban resources, such as housing availability and social life, but also on infrastructural aspects. At the outcome level, they differentiate between health and non-health (GALEA, FREUDENBERG, & VLAHOV, 2005). Medical influencing variables are not considered.

Five years later MENDIS and BANERJEE, concentrate precisely on these medical aspects. Using cardiovascular disease as an example, they framed the risks to be taken ill in terms of age and social stratification. In this way, differential exposure and vulnerabilities are contextualized by the economic development of a given city MENDIS and BANERJEE, 2010).

In contrast to this description of the urban influence on the basis of selected disease patterns, the approach of SCHLICHT, presented in 2017, concentrates on the positive influences of health-relevant urban features. In this model, people act in the context of the city and its inhabitants, who in turn are embedded in the natural environment. The enumeration of the influence variables, which are based on HUNTER and ASKARINEJAD (2015), consists exclusively of positive variables. What is missing, however, is the description of how these various variables are interlinked (SCHLICHT, 2017).

What becomes clear is that most of these models address several aspects of the WHO definition of health and several environmental aspects. All of them vary in complexity and systematization depending on perspective, background and scientific (BAI, NATH, CAPON, HASAN, & JARON, 2012; SHANAHAN et al., 2015). Even though many of these models consider a large number of influencing variables and in some cases also indicate correlations and directions of influence, this is usually done at a coarse aggregation level.

A relatively recent model that aims to tackle these limitations is the *Conceptual Modelling Approach to Health-Related Urban Well-Being* introduced in 2017 by SZOMBATHELY et al.. This model assumes that: *"[...] the success of healthy urban societies depends on an overall understanding of the complex factors that influence urban health and the interrelationships between them"* (SZOMBATHELY et al., 2017, p. 2). The authors define Health-related urban well-being (UrbWellth) on the individual level in accordance with BALLAS (2013) as follows:

> *"UrbWellth includes domains that are related to individual physical (objective health status), mental (subjective health status) and emotional (affective well-being) aspects of health, to the natural (e.g., climate) and urban specific environment (e.g., public parks) as well as to the political system (e.g., urban governance), social functioning (e.g., neighborhood) and social context (e.g., social position) in which people live"* (SZOMBATHELY et al., 2017, p. 3).

At the lowest resolution, the conceptualization of influencing variables on UrbWellth distinguishes between Citizens and Urban Environment, which are on the next level, subdivided into the sectors Individual, Society, Stressors and Morphology. As indicated by the four arrows from each sector towards the center, all sectors have an influence on UrbWellth. The intensity and nature of the impact not only depends on each sector; it is influenced by the other sectors as well, as can be seen in Fig. 1, indicated by the arrows between the sectors (SZOMBATHELY et al., 2017).

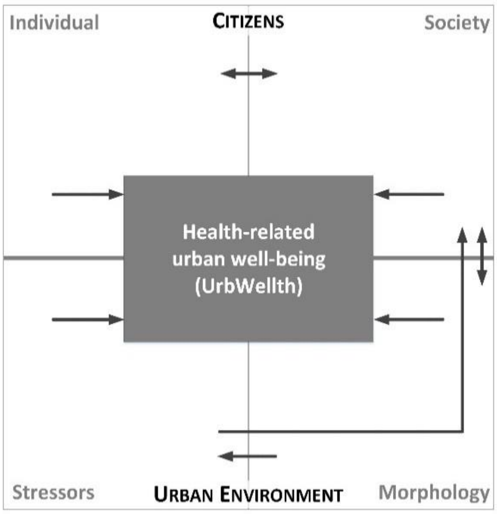

Fig. 1: Sectors and interrelations of human-environmental influences on UrbWellth
Source: SZOMBATHELY et al., 2017, p. 4.

While there is a direct interaction between the sectors Individual and Society, as well as between Society and Morphology, Morphology affects the Stressors unilaterally. The Stressors in turn have a unilateral effect on the sector Society. This is one of the major differences to most previous models: Citizens have only an influence on Stressors via Morphology (SZOMBATHELY et al., 2017).

The variables that can have an influence on UrbWellth are assigned to the sector for which they are most relevant. Thereby, not only the interdependencies of the variables within a sector are considered, but also cross-sector interdependencies, indicated by the respective arrows in Fig. 2 (SZOMBATHELY et al., 2017). The top-left sector contains variables that have an influence on health in urban areas from a medical point of view (BABISCH, WÖLKE, HEINRICH, & STRAFF, 2014; JARUP et al., 2008; KREFIS et al., 2017a; KREFIS et al., 2017b), and those that have an impact on the well-being of city dwellers from a socio-economic and socio-demographic point of view (GREGORY & URRY, 1985; POHL, 2009; STORPER, 2013. In the top-right sector, the most important socio-economic and demographic factors from the perspective of socio-spatial geography are predominantly found (JÜRGENS & KASPER, 2006; OßENBRÜGGE, POHL, & VOGELPOHL, 2009; STORPER, 2013). In general, these also have an influence on urban health from a medical point of view (KREFIS et al., 2017a; KREFIS et al., 2017b), which is indicated by the double arrow between these sectors.

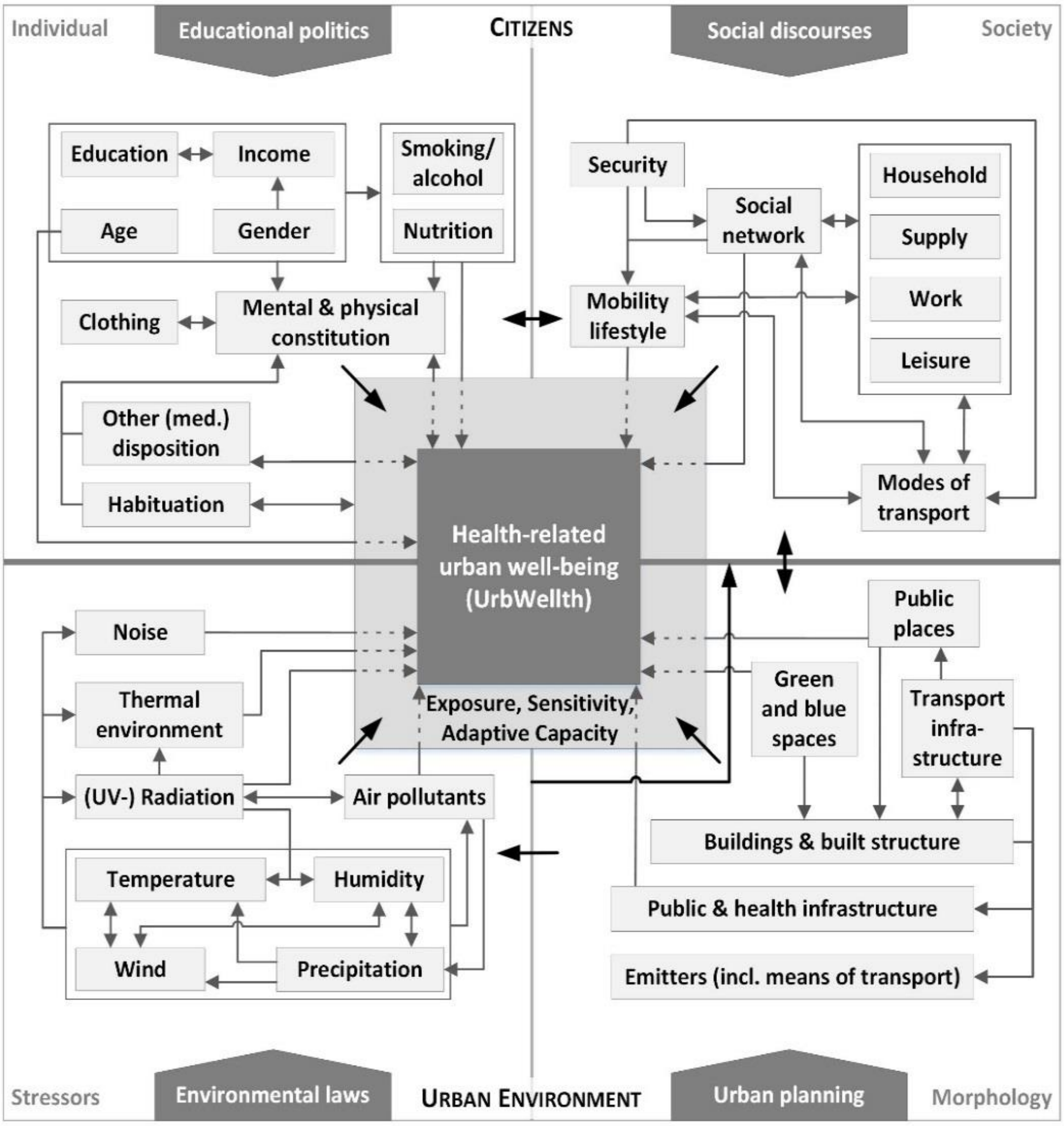

Fig. 2: Conceptual model of health-related urban well-being (UrbWellth)
Source: SZOMBATHELY et al., 2017, p. 6.

Infrastructural aspects are combined in the bottom-right sector. This includes means of transport and built environment, and is seen as enabling or preventing infrastructure as well as the production and distribution of environmental resources and stressors (GEHL, 2012) what in turn has affects human behaviour and their mobility patterns (HÄGERSTRAND, 1970, 1974).

The last sector (bottom-left) encompasses the stressors, modified and influenced by the built city. Urban structures have a considerable effect on natural resources. Water, thermal and radiation budgets as well as the wind field and the air composition differ considerably in cities from those in rural areas (OKE, 1987). The artificial surfaces and the changed roughness (due to building and constructions), as well as the anthropogenic emissions of heat and trace gases lead to effects such as the UHI effect (ARNFIELD, 2003; BECHTEL & SCHMIDT, 2011; HOFFMANN, KRUEGER, & SCHLÜNZEN, 2012). The urban setting has impacts on precipitation (HAN, BAIK, & LEE, 2014; SCHLÜNZEN, HOFFMANN, ROSENHAGEN, & RIECKE, 2009; SHEPHERD, 2005), as well as on urban air and noise pollution (MOUSSIOPOULOS, 2003). In urban areas and metropolitan regions in Europe, air pollution is mainly caused by traffic, with a high share caused by heavy commercial vehicles (MAGE et al., 1996). In addition, road traffic, aviation and industry (ROSS & WOLDE, 2001) are important sources of air pollutants and noise in cities (KHEIRBEK et al., 2014; WHO, 2011).

Another difference to other models is that the influence of the four sectors on UrbWellth is not unfiltered. Consequently, stressors such as air or noise pollution do not directly lead to a reduction of UrbWellth. This refers to the concept of vulnerability and to the idea of the human-environment system (TURNER et al., 2003). The vulnerability concept is applied in various fields, especially in the context of climate change. In this context, a tripartite structure is assumed: Vulnerability is a combination of Exposure, Sensitivity and Adaptive Capacity (FÜSSEL, 2005; THORNES, 2002). Following the definitions of the Intergovernmental Panel on Climate Change (IPCC), Exposure is defined as *"the nature and degree to which a system is exposed"*; Adaptive Capacity is *"the ability of a system to adjust to […] potential damages, to take advantage of opportunities or to cope with the consequences";* and Sensitivity is described as the *"degree to which a system is affected, either adversely or beneficially"* (THORNES, 2002, pp. 986–988). As shown in Fig. 2, a filter layer was added which contains the so-called transfer functions (SZOMBATHELY et al., 2017). Relations between whole sectors and the filter layer are indicated by the black arrows, going in to the grey filter layer (SZOMBATHELY et al., 2017).

Especially with regard to sound exposure, this filter layer and the interactions between the different sectors and variables play an outsized role. Thus, it is of relevance how the corresponding person (or group of persons) is exposed. If he works outside, for example, or in a well sound isolated room. Adaptive capacity describes the possibilities of adaptation to the given circumstances. Can the location be changed, or can windows be closed? The personal constitution has a considerable influence as well. If, for example, the person is especially sensitive to a particular source of noise, he or she will find it more disturbing than another, less sensitive person (JAKOVLJEVIC, PAUNOVIC, & BELOJEVIC, 2009). And regarding the habituation in the sector Individual, it can be assumed that the person can adapt to different noise sources up to a certain level, but in the case of noise annoyance additional confounders play a distinctive role. For example, length of residence (JAKOVLJEVIC et al., 2009).

Since this thesis primarily focuses on the influence of built environment (Morphology) on noise exposures (Stressor), and therefore discusses parts of the effect that sector three has on sector four, these interrelations and the adverse health effects of noise (in view of variables of sector one and two) are considered in more detail in the next sections.

2.2 Noise induced Adverse Health Effects

According to the WHO there are several indications that noise has a major effect on urban health and: *"[…] at least one million healthy life years are lost every year from traffic related noise in the western part of Europe. […]"* (WHO, 2011, p. V). The Noise Report published by the EEA in 2014 states too, that: *"[...] traffic is the most dominant source of environmental noise with an estimated 125 million people affected by noise levels greater than 55 decibels (dB) Lden (day-evening-night level)"* (EEA, 2014, p. 5). In Germany, noise is the second most acute urban stressor after air pollution and poses a threat to major sections of city societies. Indeed, 54% of Germans feel disturbed or harassed by traffic noise (UBA, 2015). The effect pyramid of BABISCH 2002 shown in Fig. 3 is based on a WHO publication of 1972, and was one of the first that illustrates this fundamental relationship between health, well-being and noise exposure (BABISCH, 2002).

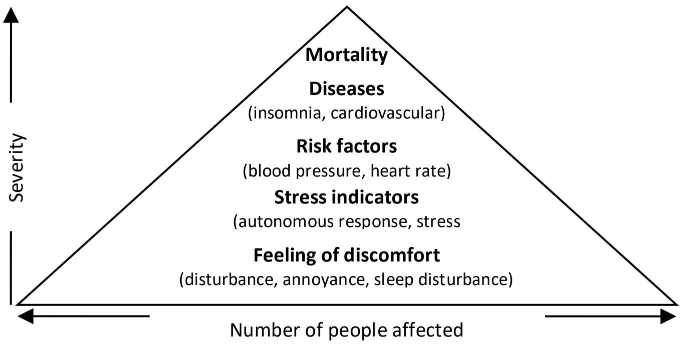

Fig. 3: WHO - pyramid of health effects of noise
Modified after BABISCH, 2002, p. XVII.

As can be seen in the pyramid, these health consequences can be of various nature. Most research has focused on the relationship between cardiovascular and respiratory diseases and noise exposure. For example, in 2014, BABISCH, WOLF, et al. found that related to a high exposure level of road traffic and aircraft noise impacts different cardiovascular health outcomes (BABISCH, WOLF, et al., 2014; BABISCH, WÖLKE, et al., 2014). JARUP et al. showed significant correlations between the occurrence of hypertension for people living close to one of the six major European airports, and an additional increase in hypertension could be seen for road traffic noise in the highest exposure category (JARUP et al., 2008). Environmental noise is also considered to be associated with respiratory diseases such as asthma, chronic obstructive pulmonary disease (DUHME et al., 1996; ISING, LANGE-

ASSCHENFELDT, LIEBER, WEINHOLD, & EILTS, 2003), and it can cause acute cardiovascular and metabolic problems. Perhaps the main effect is the release of stress hormones and the increase in blood pressure due to vasoconstriction, the effects of which can occur even during sleep (ERIKSSON, PERSHAGEN, & NILSSON, 2018).

As visible from the bottom line in Fig. 3, there is a high share of individuals who are in discomfort due to noise. Other studies focused on annoyance and could, for example, demonstrate a significant correlation between self-reported annoyance and self-reported traffic volume (DRATVA et al., 2010). Meta studies and systematic reviews of SHANNON prove these findings and correlations on the basis of new scientific medical evidence. Thus, SHANNON concluded that: *"There is sufficient evidence of a causal relationship between environmental noise and both sleep disturbance and cardiovascular disease [...]"* SHANNON, 2018, p. 63). But noise annoyance is an evaluative term that cannot be measured physically. Therefore, there are two categories of influencing factors that can be derived: those that are sound related and those that are based on personal characteristics (FÜRST & KÜHNE, 2010; JAKOVLJEVIC et al., 2009). This was recently confirmed by GUSKI, SCHRECKENBERG, and SCHUEMER, who identified that noise annoyance response usually contains three elements: *"an often repeated disturbance due to noise [...], an emotional/attitudinal response[...], [and] a cognitive response [...]"* (GUSKI et al., 2017, p.2). Regarding the personal related factors, GOLMOHAMMADI, DARVISHI, SHAFIEE MOTLAGH, AND FARADMAL come recently to the conclusion that people in poor health feel more annoyed by noise than people with a better health condition. In addition, noise annoyance increases with age and introverted people felt more psychologically stressed than extroverted people (GOLMOHAMMADI et al., 2021).

In the study conducted by KREFIS et al., a multivariate regression analysis showed that a significantly higher prevalence of depression occurs in areas with larger areas of traffic noise > 65 dba. However, further correlations exist between prevalence and depression with lower socio-economic status and lower family embeddedness (KREFIS et al., 2017). Even if in that study only the simultaneous spatial occurrence of high sound exposure and depression can be shown, a meta study of research performed between 2010 and 2016 and published by the WHO showed that environmental noise can have a wide variety of severe health-damaging effects (WHO, 2018). Particularly, annoyance is next to sleep disturbance in recent studies as a precursor and trigger of noise-related diseases including depression (GUSKI et al., 2017; HÉRITIER et al., 2014; WHO, 2018). Other recent studies by BEUTEL et al. (2020) and EZE et al. (2020) demonstrated that high traffic noise levels and noise annoyance, both jointly and independently, influence the risk of depression and that sound exposure can therefore be assumed to be causal. This is also the conclusion of the latest study of STANSFELD, CLARK, SMUK, GALLACHER, and BABISCH: *"[…] sensitivity may increase the risk of psychological ill-health when exposed to road traffic noise. Noise annoyance may be a mediator of the effects of road traffic noise on psychological ill-health"* (STANSFELD et al., 2021, p.1).

From the preceding explanations, it is clear that exposure to high levels of noise can cause damage to health in a variety of ways. For a long time, the focus of research was on cardiovascular and respiratory tract disorders. However, annoyance is also increasingly coming into focus. High and persistent annoyance, especially at night, can be a precursor to depressive disorders (WHO, 2018). SZOMBATHELY et al. and KREFIS et al. showed that the exposure level for citizens in Hamburg is dependent on age and socio-economic status, by district (KREFIS et al., 2017) but also on neighbourhood scale (SZOMBATHELY et al., 2018). Considering the findings of GOLMOHAMMADI et al., that noise annoyance increases with age, this outlines the importance of research on the noise distribution and the related annoyance for the city of Hamburg, on a high resolution.

Thus, for decision-makers at the political level it is of major importance to be able to define an effect-relationship between annoyance level and given exposure level (MIEDEMA, 2007; MIEDEMA & OUDSHOORN, 2001; WHO, 2018). For this propose, the WHO defines uniform guidelines and approaches that are incorporated into the current EU Directive (END). The scientific findings upon which the calculations for Highly Annoyed ($\%HA$) are based, are presented in the next section.

2.2.1 Assessment of Noise Annoyance

Most of the studies on exposure-response relationships are usually based on the concept of Highly Annoyed ($\%HA$) introduced by SCHULTZ in 1978. He examined the relationship between measured or modelled noise exposure and the self-reported level of annoyance. Beside the fact that non-acoustic parameters such as sensitivity to the noise source (see section 2.2) have a large influence on the annoyance level, SCHULTZ (1978) proved that if people are exposed to very high noise levels, the correlation of the acoustic parameters and annoyance is high, both for the individual and on average. Thus, he defined $\%HA$ as the top 27-29 % of an annoyance scale ranging from 0 to 100 % (SCHULTZ, 1978).

MIEDEMA and OUDSHOORN developed the concept of $\%HA$ between 1998 and 2001. In meta-analyses, the authors refer to studies published between 1965 and 1993 (MIEDEMA, 2007; MIEDEMA & OUDSHOORN, 2001). They standardise the different responses categories used in previous studies to a category system of 0 to 100 and define cut-off points. The first category was set in accordance with SCHULTZ for $\%HA$ at 72, the second one for Annoyed ($\%A$) at 50 and the third one for Little Annoyed ($\%LA$) at 28. The percentage for all of them included the 95% confidence interval and using the day-evening-night level (DENL) in dB are shown in Fig. 4 (MIEDEMA, 2007; MIEDEMA & OUDSHOORN, 2001).

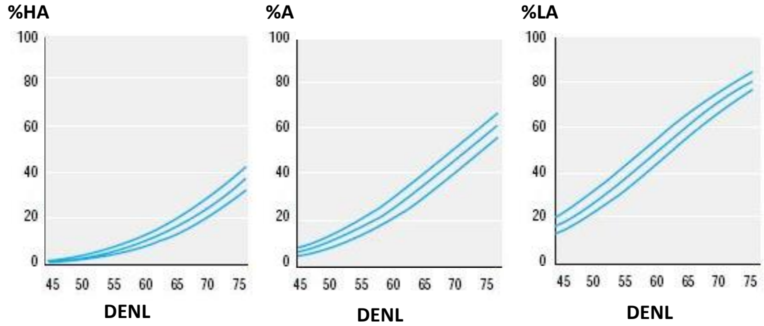

Fig. 4: The annoyance categories for road traffic as a function of DENL

Modified after MIEDEMA &OUDSHOORN, 2001, p. 412.

Meta-analyses of studies based on MIEDEMA and OUDSHOORN (2001) showed that while individual studies found highly significant results, these are not consistent with other studies (UBA, 2010b). This is possibly due to a non-uniform study design in connection with the problems in determining exposure and considering moderating factors. What is considered as another difficulty according to today's state of knowledge is that most studies limit themselves to one source of noise as a stressor (GUSKI et al., 2017; UBA, 2010b). Since this does not correspond well to reality, more recent studies are concerned with the possibility of assessing an overall noise level. GUSKI et al. demonstrate in a meta study, which included the analysis of five studies on combined noise exposure, that it is unwise to integrate different noise source combinations into one single analysis. However, the results suggest that the Domination Source Model, where annoyance refers to the strongest source, achieves good results. But due to the small number of studies, this cannot be regarded as a valid result even according to the authors (GUSKI et al., 2017).

In their recently published study on total noise annoyance, LECHNER, SCHNAITER, and BOSE-O'REILLY came to different conclusions. As part of a large-scale overall noise study in the Innsbruck area, they investigated whether traffic noise has an influence on the annoyance level to other noise sources and whether the combination of different noise sources leads to an increase in the overall annoyance level. With their data set they showed that there is no significant influence of road traffic noise on the annoyance level induced by rail and air traffic noise. Furthermore, they tested the Domination Source Model against the Equivalents Model. The second one achieved better results, but not as good as the single source models (LECHNER. et al.2019). Both, LECHNER. et al. and Lechner et al. and GUSKI et al. point out that there is a need for further research, especially in the field of total noise annoyance.

The main difficulties in the meta-analysis of studies are therefore different (measurement) concepts and approaches used. Large differences can be found in particular in the measurement variables for degree of exposition as well as in the basic assumptions for the relationship between annoyance and exposition degree. But next to the accuracy of the annoyance measurements the accuracy to determine exposure also plays an important role for achieving high explained variances (ICBEN, 2014).

MIEDEMA and OUDSHOORN countered the later argument of the strong variance in the lower section for individuals (UBA, 2010b) with the statement that for political decisions it is not the burden or reaction of individual but of the collective that is important (MIEDEMA & OUDSHOORN, 2001). And even though the concept of Highly Annoyed has been controversially discussed for a long time, it has become widely accepted today (UBA, 2010b). In 2002, the concept was established in the END as well as in the latest *Environmental noise guidelines for the European Region* published by the WHO (2018). For the calculation of the absolute risk (AR), the following dose-effect relations shall be used with regard to the adverse health effects of high annoyance:

[1] $AR = {\left(78{,}9270 - 3{,}1162 \cdot L_{den} + 0{,}0342 \cdot {L_{den}}^2\right)}\big/_{100}$

As there is a high risk of unreliable noise data for very low levels and a risk of selection of so-called survivors at very high levels, data below 42 dB and above 75 dB (L_{den}) are to be excluded (WHO, 2011, 2018).

To be able to quantify these health consequences, the WHO has developed a methodology to evaluate the global burden of disease (GBD). For traffic noise related adverse health effects, these are based on exposure-response relationships, exposure distributions, background prevalence of disease and disability weights, the burden of disease expressed in disability adjusted life years (DALYs). This calculated based on the sum of the years of life lost from premature mortality and the years lived with disability for people living with the disease or health condition or its consequences in the general population:

[2] $DALY = YLL + YLD$

$$for\ given:$$
$$YLL = numner\ of\ years\ of\ life\ lost = \sum_i N_i^m * L_i^m + N_i^f * L_i^f$$
$$for\ given:$$
$$N_i^m(N_i^f) = number\ of\ deaths\ of\ males\ (females)\ in\ age\ group\ i$$
$$L_i^m(L_i^f)$$
$$= standard\ life\ expectany\ of\ males\ (females)\ at\ the\ age\ at\ which\ death\ accours$$
$$YLD = years\ lifed\ with\ disablility = I * DW * D$$
$$for\ given:$$
$$I = number\ of\ incident\ cases$$
$$DW = disability\ weight$$
$$D = average\ duration$$

Thus *“One DALY can be thought of as one lost year of healthy life and the burden of disease as a measure of the gap between current health status and an ideal situation where everyone lives into old age, free of disease and disability”* (WHO, 2020, p. 6). The WHO conservatively estimates by applying the exposure-response function, e.g. a total of. 587.000 DALYs loss due to from noise-induced annoyance for the European Union Member States and other western European countries (WHO, 2020). Based on these results, the WHO formulates the following recommendations:

> *“For average noise exposure, the GDG strongly recommends reducing noise levels produced by road traffic below 53 decibels (dB) L_{den}, as road traffic noise above this level is associated with adverse health effects”* (WHO, 2018, p. 16).
>
> *“To reduce health effects, the GDG strongly recommends that policy-makers implement suitable measures to reduce noise exposure from road traffic in the population exposed to levels above the guideline values for average and night noise exposure. For specific interventions, the GDG recommends reducing noise both at the source and on the route between the source and the affected population by changes in infrastructure”* (WHO, 2018, p. 16).

From the last sections it is clear that due to the adverse health effects in combination with the rising number of people living in cities, it is important to know where in cities the areas highly exposed to traffic related noise are located. This recognition of noise as a harmful effect on the health of urban life is already reflected in position papers and regulations at the government level, like the Green Paper's inclusion of noise protection from 1996, which includes various regulations to reduce road, industrial and aircraft noise (EUROPEAN COMMISSION, 1996). Today there are, uniform guidelines and approaches that are incorporated in EU Directives. The latest one is *The Directive 2002/49/EC of the European Parliament and the council of the European Union* (END), which came into force in 2002, and is a development of the early joint European paper. Since all current calculations and studies are based on these guidelines, they will be explained in general terms in the next section.

2.2.2 Assessment of Environmental Noise

The *Act of Implementing the EC Directive on the Assessment and Management of Environmental Noise* of 24 June 2005 transposed the END into German national law. The aim of this Directive was to establish a common approach for the prevention of harmful effects of environmental noise and thus it contains:

(a) *„the assessment of exposure to environmental noise on the basis of noise maps using assessment methods common to the Member States;*

(b) *ensuring that the public is informed about environmental noise and its effects;*

(c) *the adoption by the Member States, on the basis of the results of noise maps, of action plans aimed at preventing and reducing environmental noise where necessary, and in particular where the level of exposure may have harmful effects on health, and at preserving the quality of the environment where it is satisfactory."* (END, 2002)

According to Article 5 of the END, the two noise indicators L_{den} and L_{night} must be calculated and according to Article 7 regarding road traffic, member states must draw up strategic noise maps for all agglomerations with more than 250,000 inhabitants and for all major roads with a traffic volume of more than six million motor vehicles per year. The procedure to be followed is set out in the Annex. In the first version of the END on environmental noise, it was initially up to the Member States to define the method of calculation, as long as it was based on ISO, 1993 and ISO, 1999. In order to guarantee further harmonisation, annex II of the directive was replaced in 2015 by a Europe-wide harmonized calculation method (EU Directive 2015/996, also identified with the acronym CNOSSOS-EU), which was to be used for noise mapping from 2018.

However, since the mapping follows a 5-year cycle, and the previous round was submitted in 2017, the first round of strategic noise mapping to use CNOSSOS-EU will be the one submitted in 2022 (MWAW, 2018). The Federal Republic of Germany therefore had to adapt the existing calculation regulations to EU requirements and later published new calculation guidelines for this purpose. Since the noise maps produced for Hamburg in 2017 will be used in this research, the provisions from that period are referred to. In the case of road noise, this concerns the *Vorläufige Berechnungsmethode für den Umgebungslärm an Straßen* (VBUS, 2006) (BUE, 2017). The VBUS is anchored in *Vierunddreißigste Verordnung zur Durchführung des Bundes-Immissionsschutzgesetzes (Verordnung über die Lärmkartierung)* (34. BImSchV, 2006) and can therefore be regarded as a legal provision for noise assessment. It is based on the well-known national calculation guidelines RLS-90, but differs from them in some essential points to align them with Annexes I and II. According to the END, the noise indicators L_{day}, $L_{evening,}$ L_{night} and L_{den} expressed in decibels (dB(A)), should be calculated as defined in ISO, 2017. The L_{den} is thus to be calculated as follows:

[3] $L_{den} = 10lg\,\frac{1}{24}\left(12 * 10^{\frac{L_{day}}{10}} + 4 * 10^{\frac{L_{evening}+5}{10}} + 8 * 10^{\frac{L_{night}+10}{10}}\right)\,dB$

The associated times are given in the VBUS, 2006:

- day = 06:00 am to 06:00 pm = 12h
- evening = 06.00 pm to 10:00 pm = 04h
- night = 10:00 pm to 06.00 am = 08h

The distinction between this three time slots is based on the common assumption that noise events in the evening and night periods create a higher annoyance than during daytime: for these time periods penalties of 5 dB(A) and 10 dB(A) are therefore added to the respective averaging levels (END, 2002; VBUS, 2006). The average annual level is calculated with the following formula:

[4] $L_{eq} = 10lg[\frac{1}{T_m}\int_{T_m} 10^{\frac{L_t}{10}}dt]$

$$for\ given:$$
$$L_t = Sound\ sevel\ in\ dB(A)\ at\ time\ t$$

To determine the emission level of road traffic $(L_{m,E})$ according to VBUS, a height of the sound source of 0.5 m above the middle of the road is assumed. If there are several lanes, it is assumed that the source is above the middle of the two outer lanes. The emission level is modified by means of several correction factors:

$$DTV = Average\ daily\ traffic\ volume$$
$$p = Truck\ percentage$$
$$D_v = Speed\ limit$$
$$D_{StrO} = Type\ of\ road\ surface$$
$$D_{Stg} = Longitudinal\ gradient$$

If no detailed information on the average daily traffic volume is available (subdivided into day, night and truck percentage), general values can be obtained from the guidelines for various types of road. Accordingly, to the VBUS the emission level $L_{m,E}$ is calculated by:

[5] $L_{m,E} \quad = L_m + D_v + D_{StrO} + D_{Stg} + D_E$

However, the propagation of sound is attenuated for a variety of reasons. First of all, if sound propagates equally in all directions into an undisturbed, homogeneous and loss-free space, a spherical wave field builds up around the source. On the way out from a sound source, sound waves therefore spread out over an increasing spherical surface. This causes the so-called energy dilution, which is expressed by the sound level reduction by distance (A_{div}) (VEIT, 2005). The second essential attenuation effect in free atmosphere is the so-called internal friction loss, expressed by the air absorption measure A_{atm} (HENN, SINAMBARI, & FALLEN, 2008). Air absorption is only noticeable from a propagation distance of $d > 200\ m$. Mathematically this is determined by the attenuation coefficient (NYBORG & MINTZER, 1955). The geometric attenuation A_{div} and the attenuation by air absorption A_{atm} are taken into account according to VBUS, 2006, jointly by the formula:

[6] $D_d = 20\, lg(d) + \frac{d}{200} - 11.2$

$$for\ given:$$
$$d = Distance\ between\ place\ of\ immission\ and\ emission$$

Next, there is the so-called ground-effect (A_{gr}) to be considered. It varies depending on the nature of the soil. To simplify matters, three ranges as well as three soil types are defined for the calculation of soil attenuation within the framework of ISO, 1999:

$$G = 0 = \ Hard\ soil\ (E.g. road\ pavement, water, ice, concrete)$$
$$G = 1 = \ Porous\ soil\ (E.g. grass\ and\ tree\ cover)$$
$$G = [0 - 1] = Mixed\ soil\ (With\ G = \ proportion\ of\ porous\ soil)$$

The distance ranges are: near the source A_s, the range near the receiver A_r and the middle range A_m as shown in Fig. 5 below.

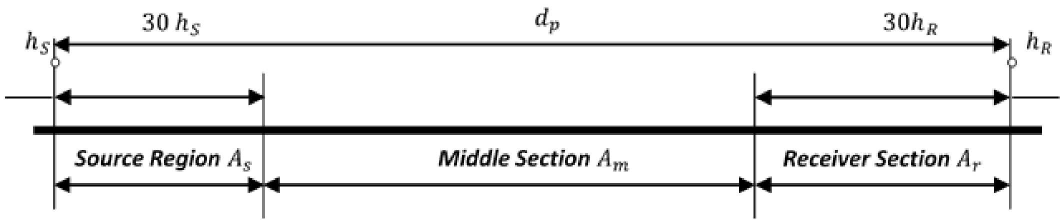

Fig. 5: Three distinct regions for determination of ground attenuation
Modified after ISO 9613-2:1996-12, p. 5.

The composition of A_{gr} is therefore calculated by:

[7] $A_{gr} = A_s + A_r + A_m$

The exact calculation as a function of the mid-band-frequency for each component can be found at ISO, 1999. But if the A-weighted sound pressure at the receiver point is of interest, the sound propagates over porous or mixed but predominantly porous soils, and if the sound is not a pure tone, ground and meteorology attenuation can be calculated according to ISO and VBUS with the following simplified formula:

[8] $D_{BM} = 4.8 - (h_m/d) * (34 + 600/d) \geq 0,$

$$for\ given:$$
$$h_m = \frac{F}{d}$$
$$D = Distance\ between\ place\ of\ immission\ and\ emission$$
$$F = Area\ between\ sound\ path\ and\ ground$$

In this case, the reflection on the ground must be considered by applying the directivity index:

[9] $D_\Omega = 10lg\left[1+(1-\alpha)\frac{d_p^2+(h_S-h_R)^2}{d_p^2+(h_S+h_R)^2}\right]\ dB,$

$for\ given:$

$a =\ Absorption\ coefficient\ of\ the\ reflecting\ surface$

Obstacles such as houses, walls and barriers play a superior role in urban space. They can attenuate and/or reflect sound in different ways due to their position, size and acoustic properties (PIERCE, 2014). According to the VBUs the attenuation due to shielding ((A_{bar}) is relevant if the obstacle at least touches the plane described by the traffic lanes and the receiver point. Additionally the level change due to shielding is only to be taken into account according to ISO, 1999 if:

- the mass per unit area $> \ 10\,\frac{kg}{m^2}$,
- the objects surface is closed and
- the horizontal dimension of the object to the perpendicular connection line source (d_l) receiver (d_r) greater than the acoustic wavelength $(\lambda)\ = (d_l + d_r) > \lambda$, as shown in Fig. 6.

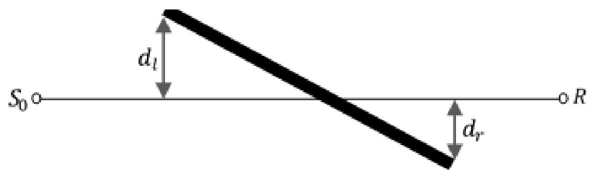

Fig. 6: Plan view of an obstacle between source and receiver

Modified after ISO 9613-2:1996-12, p. 3.

For downwind conditions the general formula according to ISO, 1999 is:

[10] $\quad A_{bar} = D_z - A_{gr} > 0$

and by diffracting around a vertical edge:

[11] $\quad A_{bar} = D_z > 0$

D_z depends on the nature of the obstacle. Distinctions are to be made between single diffraction (e.g. thin barrier) and double and multiple diffraction (e.g. buildings). The wavelength, the distance between emission and receiver points, as well as the distances between the place of emission and diffraction edge(s) or receiver point and diffraction edge(s) are considered. In addition, a meteorological correction may be required. The different calculations can be found in ISO, 1999, RLS-90, 1992 and VBUS, 2006.

In the case of traffic noise, multiple reflections occur due to urban constructions. Considering all possible reflections, the sound pressure level can theoretically increase by 8 dB. The actual increase, mainly due to the ever-present losses at the reflecting surfaces, is always below that value (ATTENBOROUGH, LI, & HOROSHENKOV, 2007; HENN et al., 2008; SINAMBARI, SENTPALI, & KUNZ, 2014). Both single and multiple reflections can lead to an increase of the immission level. The single reflection is calculated according to VBUS using the image source method, but regardless the absorption coefficient:

[12] $$L_{w,S_1} = L_w + 10\,lg(\rho)\,dB + D_\Omega$$

$$for\ given$$

$$D_\Omega = 10lg\left[1 + \frac{d_p^2 + (h_S - h_R)^2}{d_p^2 + (h_S + h_R)^2}\right] dB$$

Instead, the summand D_E is used, which considers the absorption properties of the reflecting surfaces. These are fixed according to their properties and can be taken from the VBUS. But if a section passes between two parallel, reflecting surfaces, or between closed facades of houses, where the gap proportion is $< 30\ \%$, a multiple reflection is considered according to VBUS. The sound level increase D_{ref} has to calculated by:

[13] $$D_{ref} = \frac{4h_{Beb}}{w} \le 3{,}2$$

$$for\ given:$$
$$h_{Beb} = Average\ height\ of\ retaining\ walls, noise\ barriers\ or\ house\ facades$$
$$w = Distance\ between\ the\ reflecting\ surfaces$$

If the reflecting surfaces are absorbent, *Zusätzliche Technische Vorschriften und Richtlinien für die Ausführung von Lärmschutzwänden an Straßen* should be applied (VBUS, 2006).

As A_{misc} are special attenuation effects, which are mainly needed in land use planning, it is not considered in VBUS, 2006. And thus, considering the attenuation effects above, the obtained $\mathrm{L_{m,E}}$ must be adjusted by the influencing variables in accordance with ISO, 1999 by the attenuation term, which is given by:

[14] $$A = A_{div} + A_{atm} + A_{gr} + A_{bar} + A_{misc}$$

$$for\ given:$$
$$A_{div} = Attenuation\ due\ to\ geometrical\ divergence$$
$$A_{atm} = Attenuation\ due\ to\ atmospheric\ absorption$$
$$A_{gr} = Attenuation\ due\ to\ the\ ground$$
$$A_{bar} = Attenuation\ due\ to\ barriers$$
$$A_{misc} = Attenuation\ due\ to\ other\ effects$$

Based on the specifications and calculations described, the continuous downwind (DW) octave-band sound pressure level is thus to be calculated for each receiver point by:

[15] $$L_{fT}\,(DW) = L_w + D_c - A$$

As the A-weighted long-term average sound level over all the time periods of a year is to be considered and the meteorological conditions are assumed to be favourable to sound propagation (downwind, as specified in ISO, 2017), the individual continuous sound levels $L_{fT}(DW)$ must be added up as follows:

[16] $$L_{AT}(DW) = 10lg\left\{\sum_{i=1}^{n}\left[\sum_{j=1}^{8} 10^{0.1\left[L_{fT}(ij)+A_f(j)\right]}\right]\right\}\ dB$$

$$for\ given:$$
$$n = Numbers\ of\ contributions\ i\ (sources\ and\ paths)$$
$$j = Indication\ the\ eight\ standart\ octave - band\ midband\ frequencies$$
$$A_f = Denotes\ the\ standart\ A - weighting$$

Due to the meteorological influences a time-of-day dependent meteorological correction D_{met} is to be made by:

[17] $$D_{met} = \begin{cases} 0 & if\ s_0 \leq 10(h_{GE} + h_{GI}) \\ -C_0\left[1 - 10\left(\frac{h_S+h_R}{s_0}\right)\right] & if\ s_0 > 10(h_{GE} + h_{GI}) \end{cases}$$

$$for\ given:$$
$$C_0 = \begin{matrix} Day & 2\ [dB[A]] \\ Evening & 1\ [dB[A]] \\ Night & 0\ [dB[A]] \end{matrix}$$
$$h_{GE} = Hight\ of\ emmisson$$
$$h_{GI} = Hight\ of\ immssion$$

The A-weighted average long-term sound pressure level for the regarded time period is accordingly:

[18] $$L_{AT}(LT) = L_{AT}(DW) - D_{met}$$

In this section it was shown, that traffic noise pollution is to be calculated for the respective study areas in accordance with the regulations and calculations methods explained above, and noise maps are to be produced. The received exposure in L_{den} are subsequently taken to estimate the extent by which the population is affected by traffic noise. These regulations and guidelines are implemented in various software programs such as from e.g. DataKustik GmbH; Softnoise GmbH SoundPLAN GmbH and Wölfel Meßsysteme. The use of these programs is typically not only restricted by high license fees, they also require particularly powerful hardware and a knowledge of the traffic flow as accurate as possible. Therefore, both, large-scale calculations and measurements are costly and time-consuming (GARG & MAJI, 2014; STEELE, 2001). This results in a lack of accurate data on the exposure of individuals, which explains the increased need for research in alternative ways to calculate exposure levels in urban areas.

Concerning noise as and environmental stressor beside infrastructural aspects, the built environment, i.e. the morphology, plays an important role. The approval of the impact of the building structure on the propagation of sound is also reflected at the political level. For example, at the *Handbook for Environmental Noise* of the *Federal Ministry of Agriculture, Forestry, Environment and Water Management, Austria,* are the effect of separated and concentrated traffic flows discussed on the basis of different building structures (BMLFUW, 2009). In the context of *"noise actions plans in agglomerations"* the GERMAN FEDERAL OFFICE FOR THE ENVIRONMENT states that the densest possible peripheral development can provide effective protection from road traffic noise and air pollutants (UBA, 2010a).

In the last decade in particular, the research focus has increasingly been on the relationship between different urban forms of development and their influence on sound propagation due to attenuation, reflection and absorption and thus on the exposure levels (EEA, 2014). Nowadays it is a widely accepted assumption that there is a link between urban structure and sound propagation. Thus, various studies have shown this on the basis of different morphology-related parameters that describe either the form and structure of single buildings or building arrangements, and their correlation with the corresponding exposure level. A selection of studies reflecting different approaches and underlying assumptions is presented below.

2.3 Urban Morphology as an Indicator of Noise Exposure

Early studies focused on urban surface parameters such as height and area of the buildings, and more complex ones like Porosity Index, which is a permeability indicator that measures the proportion of open space of the total investigated urban area. Thus, OLIVEIRA and SILVA were able to demonstrate that three different generalized urban forms, that differed in terms of morphology, lead to different exposure levels. For each urban setting, identical influencing variables were assumed with regard to traffic volume and road composition. It was shown that if the height of the buildings is increased, the sound exposure decreases (OLIVEIRA & SILVA, 2011; 2012, 2014). They come to conclusion that the mean sound level on the facade increases with the increase of Ratio of Open space (SILVA, OLIVEIRA, & SILVA, 2014). This stays in line with the findings of WEBER, HAASE, and FRANCK, who could prove a negative correlation between Occupied Area and noise exposure (WEBER, 2015; WEBER, HAASE, & FRANCK, 2014a). In the study conducted by WEBER et al., existing areas were changed in terms of development so that the applied metrics changed. Nine settings where tested. A particularly high influence on the level of the noise pollution was proven, when the first row of buildings was eliminated and when every second building was removed. In all tested areas the sound exposure was highest in these settings. Here, too, the height of the buildings had a particularly strong impact on the number of people heavily exposed. An increase in building height leads to a reduction in the number of people who are exposed to a burden higher than 50 dB(A) (WEBER et al., 2014b). This analysis was confirmed again on a smaller scale in 2017 by BOUZIR and ZEMMOURI for existing urban areas that were characterised by Porosity, Density as well as Compactness. The urban forms were similar to the generalized urban forms used by OLIVEIRA and SILVA. The same level of urban traffic was established for all urban configurations. The results support the statement that the level of exposure to road noise and these structural building parameters correlate (BOUZIR & ZEMMOURI, 2017).

Parameters investigated in other studies are for example, Ground Space Index and the Floor Space Index. RYU, PARK, CHUN, and CHANG showed for e.g. that Ground Space Index has a negative indirect impact and that the Floor Space Index is positively correlated with the traffic road noise level. However, contrary results were achieved in other studies, especially for the Floor Space Index. The authors attribute this to the different urban structures examined in the different studies (RYU et al., 2017). This supports the assumption that density parameters may be suitable to identify these different urban structures and stays in line with the results achieved by ZHOU, KANG, ZOU, and WANG in 2017. They investigated the possible influence of different typical building blocks in Tinjin, China, on sound propagation showed that the structural parameters for different small-scale structures correlate with noise exposure. As with RYU et al., no homogeneous traffic flows were assumed in this study, but counting data of traffic flows. The structures that have been analysed are Low-rise small, Unit community, Modern residential, High-rise. Examples can be seen in Fig. 7. The analysis of the relationship between parameters that describe the density and structure of an area and noise indexes, showed that ground and building facade noise L_{avg} have a decreasing trend with an increase in Ground Space Index in Low-rise and High-rise blocks. The standard deviation for ground and building facade noise level increase with an increase in Street coverage ratio in Low-rise and High-rise blocks. The same applies to an increasing trend for the Floor Space Index in low-rise small blocks. (ZHOU et al., 2017).

Fig. 7: Characteristics of different residential blocks development in Tianjin
From left to right: Low-rise small - Unit community - Modern residential - High-rise
Source: ZHOU et al., 2017, p.3.

HUPENG, KANG, and HONG analysed the relationship between urban streets spatial parameters on sound propagation in high-density cities. They proved that commonly used spatial parameters like e.g. the Streets Width (distance between facades), mean Facade Height and Standard Façade Height, but also new parameters Like Plan Enclosure Degree, which better takes into account the different heights of the facades within small-scale areas, are correlated to the sound level (HUPENG et al., 2019).

Further studies investigate the relationship between traffic volumes and these urban structures. In 2007 TANG and WANG investigated the influence of urban forms that differ in terms of land use on noise and air pollution caused by traffic. Parameters like Undeveloped Lot Space, Building Lot Space, Road Space, Green Space, Water Coverage and Land Consumption were used to discriminate between the areas. The results showed for example that for areas with a higher Building Lot Space the percentage of narrow roads and complex road networks is higher than in the other areas. In addition, a high density of intersections and little parking space leads to a lower traffic volume, what in turn leads to a lower overall noise level in these areas (TANG & WANG, 2007). Based on that study, WANG and KANG were able to demonstrate the morphological influence on the traffic noise distribution by comparing two structurally very different towns. Wuhan in China was chosen as an example of a high-density city compared to Greater Manchester in the UK for a typically low-density city. The correlations between noise distributions and the urban characteristics relating to urban density, such as the Road and Building Coverage Ratio have been analysed. Overall, comparisons between these two types of cities have shown significant effects of urban morphology on the traffic noise distribution. As a result, it could be shown that the examined parameters have a different influence direction on the sound level depending on the city structure. Building Coverage in Wuhan correlates negatively with both ground and façade noise levels, whereas in Greater Manchester there was a positive correlation. Also for the correlation between Accessible Space Coverage and noise levels, the results varied between the two cities (WANG & KANG, 2011). A possible reason for the increases is that a higher building coverage may result in more buildings closer to traffic and thus more noisy facades (HAO, KANG, KRIJNDERS, & WÖRTCHE, 2013).

Further studies have been carried out over the last 15 years (GIUNTA, SURIANO, SOUZA, & VIVIANI, 2015; HAO ET AL., 2013; KING, ROLAND-MIESZKOWSKI, JASON, & RAINHAM, 2012; OLIVEIRA & SILVA, 2011; SHENG & TANG, 2011; SOUZA & GIUNTA, 2011; TONG & KANG, 2021; WEBER, 2015; YU, MA, & KANG, 2019). They all came up with similar results. With the help of noise mapping they proved that different types of residential blocks result in different traffic noise burden.

Even though most studies focused on the relation of urban surface parameters, related to building properties and therefore only consider the influence of the built-up area, it also became apparent that the volume of traffic has a particularly large influence on the level of exposure. But the fact that the traffic volume varies, depending on the type of land use, has been demonstrated in various studies too. For example, WANG and KANG and ZHOU et al. show that there are correlations between Ground Space Index and noise levels as well between Ratio of Open Space and noise levels varied between the low and high density city. WEBER et al. concluded that areas with multi-storey tenement blocks and residential cores have a particularly high proportion of main roads.

What is clear from the foregoing is, that although the relationship between urban morphology and sound exposure can be demonstrated by means of surface parameter, as can be seen from the table below, the research settings differ with regard to type of investigated area, as well as with regard to the exposure determination.

Tab. 1: Exemplary research settings

Authors	*Investigated Parameter*	*Urban Setting*	*Exposure determination*
Oliveira & Silva 201, 2012 & 2014	*Height Compactness Porosity*	*Different generalized urban forms*	*Distributor roads with uniform traffic load*
Weber, Haase & Franck 2014	*Hight and Landscape metrics*	*Existing areas were changed in terms of development so that the applied metrics changed*	*Noise map acc. to VBUS*
Bouzir and Zemmouri 2017	*Height Compactness Porosity*	*Existing urban areas, that differ with regard to the surface parameters*	*The same level of urban traffic.*
Zhou et al. 2017	*Ground Space Index Floor Space Index*	*Different types of building blocks in Tinjin*	*The traffic distribution in the peak-hour period*
Silva et a. l 2017	*Sky View Factor*	*Areas in Leipzig with different geometric characteristics*	*Measurements with similar traffic flows.*
Tang & Wang 2007	*Road Space*	*Existing urban areas, that differ with regard to the surface parameters*	*Surveyed traffic volume, during 9:00e11:00 on working days*

There are studies that examine building related parameters and those that also examine street related parameters. Some use generalized forms and others real areas. Some work with uniform traffic volumes and street settings, others refer to official sound maps and others work with measurements.

The fact, that both the traffic intensity and the exposure intensity correlate with the structural parameters indicates that they do not develop independently. For example, regarding Hamburg, HOFFMANN, FISCHEREIT, HEITMANN, SCHLÜNZEN, and GASSER showed that building height, population density and street width decrease with the distance to the city centre (HOFFMANN et al., 2018). This is in line with the assumption that urban structures are a product of social processes and political decisions, thus density cannot be seen as an explanatory variable (HÄUßERMANN & SIEBEL, 1978).

It is nevertheless evident that there seems to be a connection between the structure of the buildings and, above all, between the composition of the buildings and the traffic load, as well that composition of the building has an influence on the sound propagation and thus on the resulting exposure level. There have been some attempts in recent years to use this relationship to model noise exposure maps based on the structure parameters.

Thus, GOZALO et al. developed a multiple regression model based on road and urban features to predict noise. Based on predictors such as traffic lights, crosswalks, road surface condition, lanes, law enforcement authorities, schools, floors in buildings, street length bus stops and slope, 71 % noise variability could be explained for the city of Valdivia. For Talca, based on slightly variable, 73 % noise variability could be explained (GOZALO et al., 2020).

STAAB, SCHADY, WEIGAND, LAKES, and TAUBENBÖCK create a geostatic model. Here, roads, buildings, and land use parameters were combined. Experimental results show that more than 500 samples stratified over the different noise levels are necessary to build a representative model. Using 21 selected variables, the model was finally able to explain a large part of the variability of the annual averaged road noise (L_{den}) (R^2 = 0.702) with a mean absolute error of 4.24 dB(A) and 3.84 dB(A) for built-up areas (STAAB et al., 2022). For limited areas the approach seems to be economically feasible, but for assessments on larger areas or on national level this is not yet the case. The authors assume that here noise mapping is a better alternative (STAAB et al., 2022).

The first approach is based on a very detailed knowledge of the details of the roads. However, this information is not always freely available. The second approach shows that on the basis of structural parameters, the prediction is possible by approximation, but that especially when it comes to the exact determination of the load values, the END maps are to be preferred.

Following the statement of MIEDEMA and OUDSHOORN, that it is not the exposure of the individual but of the community that is relevant for political decisions, the question is whether a globalized map could be sufficient to estimate which areas of a city are more exposed to traffic noise than others. Thus, the question arises, whether these characteristics can be used to generate a generalized map to estimate which areas are more polluted than others by classifying the study area on the basis of these structural parameters.

The interrelationship between urban structure and adverse health effects has already been studied in other disciplines. For example, in urban climatology. Here, too, the focus is on the identification of particularly highly affected areas, the level of exposure and the associated negative effects on health, based on generalized maps. The basic elements of the UHIs are taken to locate the most affected areas on the basis of the building structure. However, the classification is done on a rather low resolution. In the area of sound propagation, however, also small spatial differences have an influence. One research area in which such small-scale classifications are being tested is the classification of buildings, where structural parameters likewise play a major role. The concept of mapping UHIs and approaches for the automated classification of buildings in urban areas are therefore discussed in more detail later on. This provides an opportunity to see if the common methods used to create generalized maps could be transferable to sound propagation research.

2.4 Generalized Structure Maps

In 2014, HECHT developed an automatic classification method of building floor plans based on a data-driven pattern recognition approach based on training data with known class membership and object descriptive features. In 2014 he tested various procedures and data sets for classifying urban structures with regard to their performance in terms of the accuracy of the results and the computing effort required. He identified five different input types that differed in terms of data structure, geometric modelling, and schematic information and he defined a comprehensive set of characteristics at different levels of investigation (HECHT, 2014). The three levels between which HECHT differentiates are the micro level which includes individual buildings and building regions, the meso level which comprises a surrounding radius or a building block, and the macro level covers the settlement area or the entire area of investigation (HECHT, 2014). In addition to the assignment of a level of investigation, he provides, in accordance with NEUN and STEINIGER (2005) and STEINIGER and WEIBEL (2007) an overview of various characteristics that can be considered to describe objects with regard to their properties and relationships, as shown in Fig. 8.

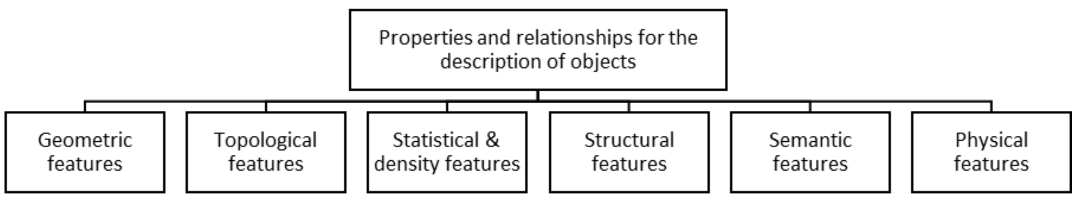

Fig. 8: Characteristics and relationships for the description of map objects

Referring to HECHT, 2014, p. 165, following PETER (2001), STEINIGER and WEIBEL (2005; 2007) and SESTER (1995).

According to STEINIGER AND WEIBEL, geometric parameters include parameters like size, shape, position and absolute or relative orientation (NEUN & STEINIGER, 2005; STEINIGER & WEIBEL, 2007). The shape-related parameters are often calculated by using so-called auxiliary objects. HECHT classifies these as centre of area, smallest enclosing rectangle, minimum perimeter or skeleton line as the centre axis of the buildings (HECHT, 2014).

Topological features contain those parameters that can be used to define the topological structure of object, for example, the number of nodes or segments of the respective polygon or holes in the polygon. Among the structural features at the micro level are parameters that are describing spatial configuration and fragmentation. Structural dimensions, such as the surface/edge line ratio or the contagion index, should be mentioned here (STEINIGER & WEIBEL, 2007). Statistical and density features refer to the geometrical and structural parameters of the single buildings, but averaged over the predefined areas or groups of objects, and are therefore on the meso or macro levels. This group includes, for example, the built-up area or the mean height in relation to the defined spatial unit, in the case of geometrical parameters. The structural features on meso or macro level include parameters that describe for example the spatial configuration and fragmentation of the respective area (HECHT, 2014; STEINIGER & WEIBEL, 2007). Semantic features are, for example, building function and other attributes of external data and physical features that are obtainable due to their spectral characteristics such as laser altitude (HECHT, 2014; NEUN & STEINIGER, 2005; STEINIGER & WEIBEL, 2007). HECHT tested 16 different classification methods in which the input parameters varied depending on the data basis. With nonlinear classification methods, eleven urban building types could be classified automatically. The Random Forest algorithm in particular was found to be highly efficient. Compared to 15 other tested machine learning algorithms, this algorithm shows the highest generalization ability and the shortest runtime (HECHT, 2014).

WURM, SCHMITT, and TAUBENBÖCK proposed in 2016 a similar mapping approach to determine Building Structure Types (BSTs) by using shape-based features but through the application of a Linear Discriminant Analysis. They proved the feasibility to classify different BSTs based on the country-wide building model at the level of detail 1 (LoD-DE1). WURM et al. classified (as can be seen in Fig. 9) five BSTs by using 26 different shape-based parameters which describe the physiognomy of individual buildings.

Fig. 9: Spatial subset of exemplary classification results
of the five building types for the test site Munich for a small area.
Colors represent building types
Source: WURM et al. 2016, p. 1911.

The parameters contained one, two- and three-dimensional features, including those which define the complexity of the respective building. The lowest contribution was performed by the one-dimensional parameters and the highest by the three-dimensional ones. The majority of the parameters used are originated from landscape analysis and are introduced by ANGEL, PARENT, and CIVICO (2010) and MCGARIGAL (2015). The Linear Discriminant Analysis indicated that the Complexity Indexes based on circle approximations according to ANGEL et al. have a particularly high contribution to the discrimination of BSTs. Among the 3D features, 3D Shape Index and Height contribute most importantly to the classification (WURM et al., 2016).

Similar mapping approaches are also used in the field of UHI and LCZ research. But whereas the generalized maps of the BSTs are mainly based on geometric and structural building parameters. In contrast, the LCZ are mainly based on density parameters. As shown in the section 2.1 *Health-Related Urban Well-Being*, heat stress is a typical urban stressor along with air and noise pollution. Especially in densely built-up inner cities, high temperatures can lead to health effects. That these areas are strongly affected is explained through the so-called UHI effect. With this effect the temperatures can be noticeably higher in the inner city than in the surrounding areas, which is caused by the urban structures in place (OKE, 1973; OKE & FUGGLE, 1972). Factors that contribute to the UHI phenomenon are, among others, the geometry of urban buildings, the thermal properties of the building substance, the radiation properties of the surfaces and the anthropogenic heat release (OKE, 1973). Densely built-up areas lead to an increase of surface area on which solar radiation can be absorbed. The absorption of solar radiation is additionally enhanced by the occurrence of multiple reflections on building walls. The use of building materials with low reflectivity (e.g. asphalt) also leads to increased absorption of solar radiation. In addition, buildings are obstacles to atmospheric currents and urban development therefore increases the roughness of the earth's surface. In simple terms, it can be said that the thermal, humid, aerodynamic and radiation characteristics of a city differ significantly from those of rural areas (ALBRECHT, 2019; OKE, 1982; STEWART, 2011).

To break down this dichotomous view between city and suburban space and to enable a more detailed analysis of the UHIs, Stewart and Oke proposed the LCZ concept in 2012. They defined Local Climate Zones LCZs as regions of uniform surface cover, structure, material, and human activity that span hundreds of meters to several kilometres in horizontal distance. Each LCZ has a characteristic screen height temperature regime. They distinguished 17 zones at local level. Four of them are illustrated in Fig. 10.

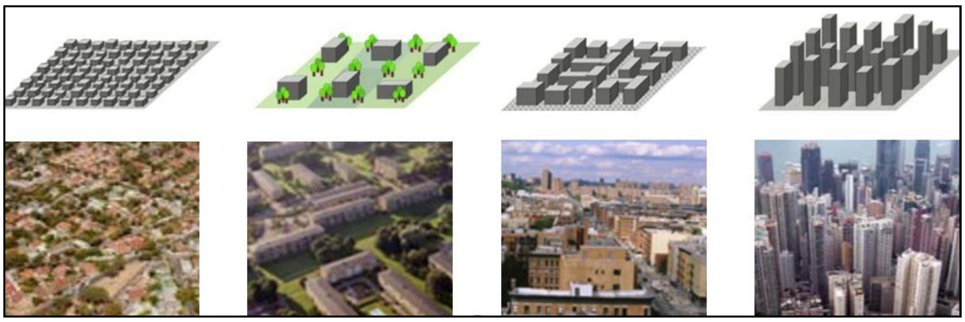

Fig. 10: Illustrated LCZs and high-angel photograph of corresponding urban area
From left to right: Compact Lowrise - Open Midrise - Compact Midrise - Compact Highrise
Modified after STEWART & OKE, 2008, pp. 1897.

The delimitation of the zones is based on parameters such as the Sky View Factor, Aspect Ratio, Mean Height, Terrain Roughness Class, Building Surface Fraction, Impervious Surface Fraction, Pervious Surface Fraction, Surface Admittance, Albedo and Anthropogenic Heat Flux. Thus, the parameters introduced by STEWART AND OKE (2012) are largely based on the building structure, in addition to the degree of sealing and the reflective properties of an area (STEWART & OKE, 2012).

Several approaches have been developed to identify LCZs using specific databases, such as satellite images and earth observation data. The set of methods includes supervised classification based on pixels (BECHTEL & DANEKE, 2012; GAMBA, LISINI, LIU, DU, & LIN, 2012; WENG, 2014), object based image analysis (GAMBA et al., 2012; WENG, 2014) and Geographic Information System based methods (LELOVICS, UNGER, GÁL, & GÁL, 2014).

Among the object-based image analysis is WUDAPT (World Urban Database and Access Portal Tools) The WUDAPT community provides 3 levels of LCZ maps. Maps of the city are referred to as the 'level 0' product as they represent the first level of information about urban areas. Level 1 and 2 meanwhile represent more detailed and higher information resolution (CHING et al., 2018; WANG, REN, XU, LAU, & SHI, 2018).

For the lowest level of detail (L0) WUDAPT uses open source remote sensing data and software tools (REN et al., 2017; REN, 2017). The classification process comprises three main steps: first, the pre-processing of the satellite raster data; second, the digitization and pre-processing of the corresponding training areas, which need expert knowledge; and third, the application of the classification algorithm. The operations are performed in SAGA-GIS developed by CONRAD et al. in (2015) and in Google Earth, while the satellite data are from Sentinel 2 or Landsat 8 OLI-TIRS (BECHTEL et al., 2015; BECHTEL et al., 2019). The final result is an LCZ map of an urban region in which each LCZ type has universal values that describe aspects of urban forms and functions (Fig. 11).

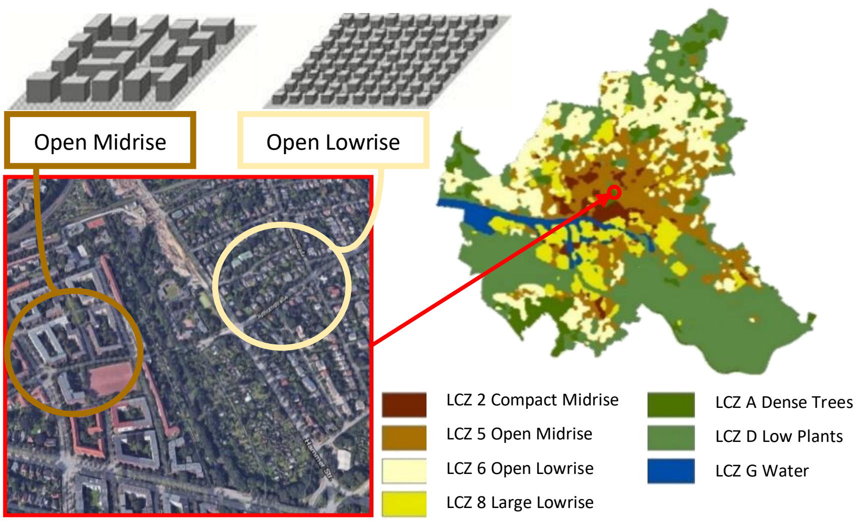

Fig. 11: LCZ for Hamburg
Referring to REN et al., 2017.
Data sources: KOTTAS, 2016.

KAVECKIS developed in 2017 on the basis of the concept of LCZ an extension to so called Urban Vulnerability Climate Zones (UVCZ). Besides the LCZ, these include future population's vulnerability to heat waves. Therefore, the identified structures can serve as an indication of which areas of a city are particularly affected by heat stress and where special preventative actions should be taken (KAVECKIS, 2017). Similar approaches to determine the extent to which people are affected by heat on the basis of urban structure were also used by FRANCK et al. (2013) and DUGORD, LAUF, SCHUSTER, and KLEINSCHMIT (2014).

In this section it could be shown that mapping based on surface parameters already exists. These are created on the basis of building parameters but also based on density parameters. In addition, the USVZ can be used to estimate where so-called hotspots are located, where exposure and adaptive capacity as well as sensitivity occur in an unfavourable relationship occur.

2.5 Conclusion and Research Objectives

In the State of Research, it has been demonstrated that the urban environment has a direct and an indirect influence on health and well-being. The interactions of the influencing variables are diverse and complex, and there is a need for further research. Due to the increasing urbanization and the associated increase in traffic volume, urban agglomerations do not only have to deal with air, but also with noise pollution. Next to the physical sound intensity, personal and psychological aspects contribute to the degree of annoyance. In order to be able to assess the consequences and thus take the necessary actions from a political point of view, common and accessible measuring instruments are required. One approach that has been established since the end of the 70s is the concept of measuring the proportion of highly annoyed persons as a function of sound levels. Despite the critical aspects mentioned above, this method it is anchored in directives on a political level. The concepts and methods available for determining the needed sound indexes to determine exposure, are usually not only time consuming and computationally intensive, but also expensive. This leads to an increased search for cost and time-saving alternatives.

One approach that has been studied increasingly in recent years is to investigate the influence of the urban structure on the level of sound propagation and the resulting exposure. All author link different structural parameters with the sound exposure and/or the traffic volume. Some authors use sound levels based on counted or modelled traffic volumes. Others take generalized forms and some use real study areas. Since the studies presented above show that urban forms have an influence on both the distribution of traffic volume and the level of noise exposure, independently of traffic volume, both factors have to be considered if exposure is derived directly from the urban structure or surface. The previous attempts to map the sound pollution by means of these parameters are based, for example, on expert knowledge regarding the road properties, or the calculation can only partially replace the time-consuming and time-intensive generation according to the END.

The creation of generalized maps and the assessment of possible health effects is also known in other research fields. Approaches to classify urban types on a smaller scale are exemplified by WURM et al. (2016) and HECHT (2014). The structural parameters are similar to those partially used in sound research as well. As was shown in section 2.4, small-scale structural parameters correlate with exposure, whereas density parameters seem to allow conclusions about the traffic load. These density parameters are similar to the ones used in the concept of LCZ mapping, which offers the possibility to derive the localization of the UHIs by identifying different landscape and city structures. Based on the similarities of the research fields, it will be examined whether the combination of these concepts can be used to detect the noise sensitivity of different urban structures.

Hence, the focus of this work is an automatic classification of the building structure based on parameters that describe the structure of buildings within an area and the density of the respective area. Thus, the research ultimately aims to generate structure maps of so-called Urban Sound Sensitivity Zones (USSZs). In addition, it will be examined whether such a map can be used to draw conclusions about adverse health effects of the exposed population. This could serve as fundamental to develop new traffic concepts in order to reduce the percentage of Highly Annoyed ($\%HA$), if necessary, and thus to increase their health level. The first leading questions of this thesis is therefore:

1. ***Does a generalized map based on surface parameters reflect the noise sensitivity of urban areas?***

To answer this question, sub-questions are defined. First, based on the research fields described above, it must be clarified, on a theoretical level, which of the parameters used for the classification of BSTs or to determine LCZs, could also be suitable for the classification of USSZ. The first sub-question that has to be answered is therefore:

1.1 Which surface parameters used in common mapping approaches have an influence on sound propagation in urban areas?

In order to emphasize the similarities that have been pointed out in the State of Research more clearly, it is shown which are the most common researched parameters regarding on their influence on the sound exposure in urban areas which are likewise used for the classification of BSTs and LCZs. Two different approaches will be analysed. The first approach works with structural parameters calculated at the building level which is defined as micro level. In the second approaches, surface parameters are investigated that are calculated for the entire area, the so-called macro level.

These theoretical assumptions serve as a guideline for determining the parameters that have to be calculated. Since the calculation of the sound exposure is not only computationally intensive, but also costly, the calculations should be possible with open sources software. Consequently, the second sub-question that has to be answered is:

1.2 Which of the surface parameters used in common mapping approaches, that have an influence on sound propagation in urban areas, can be calculated by an open source software?

Here, parameters are explored which are calculated on a vector data for the micro level and on grid data for the macro level. The parameters calculated either correspond to those of the preliminary theoretical considerations or can replace them.

The third sub-question that arises is:

1.3 Which of the calculated surface parameters highly contribute to a Random Forest classification?

Here, three different approaches are tested in which the quality of the Random Forest classification is evaluated. In order to observe to what extent these classifications allow a statement about the influence of the building structure and the resulting level of sound exposure, corresponding sound propagation scenarios are required. As it became clear in the State of Research that different building structures not only have different influence on the sound propagation, but are also affected by traffic load to a different extent, three different sound propagation scenarios are tested. One considers a uniformly distributed speed and traffic volume over the entire city, one is based on the Daily Average Traffic (DTV) and the average speed for the respective roads, and the third is based on the official noise map of the city of Hamburg. In order to find out whether conclusions can be drawn about the potential sound exposure from the three final structure maps obtained, a variance analysis is carried out for each sound propagation scenarios and each structure map. The question that has to be answered here is:

1.4 Do the noise levels of the sound propagation scenarios differ significantly between the classes of the obtained generalized maps?

Subsequently, it will be examined which of the generalized maps shows not only significant difference for one of the sound propagation scenarios but is likewise appropriate to represent the respective sound propagation scenarios. This leads to the sub-questions:

1.5 Which classifying approach is most appropriate to represent which sound propagation scenario?

This is examined by observing which approach has the highest effect size for which sound propagation scenarios.

Based on the answers to these questions, the second research question can be investigated, which addresses the question of whether statements regarding the adverse health effects of high sound exposure can also be made on the basis of the generalized maps:

2. What conclusions about adverse health effects can be drawn from the final generalized map?

Here, too, a number of sub-questions must be answered. First, it has to be verified whether the sound propagation scenario, which is best represented by the generalized map, correlates with variables that indicate adverse health effects. For this purpose, exemplary measurements are made and it is investigated at first. Based on the measurements, the following question will be investigated:

2.1 Does the final sound propagation scenario allow statements about the effective sound exposure?

It will be analysed whether $\%HA$ calculated based on the scenarios that is best presented by the final generalize likewise differs significant between the classes of the final generalised map obtained:

2.2 Does the $\%HA$ of the final scenario in accordance to the END differ significantly between the classes of the final generalized map?

It will then be examined whether the surveyed *self-reported* $\%HA$ indicated by $TRNA$ correspond to the $\%HA$ calculated based on the scenario that is best presented by the final generalize map. The question that will be analysed is therefore:

2.3 Does the relative number of self-reported $\%TRNA$ correspond to the $\%HA$ calculated in accordance to the END?

Based on these results of this three variables and sub-questions the second research question can finally be answered. Before the methodology is presented in *Materials and Methods*, the *Theoretical Considerations*, which are based on the *State of Resea*rch and whose results have a decisive influence on the methodology follow.

3 Theoretical Considerations

In the State of Research, it became apparent that a wide range of surface parameters have already been investigated with regard to their influence on sound propagation. It also turned out that similar parameters are used for classifying BSTs and LCZs. To find which parameters of these two fields of research could be suitable for the classification of the USSZ, and to answer the first sub-question: ***"1.1 Which surface parameters used in common mapping approaches have an influence on sound propagation in urban areas?"*** it is necessary to see which parameters correspond to those of the sound propagation research or are at least similarly calculated.

To proceed with this analysis in a well-structured way, the basic methodological structure of Hecht (2014) presented in section 2.4, will be followed. In addition, to narrow down the selection of possible concepts, the approaches of Wurm et al. (2016) in the case of BSTs structures and Stewart and Oke (2012) in the case of LCZs will be considered.

As stated in section 2.4 *Generalized Structure Maps*, Hecht differentiates three levels on which a parameter for classifications can be observed and calculated, which are displayed in Fig. 12. For the micro level, individual buildings and building regions are named; the meso level comprises a surrounding radius or a building block; while the macro level covers the settlement area or the entire area of investigation (Hecht, 2014).

Fig. 12: Levels of investigation
Referring to Hecht, 2014, p.165.

The thematic grouping of the parameters serves as an orientation to which level of investigation can be used, which parameters can be calculated, but also how they can be applied, and which statements are possible depending on the level of investigation. In addition to the assignment to a level of investigation, it will be looked to which of the categories of parameter characteristics provided by Hecht, in accordance with Neun and Steiniger (2005) and Steiniger and Weibel (2007), the parameters of the other research fields can be assigned.

Based on the assignment to the respective levels of investigation and different categories of characteristics, the parameters which contribute highly to both, the classification of the respective structures and the identification of the influence by building structure on sound propagation, will be further analysed. First, the parameters that highly contributed to the discrimination of BSTs in the study of Wurm et al. (2016) are discussed in section 3.2 at the micro level. This is followed by the analysis of the parameters named by Stewart and Oke (2012) for the classification of LCZs, which could also be relevant for sound propagation on macro Level in section 3.3. In addition, reference is repeatedly made to the physical laws of sound propagation and the resulting calculation regulations on both levels. Lastly, it will be clarified which of these parameters have to be calculated on the meso level for the classification in this research in subsection 3.3.4.

3.1 Level of Investigation

Typical parameters consider by WURM et al. for classifying buildings in to BSTs are area, height, width and length, but likewise shape-based parameters which describe the physiognomy of individual buildings in more detail, are often included. The former group belongs to the category of geometric surface parameters and the later to the category of structural surface parameters. Consequently the classification for example by WURM et al. mainly consists of two categories calculated on building level and can thus, as illustrated in Fig. 13, be assigned to the micro level.

As shown in the State of Research, UHIs are defined as regions of uniform surface cover, structure, material, and human activity, that span hundreds of meters to several kilometers in horizontal distance. Since larger units are often in focus, these are typically calculated at the macro level. The results are then divided into homogeneous units, the so called LCZs (STEWART & OKE, 2012). The classification is usually based on parameters like Sky View Factor, Aspect Ratio, Terrain Roughness Class or for e.g. Building Surface Fraction (OKE, 1988; STEWART & OKE, 2012). These surface parameters can be considered as density and structural. The surface parameters are therefore mostly calculated at the macro level and later on assigned to the meso level. Thus, the classification of LCZs corresponds with the macro level (Fig. 13).

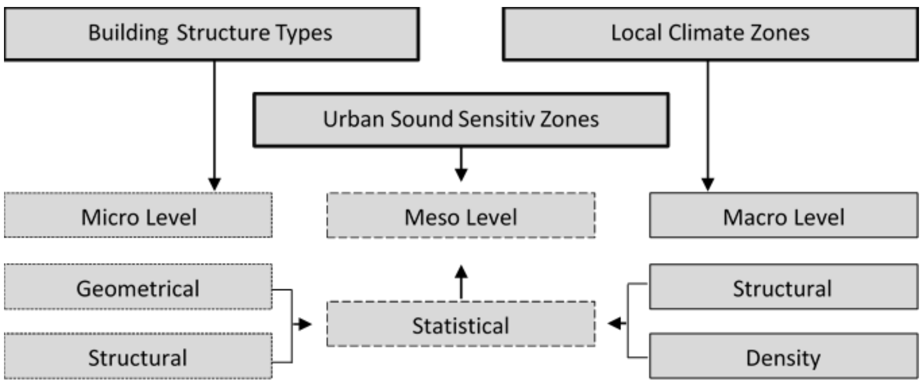

Fig. 13: Levels of investigation of the different research fields
Referring to HECHT, 2014, p. 165 and STEINIGER & WEIBEL, 2007, p. 180

If one looks more closely at the parameters that are examined in the context of sound propagation research, parameters from both approaches can be identified. The research of WANG et al. involves, for example, density and structural surface parameters such as Undeveloped Lot Space, Building Lot Space, Road Space. The early studies of SILVER et al. mainly investigate parameters calculated on the micro level like Fractal and Compactness of the individual building. In the later studies they focused on parameters like Sky View Factor as well as on Fractal and Compactness on the meso level. Thus, the surface parameters investigated in sound propagation research in urban areas are primarily based on density and statistic and density parameters, which are in turn based on geometrical and structural parameters and can, as shown in Fig. 13, clearly be assigned to the meso level.

In line with this thematic grouping, the parameters which contribute highly to both, the classification of the respective structures and to identify the influence of building structure on sound propagation, will be further analysed. First, the geometrical and structural parameters that contribute highly to the discrimination of BSTs in the study of WURM et al. (2016) are discussed. This is followed by the analysis of the parameters named by STEWART and OKE (2012) that could also be relevant for sound propagation on the macro Level. In both cases, the selection is based on the most frequently examined parameters that showed a correlation to sound exposure in the field of sound propagation in urban areas. First, the relevance of these parameters for the respective classification method is explained, before the role of these parameters in sound propagation is looked at. Since, as shown, the parameters regarding the influence on sound propagation are usually calculated at both micro and macro levels, but the investigation is carried out at the meso level, it is finally shown which of the parameters should to be determined for the meso level in this thesis.

3.2 Micro Level

Regarding the classification of buildings, WURM et al. showed that the simple geometric parameters such as Height (H), Area (A), and Perimeter (P) particular contribute considerably to the discrimination of BSTs. Regarding the research on sound propagation in urban areas A corresponds to the building foot print, and the P describes the length of building outline. In addition, in sound propagation research, there is a three-dimensional parameter of buildings investigated as well. One is the often-used Floor Space Index (FSI). It can be seen as equivalent of volume, which in turn is based on H and A, but with the difference that instead of the measured height the number of floors is taken:

[19] $$FSI = \frac{S_{\emptyset} A_c}{A_t}$$

$$for\ given:$$
$$S_{\emptyset} = Average\ number\ of\ stocks\ of\ the\ block$$
$$A_c = Constructed\ area\ of\ the\ block\ [m^2]$$
$$A_t = Total\ area\ [m^2]$$

OLIVEIRA and SILVA demonstrated in 2015 that the L_{aeq} rises slightly when the number of floors increases (OLIVEIRA & SILVA, 2011). The simulated scenarios carried out by Giunta et al. came to a similar result, where the highest average noise levels were related to the highest FSI values (GIUNTA et al., 2015).

These simple geometric parameters are all related to H and A. Thus, in different ways, the height and/or the volume of the buildings is always implicitly considered. That it is sensible to take the parameters presented above into account is founded in the physical laws of sound propagation, and is reflected in the END, in the term A_{bar}. It considers obstacles, at which the sound is reflected or refracted. The effect of single diffraction is illustrated in Fig. 14 using the example of a thin barrier (PIERCE, 2014).

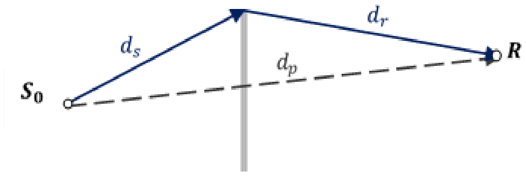

Fig. 14: Diffraction of sound by a thin barrier
Modified after ISO 9613-2:1996-12, p. 9.

Here it becomes apparent, that due to the diffraction effect of waves at edges, sound energy can reach the zone of the sound shadow, where receiver point (R) is located. The exact calculation of the obstacle effect is usually not possible. Therefore, empirical approximations are used. This is often done by using the concept of Fresnel numbers and results in (HANNAH & HUNT, 2006; PIERCE, 2014):

[20] $$A_{bar} = -10lg\frac{1}{(D'/d_p)^2 + (D'/d_p)}$$

$for\ given:$
$D' = d_s + d_r$

It is evident that the height of a house along the street has a strong shielding effect for the buildings behind, but that this effect is dependent on the height: the higher the building, the lower the sound load that can theoretically reach the sound shadow zone.

As shielding, but especially buildings, have a finite length, sound is therefore also diffracted at the edges (and possibly at the bottom edge). Each diffracted ray at the edges is associated with a specific shielding dimension $A_{bar,i}$ as shown in Fig. 15.

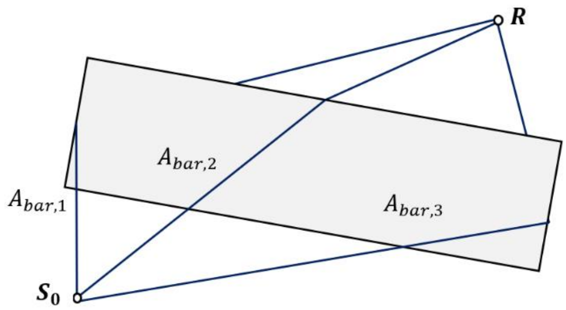

Fig. 15: Refraction on a barrier a finite length
Modified after ISO 9613-2:1996-12, p. 9.

By the interaction of the three illustrated rays a total intensity L_p at receiver point (R) is obtained by:

[21] $$L_p = L_w - 10lg\left[10^{-\frac{A_{bar,1}}{10}} + 10^{-\frac{A_{bar,2}}{10}} + 10^{-\frac{A_{bar,3}}{10}}\right] dB$$

$for\ given:$
$L_w = sound\ pressure\ level\ for\ the\ real\ source\ S_0$
$L_p = \ and\ the\ sound\ pressure\ level\ at\ R$

Just as with height, the shielding effect increases with the width of the obstacle. Thus, the parameters introduced above do not only contribute to classification of buildings, they also have a strong influence on the sound propagation in urban areas and should therefore be included in the analysis in any case.

The second category that is named by WURM et al. goes deeper into the different forms of buildings by taking their complexity into account, and can thus be assigned to the structural parameters. They name three complex parameters that highly contribute to the discrimination of BSTs. The first one is the Normalized Perimeter Index ($nPeriI$). It measures the area to perimeter ratio of a circle with the same area as the building (ANGEL et al., 2010; WURM et al., 2016):

[22] $$nPeriI = \frac{P_{A_{circle}}}{p_i}$$

$$for\ given:$$
$$P_{A_{circle}} = \ Perimeter\ of\ a\ circle\ with\ the\ area\ of\ the\ building\ p_i[m]$$
$$p_i = Building\ perimeter\ [m]$$

The second one is the Proximity Index (nPI). It is based on the calculation of the Euclidian distance between the single vertex of on object and the object centre of mass (ANGEL et al., 2010; WURM et al., 2016):

[23] $$nPI = \frac{P_{A_{circle}}}{P_{Object}}$$

$$for\ given:$$
$$P_{A_{circle}} = \frac{2}{3} r_{A_{circle}}$$
$$for\ given:$$
$$r_{A_{circle}} = Radius\ of\ smallest\ circumscribing\ circle\ around\ building\ i\ [m]$$
$$P_{Object} = \sum_{j=1}^{n} d_j \frac{1}{n}$$
$$for\ given:$$
$$d = Euclidian\ distance\ of\ the\ vertex\ to\ the\ building\ center\ of\ mass\ [m]$$

The third one is the Normalized Spin Index (nSI), which is similar to nPI (ANGEL et al., 2010; WURM et al., 2016):

[24] $$nSI = \frac{J_{A_{circle}}}{J_{Object}}$$

$$for\ given:$$
$$J_{A_{circle}} = \frac{1}{2} r_{A\ Cicle}^2$$
$$J_{Object} = \frac{1}{n} \sum_{j=1}^{n} d_j^2$$
$$for\ given:$$
$$d_j^2 = Squared\ euclidian\ distance\ of\ the\ vertex\ to\ the\ objekt\ center\ [m]$$

Additionally, they showed, that the Compactness Index (CI) achieves the height discriminatory power to classify BSTs. The CI belongs to the group of circle approximations, referred to in ANGEL et al. (2010). It is also known as Circle by MCGARIGAL. At the building level, it describes the individual shape in terms of fragmentation (MCGARIGAL, 2015) and can be calculated according MCGARIGAL (2015) as follows:

[25] $$CI = 1 - \frac{a_i}{p_i^s}$$

$$for\ given:$$
$$a_i = \ Area\ of\ a\ building [m^2]$$
$$p_i^s = Area\ of\ smallest\ circumscribing\ circle\ around\ building\ i\ [m^2]$$

The more regular the building shapes and the smaller the number of the buildings within an area, the higher the CI. Regarding the sound propagation this means: the higher the CI, the greater the presence of obstacles in an urban area; this results in an increase of shielded areas and a possible reduction of the exposure level within an area (BOUZIR & ZEMMOURI, 2017). This stays in line with the results achieved by SILVA et al. (2014) and OLIVEIRA and SILVA (2011). As the CI shows a high correlation to sound exposure level and contributes to the discrimination of BSTs as well, it is advisable to include circle approximations in the analysis.

In the case of sound propagation, next to the CI, the second most commonly investigated parameter in this group is the Fractal Index ($Fractal$). It describes the complexity of the perimeter of an urban form through the relationship between P and A of an individual building. The Fractal Index can be calculated according to MCGARIGAL (2015) by:

[26] $$Fractal = \frac{2\,ln\left(\frac{p_i}{2\sqrt{\pi}}\right)}{ln(a_i)}$$

$$for\ given:$$
$$a_i = Area\ of\ a\ building\ [m^2]$$
$$p_i = Building\ perimeter\ [m]$$

The higher the $Fractal$, the more irregular the shape of the building. Lower values are found when the building has a simpler form. If the Perimeter is instead more complex and irregular, the $Fractal$ will be greater (MCGARIGAL, 2015). SILVA et al. showed that for given investigated areas moving from the highest to the lowest $Fractal$ generate an increase of the exposure levels (SILVA et al., 2014).

The parameters that consider the complexity of the building form, as can be seen in the formulas [22]- [26], which are referred to in both research fields as P or are calculated by considering an auxiliary object. Thus, they reflect the fissuring of the individual buildings by setting the actual size of a building and an auxiliary object in relation to each other. Here, too, the mathematical similarities are thus evident.

It has been shown that parameters which consider the H, A, V and the complexity of the structure of individual buildings, highly contribute to the classification of building types and have at the same time an influence on sound propagation in urban areas. Consequently, the parameters listed in Tab. 2 should be considered in the classification of USSZ at the micro level.

Tab. 2: Surface parameters on micro level

Height	*Perimeter*	*Fractal Index*
Width	*Proximity Index*	*Compactness Index*
Area	*Normalized Spin Index*	*Ground Space Index*
Volume	*Normalized Perimeter Index*	

3.3 Macro Level

The approach in the field of mapping LCZs is, as mentioned above, different. The focus is on the properties of larger spatial units. Consequently, similar to sound propagation research in urban space, the influence of spatial composition of the unit on urban climate is investigated. Therefore, most of the parameters considered for the identification and classification are usually density and structural parameters calculated at the macro level.

A parameter, which is not only named by STEWART and OKE, but has also often been investigated in recent years in sound propagation on the meso level, is the Sky View Factor (SVF). It determines the fraction of sky hemisphere visible from ground and takes thus, as can be seen in Fig. 16, the height to with ratio into account (HÄMMERLE, GÁL, UNGER, & MATZARAKIS, 2011).

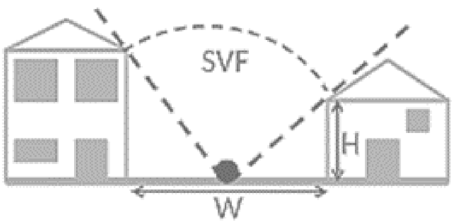

Fig. 16: Sky View Factor

Source: DIRKSEN, RONDA, THEEUWES, & PAGANI, 2019, p.3.

SILVA, FERNANDO, RODRIGUES, and CAMPOS (2018) demonstrated that the SVF has a negative correlation with noise exposure independently of the traffic class (SILVA et al., 2018). Since most authors who use the SVF refer to OKE (1988), the parallel is self-explanatory. A simplified calculation is possible as follows:

[27] $$SVF = \frac{1-cos\theta}{2}$$

$$for\ given:$$

$$\theta = tan^{-1}\left(\frac{H}{0.5\,W}\right)$$

In this category STEWART and OKE additionally name the Aspect Ratio (AR), which is defined by the mean height-to-width ratio of street canyons, building spacing, and tree-spacing (STEWART & OKE, 2012). That not only the shapes of the individual buildings, but also their formation and thus the density play a role regarding the sound propagation in urban areas, is clear when considering how this causes, for example, multiple reflections. In the case of traffic noise, multiple reflections occur due to urban constructions, as shown in Fig. 17 along the roads.

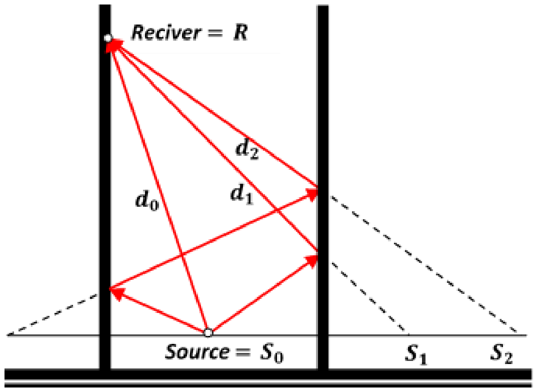

Fig. 17: Multiple reflection in a street canyon

Modified after ATTENBOROUGH, 2007, p. 419.

The sound level increase caused in this way, is explained by using the example of a street that passes through two closed facades (ATTENBOROUGH et al., 2007; HENN et al., 2008). Without reflection, the sound pressure level at the receiver point L_p at a distance d is reduced due to the so-called energy dilution, which is expressed by the sound level reduction by distance (HENN et al., 2008; VEIT, 2005):

[28] $$A_{div} = 10\, lg\left(4\,\pi \frac{d^2}{d_0^2}\right)\, dB$$

$$for\ given:$$
$$d = Distance\ between\ source\ and\ receiver$$
$$d_0 = Reference\ distance = 1m$$

Considering the reflections, it changes to:

[29] $$L_p = lg \sum 10^{\frac{L_i}{10}}$$

$$for\ given:$$
$$L_i = L_{w,S_1}$$
$$for\ given:$$
$$L_{w,S_1} = L_w + 10\, lg(\rho)\, dB + D_\Omega$$
$$for\ given:$$
$$\rho = Degree\ of\ reflection$$
$$D_\Omega = 10lg\left[1 + (1-\alpha)\frac{d_p^2 + (h_S - h_R)^2}{d_p^2 + (h_S + h_R)^2}\right]$$
$$for\ given:$$
$$\alpha = Absorption\ coefficient\ of\ the\ reflecting\ surface$$

The sound pressure level can theoretically increase by 8 dB. The actual increase is, mainly due to the ever present losses at the reflecting surfaces, always below that value (ATTENBOROUGH ET AL., 2007; HENN ET AL., 2008; SINAMBARI ET AL., 2014).

Beside the SVF and the AR, STEWART and OKE consider the Terrain Roughness Class (TRC) for the classification of LCZs. Here, the authors refer to the classification of effective terrain roughness (z_0) for city and country landscapes according to DAVENPORT, GRIMMOND, OKE, & WIERINGA, 2000. Formula [30] takes in to account, that the undisturbed geostrophic wind is slowed down by obstacles near the ground such as houses, trees or bushes. The mean wind speed ($\bar{u}$) at height (z) can be described by:

[30] $\bar{u}_z = \frac{u}{k} ln\left(\frac{z'}{z_0}\right)$

$for\ given$:

$u = Friction\ velocity$

$k = Karman's\ constant\ (\sim 0.4)$

$z' = z - z_d$

$for\ given$:

$z_d = Zero - Plane\ displacement\ height$

The roughness length z_d describes the properties of the earth's surface. z_0 is the height at which the wind speed becomes equal to zero. The wind direction and strength can also affect the level of sound exposure. The influence depends on the relative angle of sound propagation and wind vectors, and can be separated into its vertical and horizontal components. On the horizontal axis sound and wind speed add up depending on the direction. Sound propagation speed increases therefore in wind direction and vice versa. If the vertical wind gradient is positive with increasing height, there is a downward refraction. If, on the other hand, wind gradient is negative, an upward refraction occurs (DRAHOS & DRAHOS, 2012; VDI, 1988; ZIEMANN, 2002).

As shown in the State of Research, wind conditions are considered at various points in the calculation regulations. Here, a distinction is made between upwind and downwind. Since higher roughness in urban areas results in an increase in wind speed in higher altitude, the propagation speed increases with increasing height in mid-wind direction and a downward refraction occurs. This is referred to as a condition favourable for sound propagation (VDI, 1988). Since the wind conditions near the ground, especially wind direction, wind speed and wind gradient, have an influence on the sound propagation direction and sound propagation speed, it is reasonable to consider the roughness and also the roughness classification in this work. Therefore, in this work, the parameters listed Tab. 3 should be calculated at the macro level.

Tab. 3: Surface parameters on macro level

Sky View Factor
Aspect Ratio
Terrain Roughness Class

It could be shown that just the density parameters, which play a superordinate role in the field of UHIs, are also investigated in sound propagation research. Their relevance also results here from the physical laws of sound propagation. In addition to the described attenuation effects, multiple reflections can occur, especially in dense regions, which in turn increase the exposure. Furthermore, the density of the built-up area has an influence on the wind conditions in the urban area, which in turn can have a reducing or increasing effect on the sound exposure. In addition to this parameter calculated on macro level, there are further density parameters that can be calculated on the basis of the individual building parameters which are partly used as well for the classification of the LCZs. These are calculated directly at the meso level and are therefore explained in the next section.

3.4 Meso Level

A well-known parameter in the field of urban climate research on the meso level is the Building Surface Fraction which is defined as the "*Proportion of ground surface with building cover*" (STEWART & OKE, 2012). The definition shows that it is equivalent to the building coverage which is an often-investigated parameter in the field of urban structure and sound propagation. It is also called Occupation Ratio, Ground Floor or Ground Space Index (GSI). The GSI is defined as the percentage of the area that is covered by buildings/constructions which includes the total horizontal area when viewed in plane. It is calculated by:

[31] $$GSI = \frac{A_B}{A_T}$$

$$for\ given:$$
$$A_B = \sum Base\ area\ of\ all\ buildings\ [m^2]$$
$$A_T = Totali\ nvestigaion\ area\ [m^2]$$

GSI can be interpreted as a density parameter: the higher the GSI the higher the proportion of built-up area. In terms of sound propagation in urban areas, this means that the proportion of obstacles is higher and thus also the proportion of resulting sound shadow zones may rise (BOUZIR & ZEMMOURI, 2017; RYU et al., 2017; ZHOU et al., 2017). The negative correlation between the GSI and sound level exposure was confirmed by studies such as OLIVEIRA and SILVA (2011), HAO et al. (2013), BOUZIR and ZEMMOURI (2017) and SILVA et al. (2017).

A similar density Parameter that correlates uniformly in almost all studies with the level of sound exposure is the Ratio of Open Space (ROS). It is calculated by:

[32] $$ROS = \frac{S'}{S} * 100,$$

$$for\ given:$$
$$S' = Area\ of\ all\ \text{“}holes\text{”}\ [m^2]$$
$$S = Constructed\ area\ of\ the\ block\ [m^2] = \sum_i s_i$$

It measures the ratio of open space compared to the total investigated area and can therefore be seen as a counterpart to the GSI. A higher ROS is therefore associated with an increased proportion of open space within the studied area. Regarding sound propagation in urban areas, it can be deduced that sound can propagate unhindered. Therefore the sound level exposure increases with an increasing ROS (BOUZIR & ZEMMOURI, 2017). Thus, SILVA et al. came to the conclusion that the ROS and the $L_{avg,façade}$ are positively correlated (SILVA et al., 2014). BOUZIR and ZEMMOURI observed that, as ROS increases, the areas exposed to L_d > 65 dB(A) are increasing too, and that in turn the areas exposure to L_d ≤ 50 dB(a) decrease (BOUZIR & ZEMMOURI, 2017), which is consistent with the results of SILVA et al., 2014 OLIVEIRA & SILVA, 2011 and with SILVA et al., 2017.

The parameters described above, as well as the surface parameters mentioned on macro level, refer to the building density and should therefore be considered in this work for the reasons mentioned above. All surface parameters described so fare consider the building as an obstacle with regard to sound propagation. This is different for the surface parameters that are related to the degree of sealing mentioned by STEWART and OKE. The first one is the Impervious Surface Fraction (λ_i) wich is defined as the "*Proportion of ground surface with impervious cover"* and the second one is the *Pervious Surface Fraction* (λ_v), the "*Proportion of ground surface with pervious cover*" (STEWART & OKE, 2012). Since the soil properties, especially due to their degree of absorption and reflection, are also relevant for the sound propagation, a parallel can be seen. The degree of attenuation due to the soil condition has to be considered for the sound propagation too. Depending on the nature of the soil, three ranges as well as three soil types are defined for the calculation of soil attenuation within the framework of ISO, 1999:

$$G \quad = 0 = \ Hard\ soil\ (E.g. road\ pavement, water, ice, concrete)$$

$$G \quad = 1 = \ Porous\ soil\ (E.g.\ grass\ and\ tree\ cover)$$

$$G \quad = [0 - 1] = Mixed\ soil\ (With\ G = \ proportion\ of\ porous\ soil)$$

The distance ranges are: near the source A_s, the range near the receiver A_r and the middle range A_m. The composition of A_{gr} is therefore:

[33] $$A_{gr} \quad = A_s + A_r + A_m$$

In both areas, the nature of the soil and the associated reflection and absorption properties thus have an influence. Therefore, this parameter should also be considered if possible. However, it cannot be calculated from the building shape or composition. Further information is necessary here.

Regarding the question: ***"1.1 Which surface parameters used in common mapping approaches have an influence on sound propagation in urban areas?"*** it can be stated, that the parameters listed in Tab. 4 below, should to be considered. In particular, geometric and structural, but also density surface parameters, play a major role in the classification of BSTs and LCZs and can be related to the level of sound exposure.

Tab. 4: Density and statistical surface parameters on meso level

Height	*Proximity Index*	*Ground Space Index*
Width	*Normalized Spin Index*	*Sky View Factor*
Area	*Normalized Perimeter Index*	*Aspect Ratio*
Volume	*Fractal Index*	*Terrain Roughness Class*
Perimeter	*Compactness Index*	*Impervious Surface Fraction*

4 MATERIALS AND METHODS

The methods used for data collection as well as the techniques of evaluation and analysis are explained and justified in this section. The use of two research questions leads to a two-part structure presented in Fig. 18, which is proceeded by the selection of the focus areas in section 4.1 *Spatial Entities*.

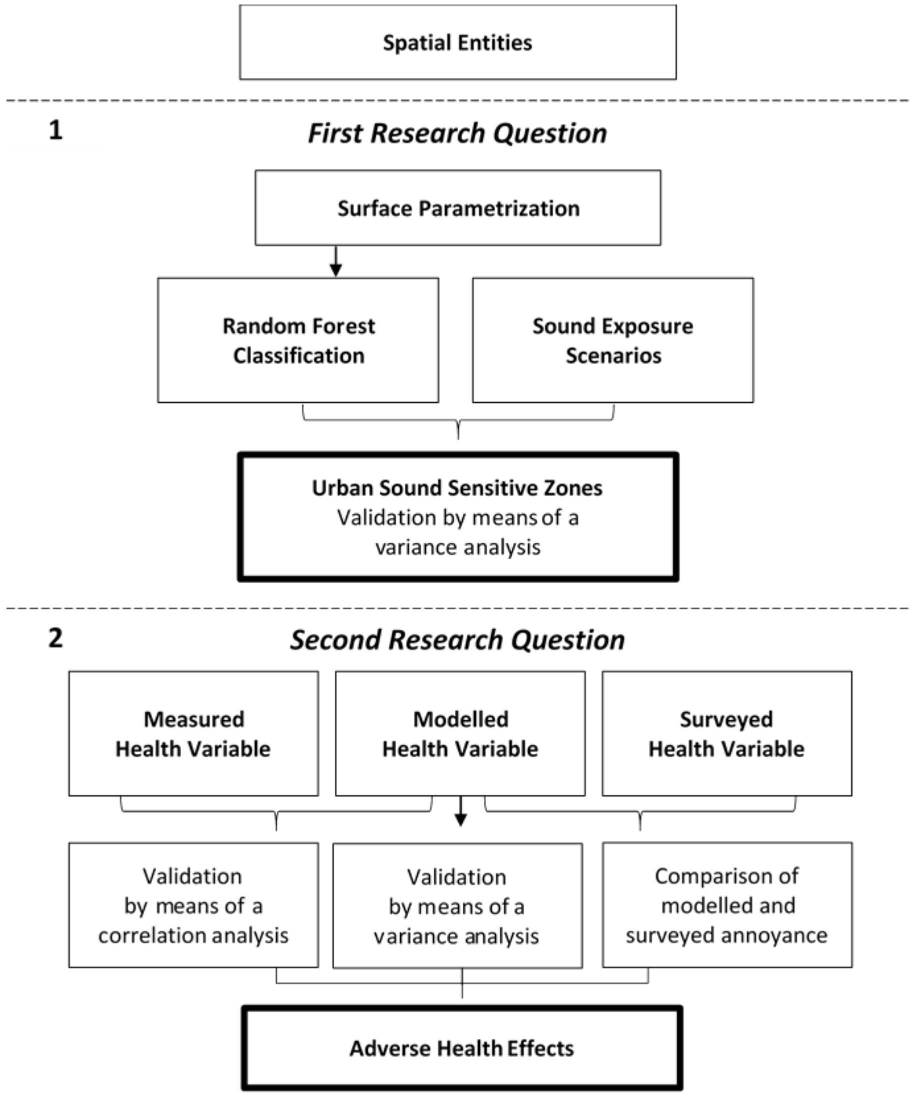

Fig. 18: Workflow Materials and Methods

To explore the first research question of ***"1. Does a generalized map based on surface parameters reflect the noise sensitivity of urban areas?",*** the selection and calculation on which the classification will be performed, is based on the outlined commonalities of the research fields and the associated surface parameters presented in section 3 *Theoretical Considerations*. Thus, in section 4.*2 Surface Parametrization*, it will be analysed which of these parameters are easily to be calculated with an open source software. This is followed by the selection and description of the algorithm by which, based on these calculated surface parameters, the possible USSZs are to be classified in section 4.3 *Random Forest Classification.* The classification settings are introduced in sub-section 4.3.1, which is followed by the accuracy assessment, that will be applied in sub-section 4.3.2. As for the validation of the USSZ the sound exposure is needed, the input parameter and the calculation methods for the sound propagation scenarios are found in section 4.4 *Sound Exposure Scenarios.* Having thus completed the computational methods for obtaining the primary data for the first question, the selection, justification, and explanation of the validation method follows in section 4.5 *Variance Analysis*.

The sections onwards from 4.6 *Health related Variables*, are dedicated to the second main research question: ***"2. What conclusions about adverse health effects can be drawn from the final generalized map?"***. Since the validation methods differ depending on the type of health variable, the respective data collection and validation methods are presented in the corresponding sections 4.6.1 to 4.6.3. In order to get an impression regarding whether the finally selected sound propagation scenario allows statements about the actual exposure, measurements are carried out. Thus, the measurement setting and the validation of the final sound exposure scenario, as well as the corresponding correlation analysis are described in section 4.6.1 *Measuring Exposure*. Following this, the modelled health variable $\%HA$, for which the calculation and analysis methods are explained in section 4.6.2 *Modelled Noise Annoyance*, is derived from the finale sound exposure scenario. Frist it is analysed if these show significant differences between the classes of the final USSZ map. To understand whether these correspond to the surveyed Traffic Related Noise Annoyance ($TRNA$), finally, the surveyed health variable, has to be collected, to verify to what extent the modelled exposure corresponds to the actual perceived exposure. Thus, the survey as well as analysing methods are presented in section 4.6.3 *Surveyed Noise Annoyance*.

4.1 Spatial Entities

The case sites for this project are located within the city of Hamburg, which is the second largest city in Germany, and is located in northern Germany. The city itself contains approximately 1.8 million inhabitants (STATISTIKAMT NORD, 2015). Hamburg is a metropolitan region with a total of about 5 million inhabitants. The settlement structure of the metropolitan region is a network of villages and towns of different size, location, function and structural design, with different economic activities within this network. A most basic classification of the area is the distinction between rural and urban settlement structure. A finer classification is the differentiation into densification areas, - urban regions, local zones, central places as well as interdependent areas of the central places. Within a place, the settlement structure can be characterized according to the assigned functions by the ratio of residential, labour, business and entertainment districts (BSU, 2007; KNIELING, 2010).

The metropolitan region is currently characterized by strong commuter flows. In addition, due to the Hamburg seaport, the metropolitan region is an internationally important shipping and logistics centre in Europe. This causes a relatively high volume of heavy traffic, especially in the port area, which is, as can be seen from Fig. 19 top-left, centrally located. Additionally, the share of private cars is high in Hamburg (FOLLMER & GRUSCHWITZ, 2020; OECD, 2019).

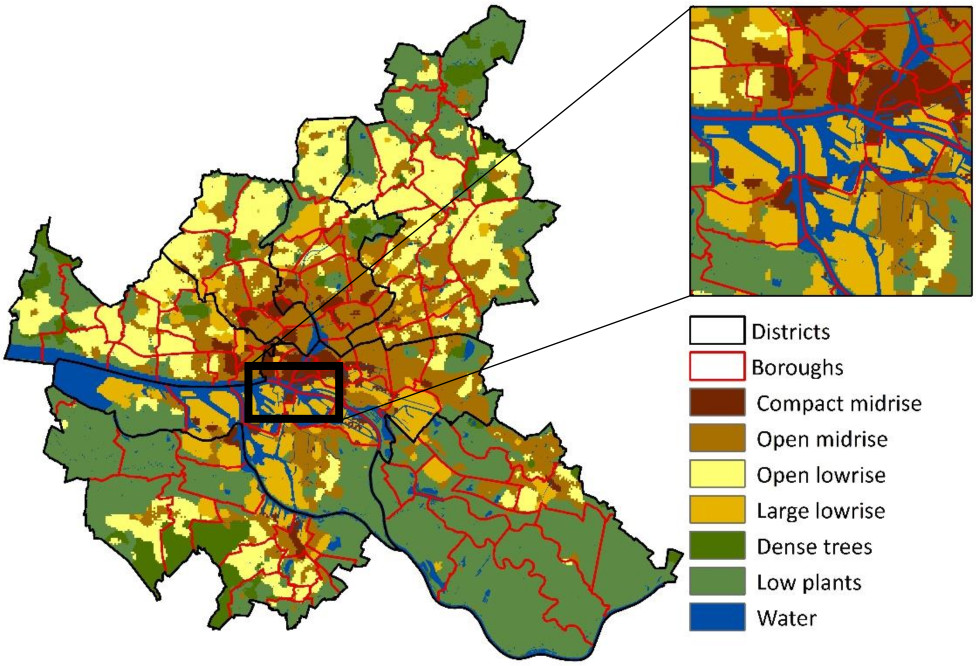

Fig. 19: LCZ, districts and boroughs of the city of Hamburg
Illustration based on data of KOTTAS, 2016 and STATISTIKAMT NORD, 2015.

The urban climate of the city of Hamburg is likewise heterogeneous, due to dense building development, high soil sealing, low vegetation in the inner city and increased emissions that are not evenly distributed throughout the city. This creates an UHIs making the central districts of Hamburg on average about 0.1°C warmer than in the surrounding area, with local peaks of 1.2°C in the city centre (ARNDS, BÖHNER, & BECHTEL, 2017; SCHLÜNZEN et al., 2009). But even on a small scale, different climatic conditions can be found and traced back to the various building structures. As explained in section 2.4 *Generalized Structure Maps*, the mapping of the LCZ has already been carried out for Hamburg by the WUDAP community. As can be seen in Fig. 19, they are distributed over the entire city area.

As the State of Research highlighted, the impact that building structure can have on sound propagation and possible adverse health effects require further examination. In particular, the single focus areas should thus be as homogeneous as possible but at the same time reflect the high variability of all the factors described above. Neither the districts nor the boroughs fulfil this requirement. Both districts and boroughs span large areas, and thus, great heterogeneity in morphology as well as socio-economic and demographic indicators can be found within the boroughs (KREFIS et al., 2017; STATISTIKAMT NORD, 2015). This also applies to the factors relevant to this research. Smaller, more homogeneous entities must therefore be established. To solve this problem, the Statistical Areas (SAs) displayed in Fig. 20, which consist of several BBs, which in turn are homogeneous with regard to selected structural and social-structural features, are used.

A wide range of socio-structural information is available for these units from the Statistical Office North. The current division into 943 SAs was implemented following the 1987 census. Since then they have been continuously adjusted, most recently in 2015 (STATISTIKAMT NORD, 2015).

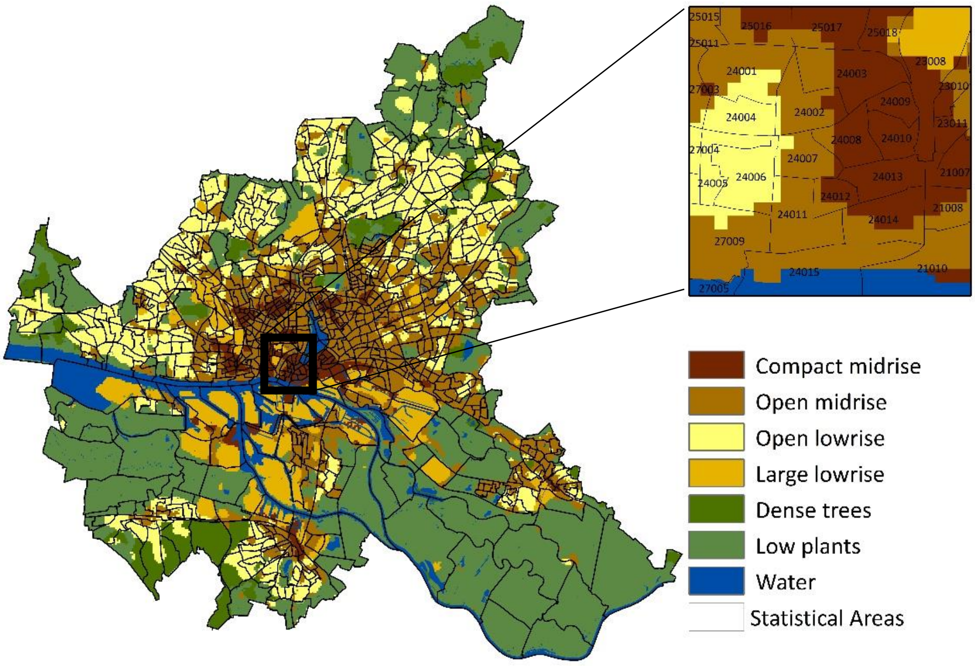

Fig. 20: LCZ and Statistical Areas of the city of Hamburg

Illustration based on data of KOTTAS, 2016 and STATISTIKAMT NORD, 2015.

As pointed out in chapter 3, for the calculation on meso level, there is a reference levels required for which the density parameters can be calculated, and the other parameters averaged. These SAs do not cross districts but occasionally cross borough boundaries. The SAs consist of different BBs, which are divided by roads, but also by open spaces, the aggregation of the surface parameter over the entire SAs, could falsify the results, especially in the case of the density parameters. For example, the open spaces, but also the streets, which would be counted as open spaces, would change the ratio of built-up area and open space in the case of the density parameters. The BBs thus comprise smaller areas that are internally-homogenous and heterogeneous to each other and are not crossed by streets. BBs are therefore a more suitable basis for the investigated question about the influence of the building structure on sound propagation. Consequently, as these SAs are made up of BBs that are relatively homogeneous, thus can be taken for the later classification but at the same time the SAs are large enough to consider the effects that result from the composition of different buildings, and are therefore more suitable than districts or boroughs.

The selection process of the Focus Areas from the SAs consists of a multi-step procedure. To take the influencing variables described above into account and to link this research closely to considerations of public health and to enable cross connection to other study results of the UrbMod project, especially to the surveyed data, the selection of the SAs is based on the same data sets used for the selection of households to be questioned in the survey, which was conducted on a project-wide basis (see SZOMBATHELY et al. 2018). The four data sets on which the selection is based, are listed and explained in the following.

(1) The L_{den}HH is taken from the strategic noise map of Hamburg, which was generated in accordance with END of the European Parliament and Council. For Hamburg, the mapping was performed according to Richtlinie 34. BImSchV and the VBUS in 2007 using the software LimA. The grid width is 10x10m and the immission height is 4m above ground level (BRÜEL & KJÆR SOUND & VIBRATION MEASUREMENT A/S; BSU, 2012; BUNDESMINISTERIUM, 2006).
(2) As the UHIs of Hamburg is most noticeable during the summer months (SCHLÜNZEN et al., 2009), the Climatologically Average Night Temperature in Summer ($CANT_s$) is taken to best represent this effect. The $CANT_s$ is based on BOETTCHER (2017). The data set was originally prepared for the analysis of "*Climate mitigation and adaptation measures for the region of Hamburg"* and is available as a 250x250m Grid (BOETTCHER, 2017).
(3) The District Types (DTs) were chosen to ensure that the chosen focus areas roughly cover the city's spatial extent, which naturally resulted in differences in building types, ages and heights. DTs divide the urban region in to eight types. Thus, the city is divided into homogeneous areas in terms of morphology and infrastructure. The LCZ according to STEWART and OKE and the UVCZ for Hamburg according to Kaveckis serve as base data. The final determination is expert-driven (KAVECKIS, 2017; SZOMBATHELY et al., 2018).
(4) Utilising the Socio-Economic Status Index (SESI) offers the possibility to answer further questions which are concerned with the socio-economic structure of the population affected by different sound exposure levels. The SESI for the SAs is based on the shares (a) of people receiving basic social security benefits; (b) unemployed adults; (c) children with a migrant background and living with single parents; and (d) people older than 64 years (equally weighted) (GEWOS, 2018; SZOMBATHELY et al., 2018). The input parameters of the socio economic status index are extracted from the social monitoring of integrated urban district development 2017 (GEWOS, 2018).

In the first step the two variables L_{den}HH and $CANT_s$ are averaged for each SA. Since the average sound exposure is of concern here rather than a temporal or spatial comparison, the arithmetic mean can be calculated. Areas for which no values are available, as well as the areas with no dwellers, are excluded.

The second step comprises a cluster analysis, where the k-Means algorithm is taken. The k-Means method is one of the most commonly used mathematical methods for grouping data and belongs to the partitioning techniques which can be applied for multidimensional approaches. It is suitable for analysing big data, as is the case in this thesis. The clusters are found by constantly repeating recalculations (iterations) until no more significant changes occur. The clusters are defined by centroids, whose components are the arithmetic means of the characteristics within the groups. The number of clusters must be selected at the start of the process. Kaiser's eigenvalue criterion can help, but it is considered imprecise and tends to select too many factors. Therefore, the ideal number of connections is checked by means of an F-test and Tukey-post-hoc (BACKHAUS, ERICHSON, PLINKE, & WEIBER, 2016; BAHRENBERG, GIESE, MEVENKAMP, & NIPPER, 2010). Thus, it is tested whether all clusters found differ significantly from one another (BACKHAUS, ERICHSON, PLINKE, & WEIBER, 2011).

In order to ensure that the final data set of the Focus Areas also show a high heterogeneity with regard to the DT, the third step is a pre-sorting. For this purpose, subgroups of all existing combination of each cluster and district type are formed. Two areas are randomly selected from each of these groups.

The SAs in which the questionnaire survey was carried out are included as well. A somewhat different focus was set when selecting the focus areas for the survey. Here, in addition to the heterogeneity of the built urban structures and the environmental stressors, the socio-economic status in particular was in the foreground. For this reason, the cluster analysis and grouping of DT type was followed by an expert selection, which was based on the *Rahmenprogramm Integrierte Stadtteilentwicklung* (RISE) of the city of Hamburg.

Since the measurements are not only intended to validate the sound propagation scenarios modelled in this thesis, but also to provide a small-scale analysis of sound exposure level, noise perception and socio-economic status, the motivation for choosing the measurement location was covering a wide range of the SESI. Six of the focus areas with a different SESI were chosen and two single measurement points are taken per focus area. Even though the socio-economic status is not the focus of this thesis, it should nevertheless be depicted approximately. Therefore, for the final focus areas the distribution of the quartiles of SESI will be compared with SESI of the initial data set.

This stratified selection process ensures that the final Focus Areas not only represent the entire heterogeneity of the city, but also that the various factors influencing sound propagation, for example, the UHIs, the building structure and the road network are represented.

4.2 Surface Parametrization

Based on the assignment to the respective levels of investigation and different categories of surface parameter characteristics presented in section 3 *Theoretical Considerations*, the parameters which contribute highly to both, the classification of the respective structures and to identify the influence of building structure on sound propagation have been identified. Now it must be determined which of these parameters can be calculated on the basis of which kind of data set and by which software.

Since, as stated in the introduction, one of the aims of this thesis is not only to enable an alternative estimation of the sound exposure of different structures, but also to show a cost-effective alternative to estimate the exposure level, an open source software should be taken for the calculation. As some calculation methods have already been implemented in SAGA-GIS for classifying LCZ, it is advisable to verify whether this software can also be taken to calculate parameters on building level, considered for the classification of BSTs.

In the State of Research, it likewise became apparent that there are parameters which are calculated on building levels as well as others which are calculated for predefined areas. These can be calculated differently on the basis of vector and grid data. Thus, a distinction is made between these two categories in this section. As can be seen in Tab. 5, the parameters which were defined in 3.2 as important to consider on the micro level, and some of the statistical and density parameter, on meso level, which are based on parameters of the single buildings, have to be calculated on vector-based data, while the density parameters need grid-based data sets.

Tab. 5: Surface parameters related to the data format

Vector-based		***Grid-based***
Height	*Proximity Index*	*Sky View Factor*
Width	*Normalized Spin Index*	*Aspect Ratio*
Area	*Normalized Perimeter Index*	*Terrain Roughness Class*
Volume	*Fractal Index*	
Perimeter	*Compactness Index*	
Height	*Ratio of Open Space*	

First, it will be seen which parameters for buildings based on vector data can be calculated with SAGA-GIS, and if they correspond to the surface parameters previously defined. The same procedure is performed for the grid-based surface parameters on the macro level.

As the State of Research found that the influence of the built-up city on the sound exposure results from the composition of buildings and rarely from a single building, the results of the vector-based data are averaged over the respective levels. For grid-based data, a grid statistic is calculated for the corresponding BBs[2].

This distinction between vector- and grid-based parameters also highlights the fact that a data set is required in vector and in grid format and as many of the parameters are calculated at the building level, it should displace the single buildings of the focus areas. The freely available data set of the Level of Detail 1 (LoD1-DE) data set provided by the City of Hamburg could be suitable. It is recommended for urban and spatial planning, architecture and real estate marketing, but likewise it is suitable as a spatial reference basis and for linking with or as background information for spatial subject-specific data for specialist information systems, for computer-aided intersection and analysis with thematic information (LGV HAMBURG, 2022), as is the case in this thesis.

The LoD1-DE model displays the buildings in simplified form. It is set up for the entire city area (≈ 750 km²) and contains approximately 360,000 buildings. The building heights were calculated by averaging all available laser data of building roof surfaces. The ground plan of the building is taken from the official digital real estate map. The buildings are displayed as "blocks" with a flat roof and are additionally blended with terrain information of the Digital Terrain Model (DTM) (LGV HAMBURG, 2022). Since for the calculation of the parameters the relative and not the absolute building height is required, the relief height

[2] SAGA Tool: Grid Statistics for Polygons

must be subtracted. To do so, the LoD1-DE dataset must first be rasterized for the attribute Height[3]. To keep the accuracy as high as possible, the size of the grid cells is set to 1x1m[s]. The relative height is obtained by calculating height difference between the rasterized LoD1-DE and the DGM of the city of Hamburg[4]. As parameters are calculated both on a shape and grid basis, the rasterized LoD1-DE must be vectorized again[5]. The Digital Surface Model (DSM) thus achieved, serves as the input data for the calculations.

Finally, the sub-question ***"1.2 Which of the parameters used in common mapping approaches, that have an influence on sound attenuation in urban areas, can be calculated by an open source software?"*** will be answered and thus based on the selected and calculated parameters, the classification can be performed.

4.3 Random Forest Classification

The classification of the BBs based on the parameters calculated as described in section 4.2 is carried out by applying the Random Forest algorithm. The rationale for using this approach is based, on the one hand, by the fact that HECHT (2014) was able to show that the Random Forest algorithm delivers a stable and accurate classification in an urban context. On the other hand, this method is also often used in the field of LCZ (ANJOS, LACERDA, DO LIVRAMENTO ANDRADE, & SALLES, 2017; HU, GHAMISI, & ZHU, 2018; YOO, HAN, IM, & BECHTEL, 2019). Furthermore, it is already implemented in SAGA-GIS based on VIGRA (CONRAD, 2020; KÖTHE, 2017)[6].

The Random Forest approach belongs to group of combined ensemble methods and is a classical decision tree model. The construction of the individual decision trees is based on random sampling of training data and a random selection of features over each constructed tree. Only one random set of characteristics is used for each constructed tree. From the data not used to construct the tree, the classification error of each individual tree can be determined, which is done with the Out of Bag Error (OOB). Considering the classification error of all trees in all OOB sets, the OOB error gives a realistic estimate of the general error level. When using the learned classifier, the classes with the most votes in all trees are assigned using the majority principle. Advantages of the Random Forest method are the high efficiency during processing, the robustness against outliers and noise, as well as the fact that no feature selection is necessary as this is done during the learning process (BREIMAN, 2001; STROBL, MALLEY, & TUTZ, 2009).

As with every supervised learning algorithm, a training data set with a known class affiliation is required, and it is important that the learning data is representative of all possible manifestations (BREIMAN, 2001; HASTIE, TIBSHIRANI, & FRIEDMAN, 2009). Thus, the classes to be identified must be known and sufficient training objects must be defined. Regarding the number of trees, authors disagree regarding the upper bound of trees: some

[3] SAGA Tool: Shapes to Grid
[4] SAGA Tool: Grid Difference
[5] SAGA Tool: Verctorising Grid Classes
[6] SAGA Tool: Random Forest Table Classification (ViGrA).

say that the OOB becomes smaller when increasing the number of trees (e.g. BREIMAN, 2001), others show that the risk of misclassification increases (e.g. HASTIE ET AL., 2009). Thus, the effect of higher trees must be considered and tested.

Most other classification approaches cannot cope with correlated input features, which is an additional advantage of the Random Forest approach. It is not only suitable for high-dimensional data, but it can also cope with complex interactions and co-variates that are highly correlated with one another (STROBL, BOULESTEIX, KNEIB, AUGUSTIN, & ZEILEIS, 2008). However, if the number of input parameters is large and the contribution of each parameter to classification small, Random Forests are likely to perform poorly due to the fact that at each split the chance can be small that the relevant variables will be selected (BREIMAN, 2001; SANDRI & ZUCCOLOTTO, 2006). This leads to the question: Which parameters can be dispensed without compromising quality, and consequently to the sub-question: ***"1.3 Which of the calculated parameters highly contribute to a Random Forest classification?***

Accordingly, there are three so-called hyperparameters that can be changes in the calculation settings that may be relevant to this thesis: the size of the training dataset, the number of trees, and the number of parameters used for classification. How these are to be determined in the present research is described in the following sub-sections.

4.3.1 Classification Settings

The selection of the training set data is typically done by experts (e.g. of WUDAP's LCZ by BECHTEL et al., 2019) or based on existing generalized maps (e.g. HECHT, 2014). In this work, the selection of training areas will be based on parameters that have a high influence on sound propagation and thus on the attenuation in urban areas. Since it has already became evident that particularly the height and the total volume of the buildings have a significant influence on sound propagation, the selection of the training areas in this work is based on these parameters. The distinction between the classes will be oriented toward the Urban Vulnerability Climate Zones (UVCZ) defined for Hamburg by KAVECKIS in 2017 (KAVECKIS & BECHTEL, 2014) in accordance with of the German energy-based planning scheme, which was established by ERHORN-KLUTTIG et al. (2011). KAVECKIS' scheme contains a total of 24 classes, of which the eleven classes shown in Fig. 21 are residential.

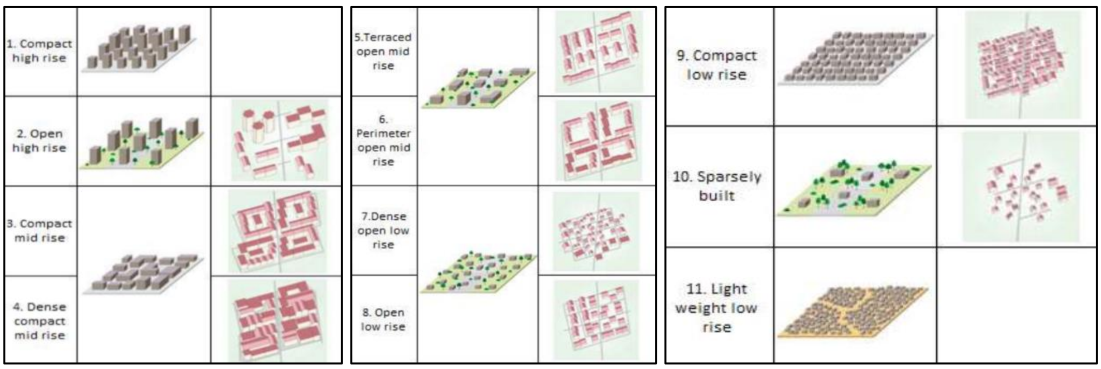

Fig. 21: UVCZ scheme with inhabited urban structure/morphology for Greater Hamburg
Source: KAVECKIS, 2017, p. 116.

As it is not possible to distinguish between residential, industrial and commercial areas within the classification-based solely on the shape of the building, only the UVCZ, which can be assumed to be inhabited are taken. Since it is likewise not possible to identify the building density of the different BBs, solely on the basis of these parameters, there will be three classes in this research. All Lowrise-categories (7 - 11) are combined to Lowrise (LR). The categories Compact Midrise (3) and Dense Compact Midrise (4) are combined to Compact Midrise (CM). The same applies to Terraced Open Midrise (5) and Perimeter Open Midrise (6) which will be in the class Midrise (MR). The average high of the two classes MR and CM is similar, but CM consist in average of more flats, and the area is thus larger. As there are only a few buildings in Hamburg that can be classified as Highrise, this class will not be considered. Thus, in this thesis, a distinction is made between three classes: Lowrise, Midrise and Compact Midrise.

The selection criteria will be based, in accordance with KAVECKIS, on the assumptions regarding the average number of floors and number of apartments in the different UVCZ, shown Tab. 6. In order to perform a corresponding attribute query in SAGA-GIS, the number of floors and number of apartments must be converted to height and approximate volume. The necessary information to transform these values can be found in the census data sheet from STATISTIKAMT NORD (2015). There, it states the average apartment size in Hamburg is 75 m² and the average floor height is three meters. As buildings smaller than 25 m² and lower than three meters are not considered as residential, but instead as garden houses, garages or side buildings, all building areas should exceed 25 m².

Tab. 6: Selection criteria for the training areas

USSZ	no. of floors	range of height [m]	no. of Flats
Compact Midrise (CM)	3 to 7	6 to 21	6 to 45
Midrise (MR)	2 to 7	6 to 21	5 to 30
Lowrise (LR)	1 to 3	3 to 9	1 to 12

For LR the area should not exceed 300 m², which corresponds to the maximum number of flats, divided by the maximum number of floors, and multiplied by an average size of 75 m². The height should be in the range of three or higher, as the maximum number of floors is three. Building height of the training areas for the category MR should equal or exceed six meters but should not be higher than 21 m (minimum and maximum height of the categories). The area of all MR buildings should be larger than the minimum number of flats multiplied by the average flat size, which corresponds for CM to ≈ 450 m² and for MR to ≈ 375 m². The final selection criteria for the categories are listed in Tab. 7.

Tab. 7: Transferred selection criteria for the training areas

USSZ		minimal height [m]	maximal height [m]	area [m²]
Compact Midrise (CM)		6	21	> 450
Open Midrise (MR)		6	21	> 375
Lowrise (LR)		3	9	25 - 300

As described above, the algorithm is based on so-called hyperparameters, which can have an influence on the result. Next to the sample size, the second hyperparameter is the number of trees, which controls how many trees are constructed. In the literature on Random Forests authors disagree regarding the upper bounds of the tree number, different tree settings are tested, in this research, after defining the training data set. The default setting in SAGA-GIS is 32 trees. To check whether a higher number of trees is necessary, they are gradually increased in steps of 32 trees. Since all classifications are based on the same data set and the identical training areas, this is tested for the vector-based classification.

The third hyperparameter which could be of concern in this thesis is the number of parameters used for the classification. As stated above, due to a high number of variables and a small contribution to classification, Random Forests are likely to perform poorly. For this reason, it is tested whether a suitable classification can be achieved with a reduced number of input parameters. Which parameters are to be eliminated after each run is based on their contribution to the classification. The contribution of each variable can be measured in two different ways, the Feature Importance (FI) and the Gini Decrease (GD) (BREIMAN, 2001; SANDRI & ZUCCOLOTTO, 2006).

FI determines the global significance of features in a trained machine learning model. The advantage of this method is that it is model-independent and can therefore use any data record, not just the training data set, to calculate feature important metrics. FI works by taking a classified data set, selecting a feature, and permuting the values for that feature across all examples, so that each example now has a random value for that feature and the original values for all other features. The evaluation metric is then calculated for this modified data record and the change in the evaluation metric from the original data record is calculated. The greater the change in the evaluation metric, the more important the characteristic is for the model (ZHANG & MA, 2012).

GD is the second general indicator of feature importance. It provides a relative ranking of the features. The optimal split within the binary trees of the Random Forest is done by measuring how well a potential split is separating the samples of the two classes in this particular node. The GD reflects the quantity of how often a particular feature was selected for a split. It therefore shows how large its overall discriminative value was for the classification (MENZE et al., 2009). STROBL et al. were able to show that FI, in particular, shows a preference for selecting correlated predictors in tree building, and that there is an additional advantage for correlated predictor variables provided by the unconditional permutation scheme used in the calculation of the variable importance measure (STROBL et al., 2008). Since it can be assumed that the parameters in this thesis are correlated, FI is not appropriate. In contrast, the GD measures how much less accurate the model would be without the variable in question, and is therefore used as a guide in this research. Parameters will be eliminated stepwise if their GD is low regarding all classes.

Even though a cross-validation is not necessary in the case of the Random Forest algorithm, it has to be verified whether a classification of sufficient quality is calculated on the basis of this training set and how the higher number of trees and the reduction of input parameters affect the classification quality. For this purpose, there are different quality measures which can be applied for the accuracy assessment in the field of automatic classification of generalized maps, as the following sub-section will discuss.

4.3.2 Accuracy Assessment

There are three main metrics that can be used to assess the quality: Overall Accuracy (OA), Producer Accuracy ($AccProd$) and User Accuracy ($AccUser$) (SMITS, DELLEPIANE, & SCHOWENGERDT, 1999; STORY & CONGALTON, 1986). Next to the OA, Cohens Kappa (κ) is often used. The OA is normally presented as a percent, with 100% accuracy being a perfect classification where all reference sites are classified correctly. Thus, it is the sum of the correctly classified buildings N_C divided by the number of all classified buildings.

[34] $$OA = \frac{N_C}{N}$$

κ is calculated from the expected random match p_e and actual match p_0 (GROUVEN, BENDER, ZIEGLER, & LANGE, 2007):

[35] $$\kappa = \frac{p_0 - p_e}{1 - p_e}$$

Thus, κ is not an actual index of accuracy, but an index of overall agreement that goes beyond chance. In contrast to OA, κ considers the imbalance in class distribution and thus intends to produce low values when the balance of classes is low (WARDHANI, ROCHAYANI, IRIANY, SULISTYONO, & LESTANTYO, 2019), which is given for the classification of the USSZ for Hamburg. Compared to LR and MR, the CM in particular is much rarer in Hamburg. Thus, OA as well as κ will be considered in this thesis. If there are differences between these two values, it must be identified which classes are matched poorly. This is where the $AccProd$ and $AccUser$ can be utilised.

$AccProd$ provides the percentage of objects of the reference data for a given class that are correctly identified by the classifier (STORY & CONGALTON, 1986). $AccUser$, in contrast, describes the accuracy from the point of view of a map user, not the map maker, and therefore gives the percentage of items classified as a particular class matched to the reference data (STORY & CONGALTON, 1986). Essentially, it identifies how often the class on the map actually occurs on site. This is referred to as reliability (SMITS ET AL., 1999; STEHMAN, 2009; STORY & CONGALTON, 1986). Since the probability of the correct assignment is of concern in this thesis, the $AccUser$ is referred to when taking a closer look at which classes are poorly matched.

In principle, the generated classification would be tested against a reference dataset which contains real world data, to prove how well the generalized map matches reality. Since, in this work, the accuracy of the classification itself is of importance, the accuracy assessment will be done with regard to, if the approaches assign different classes to the same BBs. Thus, instead, these criteria will be taken to prove the quality of the different settings. All of these indicators are implanted in SAGA-GIS[7],thus, OA and κ as well as $AccProd$ and $AccUser$ and the corresponding Confusion Matrix can be displayed.

[7] SAGA Tool: Confusion Matrix (Table Fields)

As can be seen from the Confusion Matrix shown in Tab. 8, the Confusion Matrix is created by dividing the number of correctly classified objects in each category by the SumProd (for MR = 300/306). The $AccUser$ represents the probability that an object classified into a given category actually represents that category in the refence data set, and is calculated by dividing the number of correctly classified objects in each category by the SumUser (for MR= 300/310).

Tab. 8: Confusions Matrix RF/32/1 vs. RF/32/2

	MR	CM	LR	SumUser	AccUser
MR	**300**	2	8	310	96.77
CM	1	**373**	0	374	99.72
LR	5	0	**107**	112	95.53
SumProd	306	375	115		
AccProd	98	99	93		

Regarding the sample size and the number of trees, the accuracy assessment will be performed by comparing the results of two runs with the initial settings. In this way it can be verified whether they lead to a similar result or not, or in other words, how stable the corresponding setting is. The first step is to look at OA and κ to get an idea of how similar the overall results are. The second step is then examining how many objects are assigned to the same class in both runs. Thus, in this thesis the $AccProd$ represents how often an object in a classification run x (= RF/32/1) is classified in the same way in run y (= RF/32/2). Thus, it can be identified which classes are particularly difficult to classify. The same procedure is used when comparing the quality change due to parameter reduction. Here, the focus is also on how the object assignment to the classes changes due to the reduced number of input parameters. For this reason, a run with all input parameters is taken as a reference data set in order to test how the classification differs on the basis of the reduced parameters. Here, $AccUser$ can be used to determine whether the different settings produce different results in terms of the class to which the objects are assigned.

The actual validation of the model is therefore not carried out on the basis of a reference data set, which indicates the class affiliation of the objects in real world, but on the basis of the validation of which of the classifications found is most suitable for providing information about the level of sound pollution of the corresponding classes. Therefore, in order to validate whether the classes of generalized maps found in this way reflect the level of sound exposure as a function of the urban structure, different sound propagation models are required. Their calculation and the input parameters considered are presented in the following section.

4.4 Sound Exposure Scenarios

The sound exposure is calculated by means of three different scenarios, all needed to comprehensively answer the first research question. As shown in the section 2.4 in the field of urban sound propagation often different sound propagation scenarios are used to investigate the interconnection between urban surface parameters and the exposure level. Some are based on EU directives and real-world conditions, others assume a uniform traffic flow and others work with measured data. Additionally, in some studies is was shown that the traffic volume is also related to surface structure. Thus, it is the question, whether the classification based on these parameters only represents the influence of the urban structure on the sound propagation or if the associated traffic volume is likewise represented. Three different sound propagation scenarios will therefore be calculated in order to validate the final USSZ map.

In order to determine the suitability of the finally selected scenario, that is best represented by the final generalized map for estimating the actual exposure, it is validated by measurements. The modifications of the scenarios and the procedure for the measurements, as well as the choice and the justification of the analysing methods will be explained in this section. The input data of the buildings is once more the LoD1-DE Data set for the city of Hamburg, discussed in section 4.1 *Spatial Entities*. Since the structure of the building is most important, three scenarios are calculated to see which input parameters and classification is best suited.

The first scenario is based on the Strategic Noise Map of the city of Hamburg and is used as a comparative model, which is referred to as L_{den}HH in the following. The Strategic Noise Map in grid format does not contain the data for the location of buildings, but instead has a three-meter buffer surrounding the buildings. Subsequently, these enlarged polygons were combined with the noise map, assigning the arithmetic mean of the modelled noise in L_{den} to the polygons. The L_{den} is then attached to each building by calculating the arithmetic mean of all values for each building with this three-meter buffer.

For the second and third scenarios, the facade sound level is calculated using the software CadnaA developed by the DataKustik GmbH. The software has implemented the VBUS (2006) based on the ISO, 1996 (DataKustik GmbH, 2018). Two data sets of traffic volume serve as input date. The first data set relies on counting data and was prepared and provided by the Ministry of Economics, Transport and Innovation for the generation of the Hamburg noise map following the guidelines of the END From this the truck share is taken. However, as the traffic load for individual traffic is required on a smaller scale than available for the generation of the noise maps, a modelled data set is used in addition. This data comes from a microscopic transport model that was generated in VISIUM by members of the TU-Harburg as part of the project *Auswirkungen von steigenden Energiepreisen auf die Mobilität und Landnutzung in der Metropolregion Hamburg* (Gertz & Maaß, 2015).

Since the influence of the buildings as well as the influence of the traffic volume must be considered separately, two more scenarios based on different traffic volumes are calculated. As the main aspect of this work is to investigate the influence of the building structure on the façade sound level, all other factors must be kept constant. Therefore, the heavy-load transport is not considered in the second scenario, which is referred to as L_{den} 75 in the following. The speed was set to 50 km/h for all roads and in addition, a uniform traffic volume for all roads is established at the 0.75 percentile of the traffic volume over all study areas.

For the third scenario, the Daily Average Traffic (DTV) and the average speed for the respective roads is taken. This model is referred to as L_{den} DTV in the following. In accordance with the guidelines presented in section 2.2.2 *Assessment of Environmental Noise*, vegetation attenuation was not considered. In the case of multiple lanes, outer lanes are calculated separately. To keep all other influencing factors constant, uniform roads and road surfaces are assumed for both scenarios calculated in CadnaA. The main differences between the three scenarios are listed in Tab. 9.

Tab. 9: Differences of the input parameters for the noise scenarios

Scenarios	Traffic volume	Speed
L_{den}75	75 percentiles of traffic volume over all study areas	50 km/h for all roads
L_{den}DTV	Modelled DTV	Average speed per road
L_{den}HH	Acc. VBUS	Acc. VBUS

The building evaluation in CadnaA allows the calculation of levels on the facades of buildings under noise impact caused by traffic. Receiver points are assigned to the facades of buildings with a height of 4 m in 0.05 m distances, and the calculation considers reflections of the sound path on objects of 1st order (DATAKUSTIK GMBH, 2018). An example of a building evaluation is shown in Fig. 22. On the basis of the noise maps, it can be assessed at which facade points an immission limit value is met or exceeded. For each building, the maximum levels L_{den} (left in the circle) and L_n (right in a circle) are calculated (DATAKUSTIK GMBH, 2018). The Building Evaluation values are averaged over the respective building blocks.

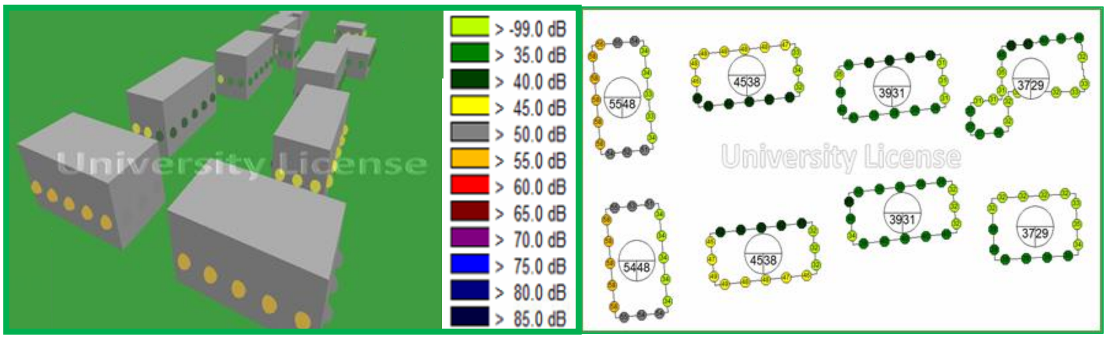

Fig. 22: Facade sound levels and building evaluation

The sound propagation scenarios generated in this way can now be used to verify whether the classes found using the Random Forest algorithm differ in terms of sound exposure and whether certain classifications are better suited to represent particular scenarios. The scenarios calculated in CadnaA enable investigations into whether the received classification only reflects the influence of the development structure, or whether the connection between the development structure and the traffic volume is also represented. For this purpose, a variance is performed. The selection of the appropriate method is described in the next section.

4.5 Variance Analysis

To address the question: ***"1.4 Do the noise levels of the sound propagation scenarios differ significantly between the classes of the obtained generalized maps?"***, the first step is to look at how strongly the L_{den} values differ between the three classes. The Standard Deviation (SD) of the L_{den} within the classes can be compared in the two ways. Either by comparing the SD with regard to the scenario or with regard to the classification approach. This way it can be deduced to what extent the L_{den} values vary within the classes on the building block level. This offers a first impression of how well each classification represents the sound exposure of the respective scenario. Since values of the same entity (L_{den} in dB(A)) are compared here, the standard deviation can be applied.

Subsequently, a variance analysis is performed. As the independent variable is the sound exposure level and the dependent the USSZ, the dependent variable is nominally scaled, a single factor variance analysis is inapplicable. In addition, it is not known whether the sound exposure expressed in L_{den} is normally distributed. Therefore, the variance analysis is tested by means of the Kruskal Wallis Test.

The Kruskal Wallis test is a nonparametric approach designed to analyse two or more independent groups. For this reason, it is also called rank variance analysis (RASCH, FRIESE, & HOFMANN, 2021). The assigned ranks should be evenly distributed across all groups under the null hypothesis. The H-value can be used to test whether the observed distribution of ranks differs systematically from the random one. The empirical H-value must be greater than or equal to the critical value. This test is suitable for independent samples. Since it is a comparison of central tendencies by means of ranking, in which the data do not have to be normally distributed, it can be applied without further analysis of the data. In addition, outliers are due to the ranking not overestimated, as it is sometimes the case with rational scaled date, where the mean is calculated (KRUSKAL & WALLIS, 1952; RASCH ET AL., 2021).

A problem is, however, that a Type I error might occur, which means that a false positive conclusion is drawn. This happens because with the Kruskal Wallis test it is only checked whether the groups differ, but not for which of the groups this applies. Therefore, a post-hoc test, a so-called pairwise comparison, must be performed. This is done with a Dunn post-hoc test. The test is carried out on each pair of groups. As a multiple test is being carried out, an adjustment to the p-value is done by applying the Bonferroni adjustment. This is to multiply each Dunn's p-value by the total number of tests being carried out (DINNO, 2015). The variance analysis can be taken to test whether classes differ significantly with respect to sound exposure, but not how large this effect is (DINNO, 2015; RASCH ET AL., 2021). Therefore, the effect size must then be calculated for the approaches that show significant differences.

Based on the effect size, a statement can be made not only about how strong the differences are overall, but also between which of the classes the difference is strongest. In each case, the effect is calculated between two of the classes. The effect sizes are calculated as follows:

[36] $$Effect\ sizes = \frac{Std.Test\ Statistic}{\sqrt{n}}$$

The coefficient assumes the value from 0 (indicating no relationship) to 1 (indicating a perfect relationship) (COHEN, 2008).

Thus, the sub-question: ***"1.5 Which classifying approach is most appropriate to reflected which sound propagation scenario?*** will be answered and based on the sound propagation scenario and the classification for which the effect size is highest, the second research question is now able to be investigated. The exact procedure is explained in the remainder of this chapter.

4.6 Health related Variables

In order to address the second research question ***"2. What conclusions about adverse health effects can be drawn from the final generalized map?",*** it must be examined to what extent the classes represented by the final classification of the USSZ allow conclusions to be drawn about the actual sound exposure. For this purpose, measurements are carried out and the health variables derived from the final L_{den} scenario that is represented best by the USSZ are compared with survey results. Even if the DAYLs for other illnesses are higher, the overall health burden is high for annoyance, as shown in Fig. 3. Since some recent studies show that annoyance may be a precursor to other diseases, its importance for health should not be underestimated. In addition, self-assessed annoyance is easier to assess than specific diseases that need to be recorded by physicians. Thus, the research focuses in this thesis will be on the percentage of being highly annoyed ($\%HA$) and the self-reported noise annoyance ($TRNA$) as an adverse health effect. The setting of the measurement as well as the selection and calculation of the modelled and surveyed variables used for this purpose are explained in this section.

4.6.1 Measuring Noise Exposure

To obtain the highest possible accuracy, class 1 sound level meters from Cirrus (type CR:161B) were used, which comply with the standards and guidelines of Norm IEC 61672-1:2013. In order to get both an average value for the entire building and a facade level on the road-side, one sound level meter was placed on the roadside and another one to the off-road-side of the house. In accordance with the guidelines ISO, 2017, the sound level meters were located at a distance of 1.5 m from the facade of the building and the microphones were adjusted at a height of 1.55 m. As the data will also be used to see if the measurements correlate better with perceived disturbance from noise than the models, all noise measurements were carried out between 4 p.m. and 7 p.m. on a Tuesday afternoon. Therefore, only noise levels during the day will be accessible. This time period was chosen to include the heavy traffic volumes during rush hour. Moreover, it can be assumed that a relevant proportion of the residents are already at home at this time and thus are affected by the noise observed. As meteorological conditions influence sound propagation, the meteorological variables of temperature, wind and precipitation were controlled, by taking measurements only on days with similar weather conditions, to assure as comparable conditions as possible. Due to bad weather conditions during the measurement period, only six measurements could be carried out.

In order to make statements about the sound pressure level within a certain observational period T and to be able to compare sound pressure levels from different sources, there are various statistical parameters which can be calculated from the measured values. The averaging process is analogous to the energetic sound pressure level addition, whereby $\sum_i 10^{0.1L_i}$ must be divided by the total number of time periods (or sources) before they are scaled logarithmically (WILLEMS, DINTER, & SCHILD, 2006):

[37] $$L_{eq} = 10lg(\frac{1}{T}\int_0^T 10^{0.1L(t)dt})$$

$$for\ given:$$

$$T = \sum_{i=1}^{n} T_i$$

If each time period T_i has the same length, the determination of the equivalent continuous sound level is simplified to an L_m (Willems et al., 2006):

[38] $$L_m = 10lg\left[\frac{1}{n}\sum_i^n 10^{0.1L_i}\right]$$

Since the measured values are not facade levels and the measured height also differs from the calculation height of the initial scenarios, a separate scenario must be calculated here. A precise calculation is carried out for the coordinates of the measuring stations at the height of 1.5 m. In addition, the initial scenarios include the L_{den} value, but the measurements only take place during the day and last for only three hours. In order to obtain a more suitable reference value, the L_d is calculated here and the reflection level was increased for this calculation as well.

To get an impression of whether the data suggest a correlation, a bivariate correlation is first performed. Since both variables are metric data, the Pearson correlation can be calculated. If the scenario is suitable for representing the real-world data, then the question: ***"2.1 Does the final sound propagation scenario allow statements about the effective sound exposure?"*** can be answered positively, and a modelled health variable can be derived from the final propagation scenario in the next step. This procedure is described in the next section.

4.6.2 Modelled Noise Annoyance

The relative risk of being highly annoyed presented in section 2.2.1 is used here as the modelled variable. The percentage of Highly Annoyed ($\%HA$) is calculated as shown earlier in accordance with END as follows:

[39] $$\%HA = {(78{,}9270 - 3{,}1162 \cdot L_{den} + 0{,}0342 \cdot {L_{den}}^2)}/{100}$$

The question is now, whether the USSZs only differ in terms of sound exposure level, or if this is true for the risk of being highly annoyed too. As can be seen from the *State of*

Research section 2.2.1, a dose-response relationship can only be calculated from L_{den} values > 42 dba. For this reason, it has to be examined whether this significant difference can also be detected for the variable $\%HA$, and how large the effect size is in that case. In order to address the sub-question ***"2.2 Does the $\%HA$ of the final scenario in accordance to the END differ significantly between the classes of the final generalized map?"*** the Kruskal Wallis test has to be performed and the resulting effect size is calculated. However, in order to keep the risk of ecological fallacy as low as possible, this is not done at building block level, but at building level. The focus areas include a total of 24,232 buildings. If the variance analysis is carried out on the basis of the individual buildings, the sample would be extremely large. A consequence is that almost arbitrarily small mean differences become significant. This is due to the fact that the sample size is considered the standard error in the denominator of the calculation. Therefore: the larger the sample, the smaller in the standard error. The standard error in turn is included in the calculation of the test statistics in the denominator as well. Smaller standard errors therefore result in larger empirical t-values, which is why even tiny "effects" achieve significance (LIN, LUCAS, & SHMUELI, 2013). In order to avoid the sample being too large and the small differences appearing to be significant, the Kruskal Wallis test is done on a random sample of 285 buildings per class. If the final scenario approximates the measured values and if the $\%HA$ for the final classes differ significantly with at least a medium effect size, the potential health risk can be inferred from the generated map.

Finally, it will be examined whether the $\%HA$ based on the EU directive resulting from the finally selected scenario which is best reflected by the final classification correspond to the surveyed self-reported Noise annoyance. The procedure for the survey and the technique for comparing the calculated and requested exposure is explained below.

4.6.3 Surveyed Noise Annoyance

The UrbMod project conducted a household survey to collect primary data on noise perception at a high spatial resolution in urban blocks and thus accounts for small-scale differences in exposure. In 24 of the focus areas (divided in to 63 subareas in total), data was collected in written form and the pre-tested questionnaires were hand-delivered into residential mailboxes. Each surveyed location contains 150 to 400 households (6,620 in total). One adult per household was asked to respond and return the survey. For the questionnaire, different assessment instruments related to health are evaluated. It comprises 51 questions in total, but with only eight questions on noise annoyance. In this research the question*: "To what extent do you feel annoyed in your apartment/house by road traffic noise?"* is looked at. It will be referred as *Traffic Related Noise Annoyance* ($TRNA$) in the following. The answer scale is a four-level Likert scale, consisting of: *very much, quite, somewhat* and *not at all* (Szombathely et al., 2018)[8].

[8] Some of the questions regarding self-reported annoyance are analysed and published by Szombathely et al. (2018). The complete questionnaire (in German) can be obtained from the authors

Based on the comparison of $\%HA$ and $TRNA$ it will be clarified whether the curve of the $\%HA$, based on the L_{den}DTV scenario calculated in accordance with the END, adequately reflects the actual annoyance for Hamburg's population. For this purpose, the proportion of those who are highly exposed to the total number of respondents is compared with the result of the relative risk of being highly exposed $\%HA$. In order to make the two values comparable, the absolute number of people that answered the question about $TRNA$ with very much must likewise be converted into a percentage. The conventional level classes in 5dB(A) steps are appropriate here. From this comparison it can be deduced whether the $\%HA$ based on the calculated scenario and the END reflects the data collected - i.e. whether conclusions can be drawn from this classification about the level of the actual affected persons. Thus, the question **"2.3 *Does the relative number of self-reported* $\%\boldsymbol{TRNA}$ *correspond to the* $\%\boldsymbol{HA}$ *calculated in accordance to the END?"*** can be addressed. And based on the results of the data and analyses described above, the second research question: ***"2*. *What conclusions about adverse health effects can be drawn from the final generalized map?"*** finally is to be answered.

5 RESULTS AND DISCUSSIONS

The presentation and discussions of the results is orientated on the workflow presented in section 4 *Materials and Methods*. Thus, the two main parts are again preceded by the section 5.1 *Spatial Entities* which is split in two sub-sections. The results of the selection process including the k-means cluster analysis to define the finale Focus Areas out of the SAs is presented in 5.1.1 *Focus Areas*. As the different resolutions of the surveyed and calculated data on different levels of investigation and the associated possibilities of aggregation lead to limitations, these limitations are discussed in the following in the sub-section 5.1.2 *Level of Investigation and Spatial Aggregation*.

The sections 5.2 to 5.5 are dedicated to the findings with regarding the first main research questions: ***"1. Does a generalized map based on surface parameters reflect the noise sensitivity of urban areas?"***. The work flow that has been flowed is shown in Fig. 23 below.

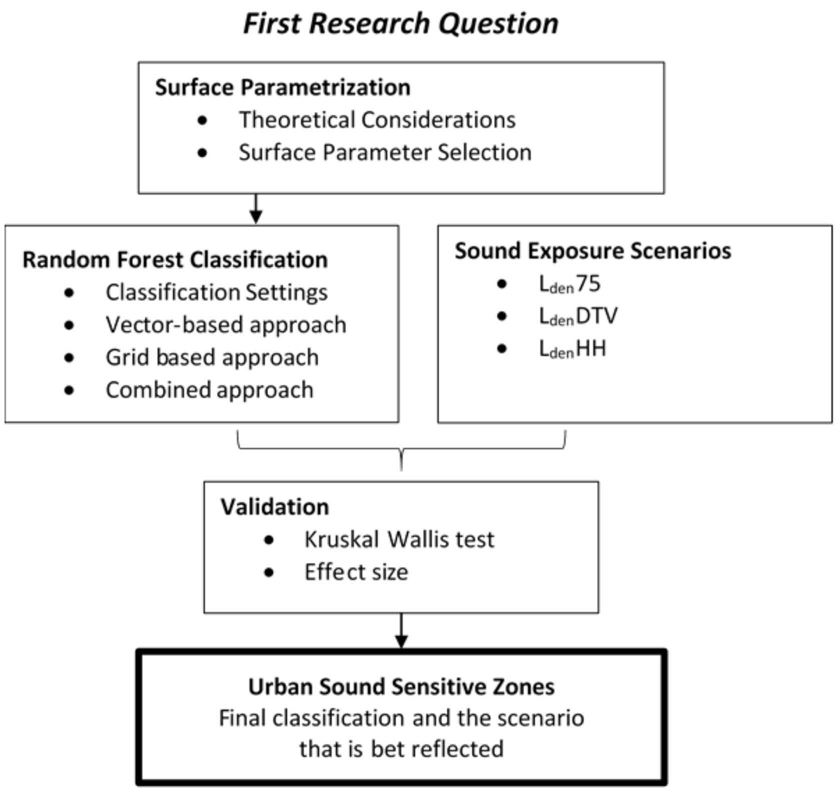

Fig. 23: Workflow first research question

As the first sub-question was already answered in the Chapter 3 *Theoretical Considerations*, in section 5.2 *Surface Parametrisation* the finale parameter set for the three classification approaches will be presented in this section first. Next the results of the classification of the USSZ based on the three different approaches are proposed and discussed in the section 5.3 *Random Forest Classification*. This section is divided into sub-sections; the selection of the training sample and the classification settings are described first in 5.3.1. The quality of the settings is discussed on the basis of the criteria κ, OV and $AccUser$

introduced in section 4.3.2. The same applies to the three different classification approaches, which are based on three different initial set of surface parameters, of which the results are discussed separately in the sub-sections 5.3.2-5.3.4. Subsequently, the three sound propagation scenarios needed to validate the generalised structure maps obtained are presented and briefly discussed in section 5.4 *Sound Exposure Scenarios*, bevor, based on the previously calculations, the results of the analysis of variance by means of a Kruskal Wallis test regarding the significant differences of exposure level is proposed in the subsection 5.5 *Variance Analysis of the Sound sensitive Zones*. Based on the associated effect size, between the three classes LR, MR and CM the first research question could be answered in this section.

Onwards from section 5.6 Health related Variables the second main research question: ***"2. What conclusions about adverse health effects can be drawn from the final generalized map?"*** is addressed. Based on the previously calculation, the results of the analysis of variance by means of a Kruskal Wallis test regarding the significant differences of exposure level expressed as $\%HA$, between the three classes LR, MR and CM are proposed and thus the first sub-question is to be answered. The work flow that has been flowed is shown in Fig. 24 below.

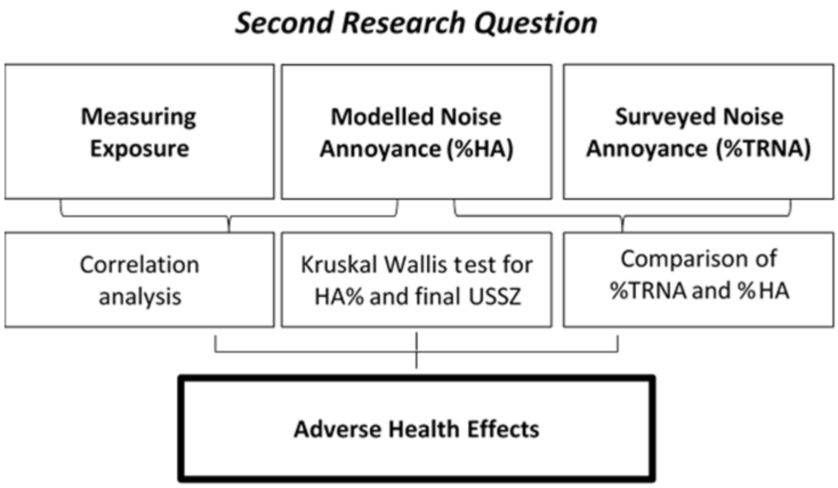

Fig. 24: Workflow second research question

First it was tested whether the measured exposure can be assumed by the final sound propagation scenario, that was represented best by the final USSZ map, by a means of a correlation analysis in sub-section 5.6.1 *Measuring Exposure*. Next it was analysed if the modelled $\%HA$ likewise the L_{den}, differs significantly between the USSZ classes of the finally chosen generalised map in sub-section 5.6.2 *Modelled Noise Annoyance*. This was done again by the means of a Kruskal Wallis test. It was then investigated, if the modelled $\%HA$ represents the surveyed $TRNA$. in sub-section 5.6.3 Surveyed Noise Annoyance. Bringing this finding together, the second question could be answered in the last sub-section: 5.7 *Adverse Health Effects.*

5.1 Spatial Entities

The results of the Focus Area selection process is proposed in section 5.1.1. Since the data were collected at different resolutions, they need to be aggregated or disaggregated for some analysis steps. The limitations to be considered for the different data types and levels are discussed in section 5.1.2 *Level of Investigation and Spatial Aggregation*.

5.1.1 Focus Areas

Since the SAs for which no values are available, as well as the areas with no dwellers were excluded, 601 SAS were included in the selection process. Regarding the number of clusters, the F-test for the z-transformed L_{den}HH, which is the most important variable for this study, was highest for six cluster. But the Tukey-post-hoc proofed that in the case of six clusters, there is no significant differences between cluster 1 and 5. If five clusters are taken instead, the test showed a significant difference at $p < 0{,}000$ between almost all groups, only for cluster 1 and 5 is still only significance at level of $p < 0{,}053$, what is in an acceptable range. As can be seen in Fig. 25 (top), for these two variables the optimal number of clusters is therefore five.

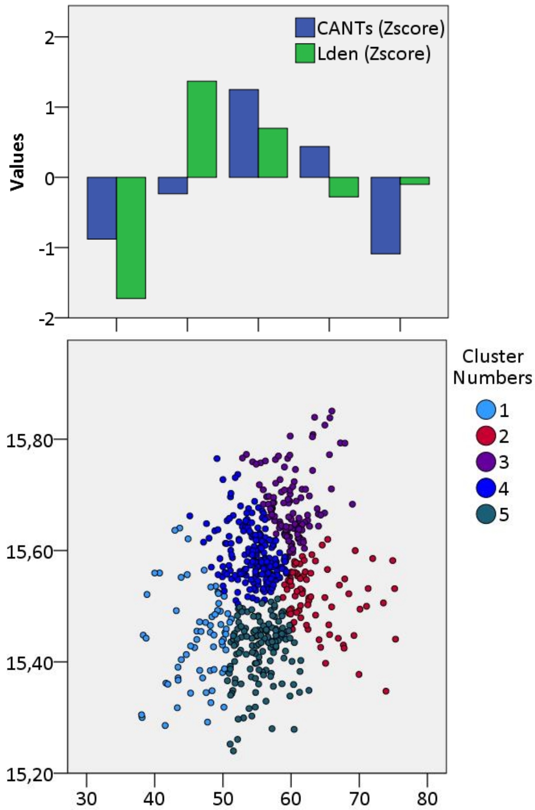

Fig. 25: Final cluster of the combination of L_{den} an CANTs

The final cluster affiliation is shown Fig. 25 (bottom). In the first cluster, areas with a low $CANT_s$ and a very low L_{den}HH are combined. Cluster two comprises areas with an almost average $CANT_s$ and a very high L_{den}HH. Cluster three identifies areas with a very high $CANT_s$ and medium high L_{den}HH. The areas with a medium high $CANT_s$ and medium low L_{den}HH are found in cluster four. The fifth cluster, combines very low $CANT_s$, with an average L_{den}HH.

The following pre-sorting of all existing combination of the clusters found and the DT showed that not every combination of cluster and DT occur, hence 47 focus areas where finally chosen. Together with the SAs in which the survey will be conducted, there are thus 80 SAs that have been defined as Focus Areas, which are evenly distributed across the city, as can be seen in Fig. 26.

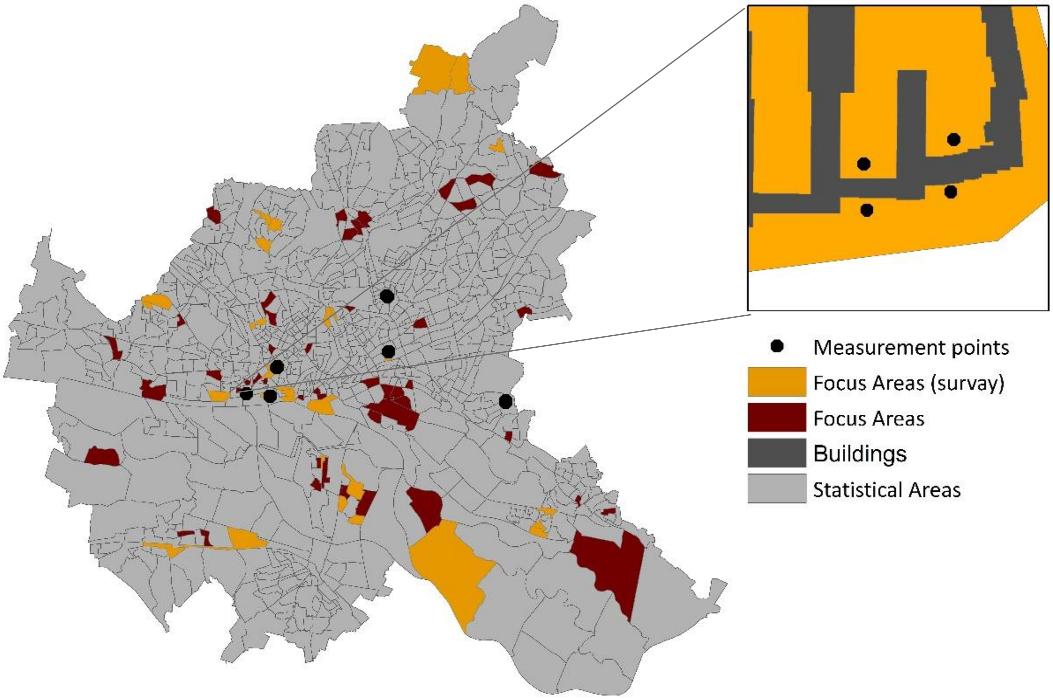

Fig. 26: Focus Areas

Regarding the SESI, areas with a high Socio-Economic Status Index are slightly over-represented, but the median is almost equal. As the SESI is only of minor importance in this study, this is within an acceptable range.

Although the focus areas were selected on the basis of the SAS, it is neither meaningful, nor possible to collect or calculate all variables at the same resolution and thus the calculations, measurements and surveys where carried out at different resolutions within in this focus areas, the following subsection addresses possible aggregation levels of the datasets to be collected.

5.1.2 Level of Investigation and Spatial Aggregation

As has become clear, especially in the field of building classification, surface parameters are usually calculated at the building level. In the case of sound propagation research and for the identification of LCZs, the analysis is usually based on statistical and/or density parameters for larger areas that are as homogeneous as possible. This results in the circumstance that the surface parameters in the case of vector data will be calculated on building level and for the entire set of SAs in the case of grid data. In addition, there are density parameters that result, for example, from the ratio of built-up area to open space. A reference level is therefore needed for which these different parameters can be averaged or calculated.

As shown in section 4.1 *Spatial Entities*, these are the BBs. In the case of surface parameters calculated at the building level, on vector basis, the arithmetic mean can be calculated for all buildings within a BB. But the grid-based surface parameters are calculated at the level of the entire SAs and thus a grid statistic is calculated for the corresponding BBs.

The results of the sound propagation scenarios are facade levels of individual buildings. In order to be able to investigate whether the classes found, differ significantly in terms of sound exposure, either the identified classes have to be assigned to the individual buildings, or the facade sound levels of the buildings have to be averaged across the BBs. The L_{den} values must therefore be aggregated. A logarithmic mean for the values of the L_{den} point data is not necessary, since this is part of the analysis was about the average exposure on the BBs and not a comparison over time or space.

This is different when the final scenario is validated by the means of sound measurements. The measurements took place around a respective building and the height is 1,5 m. Therefore, as described in section 4.6.1 the sound propagation scenario for the validation of the measurement are exact point calculations at the same place and height as the measurement devices were placed. The measurements are taking place over a time period of three hours. But few noises are constant over time, the sound pressure level rather change continually. To be able to make statements about the sound pressure level within a certain observation period T and to compare sound pressure levels from different sources, there are statistical parameters which can be calculated from the measured values. Since the levels in decibels are not measured in a linear scale, they cannot simply be added. The sound pressure levels must rather be summed up energetically according to the following equation (Willems et al., 2006):

[40] $$L_p = 10lg \sum_i 10^{0.1L_i}$$

$$for\ given:$$
$$L_i = Single\ Sound\ Pressure\ Level$$

The averaging process is analogous to the energetic sound pressure level addition, whereby $\sum_i 10^{0.1L_i}$ must be divided by the total number of time periods (or sources) before they are scaled logarithmically (Willems et al., 2006):

[41] $$L_{eq} = 10lg(\frac{1}{T}\int_0^T 10^{0.1L_i}dt)$$

$$for\ given:$$
$$T = \sum_{i=1}^{n} T_i$$

Even though the survey is complete within the focus areas, it never covers all buildings within a BB or even a whole SA, but only a few buildings within the BBs have been surveyed. Due to data protection guidelines, a certain degree of anonymity must be guaranteed, especially for health-related questions. An exact allocation to individual buildings, or even flats, is therefore not possible. But transferring the results to higher levels of aggregation, is problematic. The spatial aggregation of socioeconomic variables in particular can lead to so-called ecological fallacy (PEARCE, 2000). The ecological fallacy is a recurring phenomenon, especially in the social and environmental sciences. This results in a false assumption about an individual based on aggregated data for a group (BAHRENBERG et al., 2010). Therefore, socio economic survey data in particular should not be aggregated to a greater extent than is absolutely necessary. Hence, whenever the survey results are included in the analysis, all other variables must be aggregated or assigned to the designated survey areas. In order to avoid this effect or to keep it as low as possible, the health variables are additionally calculated at building level. As can be seen in Fig. 27, the data are thus calculated and collected at up to four different levels of resolution.

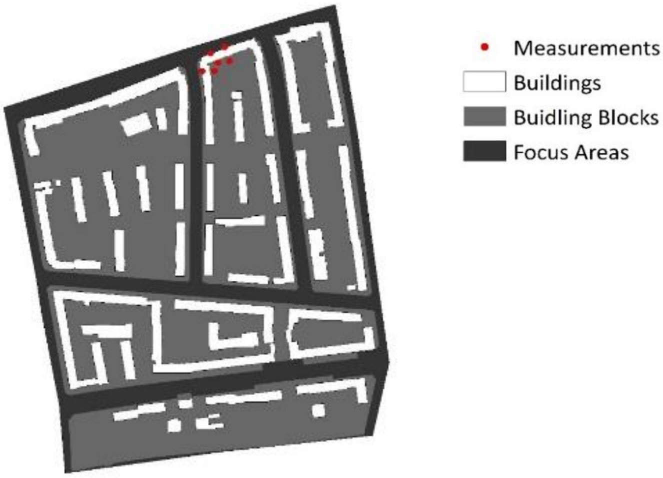

Fig. 27: Aggregation level

Once it has been clarified on which resolution the respective data was generated and what had to be considered for the respective aggregation, the selection of the parameters to be calculated for the classification follows.

5.2 Surface Parameter Selection

After having identified the most important parameters that are used for the classification of BSTs and UHIs and which at the same time are considered in sound propagation research in section 3 *Theoretical Considerations*, the second sub-question: ***"1.2 Which of the surface parameters used in common mapping approaches, that have an influence on sound propagation in urban areas, can be calculated by an open source software?"*** could be investigated. As the surface parameters at the building level where calculated on the basis of vector data sets and those at the macro level on grid-based data sets, a distinction is made in the following between those two categories. The surface parameters where derived from the LoD1-DE datasets that is freely available (see section 4.1).

5.2.1 Vector-based Parameters

SAGA-GIS has implemented various tools to calculate the properties of polygons. Especially with the tool Polygon Shape Indices several geometrical features can be obtained on building level. The calculations are based on Lang and Blaschke (2007), FORMAN and GODRON (1986) and MERKUS (2009). The first set of parameters belongs to the group of geometrical parameters. It contains Area (A) and Perimeter (P). Furthermore, different ratios of this parameters can be calculated. In this analysis, $\frac{P}{A}$ and $\frac{P}{\sqrt{A}}$ where calculated. The surface parameters that consider the height must be present either as the measured height or the number of floors of the buildings. In this thesis, these are prepared accordingly to the description in section 4.1 *Spatial Entities*.

In addition to this simple geometric surface parameters, this tool offers the possibility to calculates various parameters using the so-called auxiliary objects. The first set in this category belongs to the circle approximations, which will shortly be interduce in the following. The Equivalent Projected Circle Diameter $(Deqpc)$ is the diameter of a circle that has the same area as the occupied area of the building which corresponds to the compactness index. The $Sphericity$ is calculated as the ratio of the perimeter of the equivalent circle to the real perimeter whereas the $Shape\,Index$ is the inverse of the $Sphericity$. The Diameter of Gyration $(Dgyros)$ is calculated as twice the maximum vertex distance to its polygon part's centroid. This radius can be determined by rotating the corresponding building around its geometrical canter of gravity. The Maximum Diameter $(Dmax)$ is the Maximum Distance between two polygon part's vertices. It corresponds therefore to the largest circumscribing circle. Additionally the ratios $\frac{Dmax}{A}$ as well as $\frac{Dmax}{A^2}$ where considered (LANG & BLASCHKE, 2007; MERKUS, 2009; SAGA-GIS TOOL LIBRARY).

The next set of parameters that can be calculated with this tool comprises the so-called feret parameters, originated in the field of particle research. The Feret Diameter is not a diameter in the actual sense, but rather a group of parameters, all of which are defined by the distance between two tangents to the polygons contour in a specified measuring direction (Merkus, 2009). In the case of the Maximum Feret Diameter $(Fmax)$ it is determined internally for a sufficient number of angles and the largest value is selected. For irregular buildings, the feret diameter varies more than for spherical. the $Fmax$ is therefore always greater than the diameter of the circle with the same projection area (Deqpc) (Merkus, 2009; Sympatec GmbH, 2020). The Minimum Feret Diameter $(Fmin)$ and the Mean Feret Diameter $(Fmean)$ are calculated the same way, but the smallest diameter or respectively the average value are selected. The $Fmax90$ is measured at an angle of 90 degrees of the $Fmax$ direction and $Fmin90$ at an angle of 90 degrees to the $Fmin$ direction (Merkus, 2009; SAGA-GIS Tool Library; Sympatec GmbH, 2020). As in the case of buildings, the ratios of feret diameters $\frac{Fmin}{Fmin90}$ and $\frac{Fmax}{Fmax90}$ can be used to describe the length to width ratio; and thus, they will be considered in the later analyses as well. Feret Volume $(Fvol)$ is the diameter of a sphere having the same volume as the cylinder constructed by $Fmin$ and

$Fmax$ and belongs therefor to the group of smallest enclosing rectangle (Merkus, 2009; SAGA-GIS Tool Library; Sympatec GmbH, 2020).

The first set of surface parameters, that where calculated are the identical parameters that are used in the approaches of building classification. The set includes the similar parameters, because likewise the ones introduced in the chapter 3 *Theoretical Considerations*, the calculations are either based on P and A or include axillary objects in the calculation. Thus, the geometric as well as the structural parameters are covered, almost.

Only an equivalent to $Fract$ or CI is missing. Thus the $Fract$ will be calculated on micro level by applying the Field calculator[9] by the flowing formula:

[42] $Fract = (2 * ln([P]))/(sqrt(pi()))/(ln([A]))$.

To take at least one density parameter calculated on vector -basis in to account, the ROS is on the meso level was chosen. This calculation was done by summing up the A of all buildings within the respective BB. Subsequently, as can be seen in the formula below, the ratio to the total A of the BB was formed.

[43] $ROS = ([A\_BB] - [SUM\_A\_B)]/[\ A\_BB] * 100$

Thus, both the simple geometric and the structural parameters as well as at least one density parameter can be calculated in SAGA. The Tab. 10 shows all surface parameters that where considered on a vector basis in this work.

Tab. 10: Finale vector-based surface parameters

Area (A)	*Shape Index*	*FminDir*
Perimeter (P)	*Dmax*	*Fmean*
P/A	*DmaxDir*	*Fmax90*
P/sqrt(A)	*Dmax/A*	*Fmin90*
Height	*Dmax/A²*	*Fmax/ Fmax90*
Volume	*Fmax*	*Fmin/ Fmin90*
Dgyros	*FmaxDir*	*Ratio of Open Space*
Deqpc	*Fmin*	*Fractal Index*

5.2.2 Grid-based Parameters

One of the reasons why the program SAGA-GIS is chosen is, as mentioned earlier, that some tool for the calculation of the parameters on a grid basis for the classification of LCZs are already implemented. For example, parameters like Visible Sky (VS), Sky View Factor (SVF) and related parameters like Terrain View Factor (TVF) was well as Average View Distance (AVD). These parameters are calculated in SAGA according to BÖHNER and ANTONIĆ (2009), HÄNTZSCHEL, GOLDBERG, and BERNHOFER (2005) and (OKE)[10] and are mainly based on the simplified calculation of the SVF presented in section 3.2. In addition, the Topographic Openness, which expresses the dominance (positive = PO) or enclosure (negative = NO) of a

[9] SAGA Tool: Polygon Shape Indices (no. Directions = 18)
[10] SAGA Tool: Sky View Factor

landscape or location, will be considered. Openness is related to how wide a landscape can be viewed from any position (SAGA-GIS Tool Library)[11]. The calculation is based on YOKOYAMA, SHLRASAWA, and PIKE (2002). With these parameters the density on the macro level can be covered.

To consider also the roughness, the tool Vector Ruggedness Measure (RUG) [12], which is likewise implemented in SAGA-GIS can be taken. The Ruggedness concept was developed by RILEY et al. (1999) to express the amount of elevation difference between adjacent cells of a DEM. It calculates the difference in elevation values from a center cell and the eight cells immediately surrounding it. Then it squares each of the eight elevation difference values to make them all positive, sums them, and takes the square root. In SAGA-GIS it is calculated according SAPPINTON, LONGSHORE, and THOMPSON (2007).

All of these parameters determine the unobstructed hemisphere given as percentage and/or the view distance and implicitly involve both geometric and density features of the areas. Thus, both height and building density determine on all of these parameters. The third parameter category, presented in section 3.2, refers to the soil property. Since this cannot be derived directly from the shape of the building or from the arrangement of the buildings, it will not be considered in this work. The Tab. 11 summarizes the surface parameters that where calculated.

Tab. 11: Finale grid-based surface parameters

Sky View Factor	*Vector Ruggedness*
Visible Sky	*Topographic Openness*
Terrain View Factor	*Positive Openness*
Average View Distance	*Negative Openness*

In this section and chapter 3 *Theoretical Considerations* the first two sub-question ***"1.1 Which surface parameters used in common mapping approaches have an influence on sound propagation in urban areas?"*** and ***"1.2 Which of the surface parameters used in common mapping approaches, that have an influence on sound propagation in urban areas, can be calculated by an open source software?"*** where addressed. It could be shown, that there are different parameters that are calculated based on different data formats at different levels of investigation. While the classification of BSTs is based on micro-level surface parameters, the LCZs are predominantly based on macro-level surface parameters. In the field of sound propagation research, there are mainly statistical and density parameters on the meso level, whose calculation, however, is based on the surface parameters of the other two research fields. It was then shown that there are Vector-based and Grid-based approaches to classify structures in urban space, which are likewise investigated in the field of research on interaction between building structure and noise exposure that can be calculated with the help of the open source software SAGA-GIS based

[11] SAGA Tool: Topographic Openness
[12] SAGA Tool: Vector Ruggedness Measure (VRM)

on the freely available Lod-DE1 data set of the city of Hamburg. The next step, that was performed, was the classification based on the selected and calculated surface parameters.

5.3 Random Forest Classification

Based on the results of the first two sub-questions three different classification approaches will be tested in this section to answer the third sub-question: ***"1.3 Which of the calculated surface parameters highly contribute to a random forest classification?"***. One approach was based on a vector-based, one on a grid-based and the third on a combined surface parameter set. As the finale classification was performed for all approaches with the identical data set of BBs, the selection of the training areas, the test of the ideal sample size as well as the test of number of trees, where conducted for the Vector-based approach, but will likewise be applied for the calculations based on the grid-based and the combined surface parameter set.

5.3.1 Classification Settings

As shown in section Random Forest Classification, supervised learning techniques require training data sets with a known class affiliation. Based on the selection criteria for the training area, defined in 4.3.1 *Classification Settings*, the BBs, that have met on average the selection criteria where selected by attributes. From this selection the training data set was randomly chosen for each of the classes. As can be seen in Tab. 12, a total of 255 of the 796 building blocks where thus defined as training areas. This corresponds to 32 % of all BBs. Within these 255 BBs are 26 % of the buildings of the entire focus areas located.

Tab. 12: Sample size of the training areas

	Building Blocks	Buildings
CM	35	200
MR	74	550
LR	148	5500
Total no.	796	16,000
Percentages	≈ 32 %	≈ 26 %

The comparison of two runs with the setting 32 trees and 21 input parameters shows that a good result could already be achieved. A κ of 0.967 and an OA of 0.980 (Tab. 13) is sufficient and thus, no further increase of the sample size was necessary. Next, the ideal number of trees for the Random Forest classification was tested by increasing number of trees stepwise. Two runs with the identical number of trees, where afterwards compared vs. each other. As can be seen in Tab. 13, this resulted in $\kappa > 0.956$ and $OA > 0.964$ for all runs.

Tab. 13: Overall Accuracy for classifications based on a different number of trees

	32 Trees	64 Trees	96 Trees	108 Trees
κ	0.967	0.956	0.977	0.988
OA	0.980	0.974	0.986	0.992

But κ was always slightly lower than OA, what indicates that there are classes that are slightly harder to classify then others. This was confirmed by $AccUser$. Even though, runs with 32 trees achieve good results, the comparison by means of the $AccUser$ showed, as can be seen in Tab. 14, that due to the higher number of trees the distinction between CM and MR was clearly improved. Especially regarding the class CM $AccUser$ rises from 0.955 for 32 trees to 0.981 for 108 trees.

Tab. 14: User Accuracy for runs with rising no. of trees

USSZ	32 Trees	64 Trees	96 Trees	108 Trees
LR	0.997	0.983	0.995	0.997
MR	0.967	0.960	0.987	0.990
CM	**0.955**	0.980	0.954	**0.981**

Since the best results where therefore achieved by runs with 108 trees, all subsequent classifications where performed with this number of trees. Based on these classification settings, it could now be analysed if the number of input parameters can be reduced for the vector- and Grid-based approach without having a too high loss of accuracy.

5.3.2 Vector-based Approach

The input parameters for the classification where reduced stepwise and the reduction of the parameters to the minimum number necessary to obtain a classification of high accuracy was done by means of the GD. The parameters that have contributed the least to the classification in the previous run where eliminated. The eliminated parameters of each run are listed in Tab. 15.

Tab. 15: Reduction by Gini Decrease - vector-based parameters

Reduction 1		Reduction 2		Reduction 3	
Parameters	**Gini Decrease**	**Parameters**	**Gini Decrease**	**Parameters**	**Gini Decrease**
FminDir	0.903	Fmean	4.072	Fmax	9.426451
Fmin	0.833	P/A	3.210	DmaxDir	5.506504
Dmax/A	0.823	DmaxDir	3.179	Fvol	5.262794
Fmax90	0.821	Fmin90	2.345		
FRAC	0.670	FmaxDir	1.734		
P/sqrt(A)	0.529	Fmax/Fmax90	1.375		
Shape Index	0.317	Fmin/Fmin90	1.355		
Perimeter	0.286				
Sphericity	0.264				

First, all parameters whose GD is < 1 where omitted. This was followed by a reduction by all parameters whose GD < 5. The third reduction eliminated all parameters whose GD < 10. To proof how stable and accurate these classifications are, two runs of each input parameter setting are again tested versus each other. As can be seen in Tab. 16, κ as well as OA are almost not affected regarding the internal accuracy of the reduced parameter sets. On the contrary, both indicators increase (apparat from reduction 2) with decreasing input parameters. This had to be expected, since there are fewer combination possibilities and thus also a low error probability occurs.

Tab. 16: Internal Overall Accuracy of vector-based parameters reductions

	Reduction 1	Reduction 2	Reduction 3	Reduction 4
κ	0.983	0.9753	0.982	0.990
OA	0.990	0.9849	0.989	0.994

Yet, the question is whether a different classification is found with fewer input parameters than on the basis of all parameters. As can be seen in Tab. 17, this is the case. For all reductions decreases both, κ as well as OA. What also becomes apparent is that κ degrades more (from 0.977 down to 0.873). This indicates that certain classes are classified differently as the number of parameters decreases.

Tab. 17: Overall Accuracy - vector-based parameter reductions vs. initial parameter set

	Reduction 1	Reduction 2	Reduction 3	Reduction 4
κ	0.977	0.962	0.926	0.873
OA	0.986	0.977	0.954	0.923

This is confirmed by a look at the $AccUser$. As can be seen Tab. 18, for all reductions the $AccUser$ decreases for all three classes. This effect is highest for the class CM. It decreases from 0.953 to 0.805. For the MR class the decrease is slightly lower (from 0.994 down to 0.958). For the LR class the classifications are seminary and $AccUser$ stays high until the reduction 4. As thus any further reduction than reduction 3 leads to a lower $AccUser$ regarding all classes, no further reduction will be considered in the following.

Tab. 18: User Accuracy - vector-based parameter reductions vs. initial parameter set

	Reduction 1	Reduction 2	Reduction 3	Reduction 4
LR	0.989	0.999	0.984	0.929
MR	0.994	0.952	0.924	0.958
CM	0.953	0.972	0.944	0.805

Consequently, in the case of the Vector-based approach, a reduction of the parameters from 24 to 6 parameters is possible without causing large differences in quality. But the different reduction runs lead to different results. Since the focus here is on the statement as to whether these classifications are associated with significant differences in sound exposure, these four classifications will be tested later on regarding the different sound exposure level.

5.3.3 Grid-based Approach

For the grid-beast approach fewer input parameters are in the initially parameter set, thus the contribution to the classification measured by GD was higher for all parameters and therefore, as can be seen in Tab. 19, only two reduction where be possible.

Tab. 19: Reduction by Gini Decrease - grid-based parameters

Reduction 1		Reduction 2	
Parameters	**Gini Decrease**	**Parameters**	**Gini Decrease**
VS	5.800	SVF	15.173
SVFS	6.190	AVD	17.105
		PO	18.192

For the grid-based surface parameters the first classification showed weaker results than regarding the Vector-based approach. The comparison of two runs with the initial set of parameters achieved a lower κ, and a lower OA; but the $OA > 0.95$ can still be considered sufficiently good. Likewise, for the Vector-based approach, the accuracy of the individual classifications increases, as can be seen in Tab. 20, when reducing the input parameters. But the difference between κ and OA is somewhat higher. This suggests that greater differences occur here when assigning the BBs to one class for the Grid-based approach.

Tab. 20: Internal Overall Accuracy of grid-based parameter reductions

	All	Reduction 1	Reduction 2
κ	0.916	0.925	0.966
OA	0.952	0.957	0.981

This is confirmed by the comparison of the reduction runs with the initial classification. It leads to a classification that differs even more from original classification than in the case of the vector-based data. κ and OA for the second reduction are only 0.775 and 0.877 as can be seen in the table below.

Tab. 21: Overall Accuracy - grid-based parameter reductions vs. initial parameter set

	Reduction 1	Reduction 2
κ	0.915	0.775
OA	0.952	0.874

But likewise, to the parameter reduction in the Vector-based approach, the discrimination between MR and CM deteriorates as the number of input parameters decreases. As can be seen in Tab. 22 this case; $AccUser$ falls to 0.597. This could be due to the fact that, as can be seen from the in Tab. 19, in the first run already all parameters contribute with a $GD > 5$ to the classification, and are those necessary to distinguish between the classes.

Tab. 22: User Accuracy - grid-based parameter reductions vs. initial parameter set

	All	Reduction 1	Reduction 2
LR	0.944	0.964	0.929
MR	0.965	0.950	0.872
CM	0.954	0.900	0.597

As any further reduction than the first one leads to a lower $AccUser$ especially between MR and CM no further reduction undertaken. Consequently, in the case of grid-based surface parameters, only a reduction of the parameters from 8 to 6 parameters is possible without causing large differences in quality. But likewise, for the Vector-based approach the different reduction runs lead to different results. Thus, the first two classification will be tested separately regarding the difference in sound exposure.

5.3.4 Combined Approach

For the third approach, surface parameters that highly contribute to the vector- and the grid-based classifications were taken but additionally it was considered which of those parameters show a high correlation, with L_{den} as well as which parameters, were identified as important regarding the sound propagation. In addition, it was ensured that parameters types are included. The finale set is shown in Tab. 23.

Tab. 23: Parameter set for the Combined classification

Geometrical	A	H	P	Vol
Structural	Dgyros	Dmax	Fvol	
Density	ROS	TVF	SVF	

As a look at the contribution of the individual parameters to the classification and the correlation with the L_{den}, (Tab. 24) showed, most vector-based parameters seem to be clearly more efficient and the correlation is higher too. Nevertheless, not all parameters that contribute highly to the classification correlate highly with L_{den}. But especially $Depqc$, ROS and $Dgyros$ seem to be closely related to both aspects. Regarding the gird-based parameters only TVF and SVF showed considerably correlations; but the GD is relatively low.

Tab. 24: Gini Decrease & Correlation - combined parameter set

Parameter	Gini Decrease	Correlation	Parameter	Gini Decrease	Correlation
Depqc	35.067	0.29	TFV	5.508	0.18
A	29.272	0.17	SVF	4.053	-0.17
ROS	27.226	0.22	H	3.537	0.33
Dgyros	25.077	0.25	VOL	2.926	0.23
Fvol	9.593	0.29	P	2.898	0.19

The results of this classification will be considered by a comparison with the previous two approaches. In this way, the differences can be highlighted. Thus, the results of the Combined classification approach are therefore compared in the following with the classification resulting from reduction run 3 of the Vector-based and reduction run 1 of the es Grid-based approaches.

As can be seen in Tab. 25, almost identical values for κ and OA can be obtained by the combined and the vector-based parameter set, thus for this two approaches the results are slightly more stable than in the case of the grid-based classifications.

Tab. 25: Internal Overall Accuracy - all approaches

	Vector	Grid	Combined
κ	0.988	0.916	0.989
OA	0.992	0.952	0.993

The allocation to the classes seems to be easier to be identified as well. This was confirmed by the comparison of the $AccUser$ of the initial runs of all three approaches. As can be seen in Tab. 26. the values for the Combined approach are higher than in the case of the Vector- and Gird-based approaches.

Tab. 26: User Accuracy - initial parameter set - all approaches

	Vector	Grid	Combined
LR	0.987	0.944	0.988
MR	0.981	0.965	0.997
CM	0.930	0.954	0.991

As can be seen the strongest differences seem to be particularly founded in the different classification of the CM classes. For the Combined approach $AccUser$ > 0.988 for all three classes whereas $AccUser$ is only 0.930 for CM for the Vector-based approach and 0.944 for LR for the Grid-based approach.

This obviously difficult classification of the class CM is also reflected by the three classification approaches based on the initial parameter sets, illustrated in Fig. 28 by selected displayed BBs. As can be seen, it seems to be particularly difficult to classify BBs that consist of CM buildings and have a high proportion of open space.

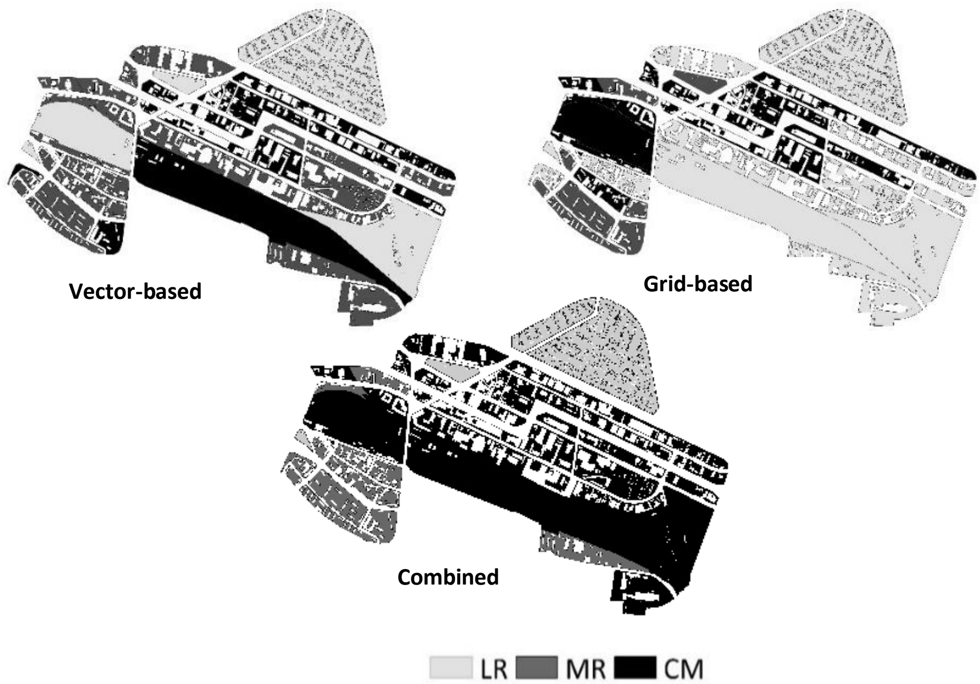

Fig. 28: Example of final classifications of USSZ

This is confirmed by means of the $AccUser$. As can be seen in Tab. 27, regarding the vector-based classification against the Grid-based, CM is only classified the same way to a little over 50 percent ($AccUser$ = 0.532). The highest values are obtained by the comparison of the Vector-based and the Combined approach. Thus, the Combined classifications are somewhat closer to the Vector-based approach than to the Grid-based approach.

Tab. 27: Users Accuracy - classifications vs. each other

	Vector vs Grid	Vector vs Combined	Gird vs Combined
LR	0.905	0.930	0.719
MR	0.665	0.920	0.813
CM	0.532	0.798	0.775

This could be due to the fact that the MR and CM classes differ mainly in regarding density and compactness of the individual buildings. These two aspects are particular well represented by the parameters SVF and TVF. Thus, it could be, that although the overall contribution to classification is relatively small, it is these two parameters that improve the discrimination between CM and MR.

The question ***"1.3 Which of the calculated surface parameters highly contribute to a random forest classification?"*** can therefore be answered in that way, that on the basis of each of the three approaches a stable classification is possible, even when the input parameters are reduced, but that in particular the larger buildings surrounded by open space are not classified the same way. Since in this thesis not the classification of the buildings itself, but the interconnection between the classes and the height of the sound exposure level is in the foreground, sound propagation scenarios had been prepared for further validation. The results of the calculated sound propagation scenarios and first results of the analysis are presented in the next section.

5.4 Sound Exposure Scenarios

In order to be able to examine the next two sub-questions***: "1.4 Do the noise levels of the sound propagation scenarios differ significantly between the classes of the obtained generalized maps?"*** and: ***"1.5 Which classifying approach is most appropriate to represent which sound propagation scenario?"*** three different sound propagation scenarios have been calculated, to proof if the final USSZ only reflect the building structure related influences, or likewise other influencing variables, such as the traffic flow depending on the respective zone. The results of the sound propagation scenarios L_{den}75 and L_{den}DTV calculated in CadnaA are available at the building level. For the L_{den}HH scenario, values were assigned to buildings as described in 4.4 *Sound Exposure Scenarios*.

As can be seen from the descriptive statistics displayed in Tab. 28, the lowest values regarding the SD were obtained by the L_{den}75 and the highest by the L_{den}DTV scenario. The mean of the L_{den}75 is considerably lower than for the L_{den}DTV. The differences of the two scenarios calculated in CadnaA can be predominantly attributed to the different input parameters. In particular, the circumstance that the L_{den}75 has significantly lower sound levels is possible due to the fact that a uniform traffic load with an average speed over the entire urban area of 50 Km/h was calculated.

Tab. 28: Descriptive statistics for the sound propagation scenarios

Scenarios	N	Range	Minimum	Maximum	Mean	SD
L_{den}75	22812	62.10	1.90	64.00	38.36	9.10
L_{den}DTV	22739	84.90	1.00	84.90	46.43	10.45
L_{den}HH	18092	41.00	36.00	77.00	51.21	7.05

Even though the heights value is created by the L_{den}DTV scenario. The values of the L_{den}HH are in general higher. This is particularly evident in the mean value, which is highest at 51.21 dB(A), although only values ≥36 dB(A) and 77dB(A) ≤, are available for this scenario. This higher mean of the L_{den}HH could lead to the assumption that both CadnaA scenarios underestimate the exposure compared to this scenario. But it must be considered that in the case of the L_{den}HH scenarios not only all parameters according to the regulations are considered but that in addition, the initial data set of the L_{den} scenario is a 10*10 m point grid data set in the immediate surroundings (3 m) of the buildings and not facade levels, as it is the case for L_{den}75 and L_{den}DTV. Consequently, the sound levels of the L_{den}HH scenario are closer to the source. Since sound levels decrease with distance, this is a possible reason for the higher values of this scenario.

Due to the reason discuss above, a direct comparability of the values is not advisable. For this purpose, it was not the values themselves that are compared, but the SD of the building evaluations within the respective BBs.

As visibly for the selectively displayed BBs in Fig. 29, the L_{den} values for the individual building differ in terms of variance, within the BBs, regarding all three scenarios.

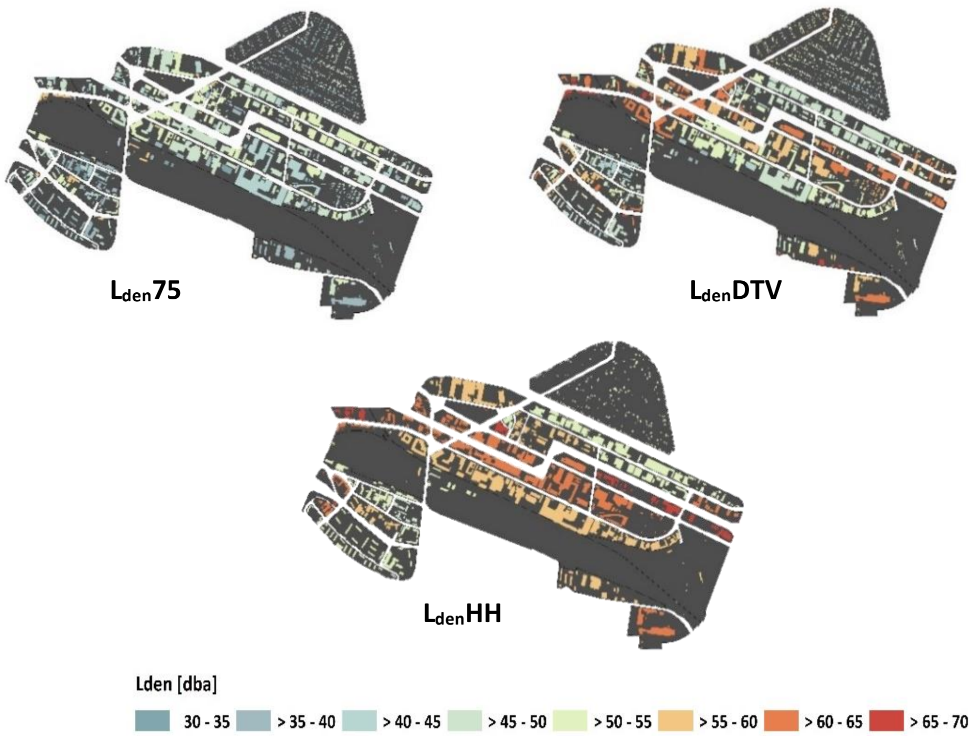

Fig. 29: Sound exposure on building level

This is likewise reflected by the SDs displayed for selected BBs (see Fig. 30). The span of SD is lowest for L_{den}HH (SD = 0.00-10.59) and highest for L_{den}HH (SD = 0.14-18,38).

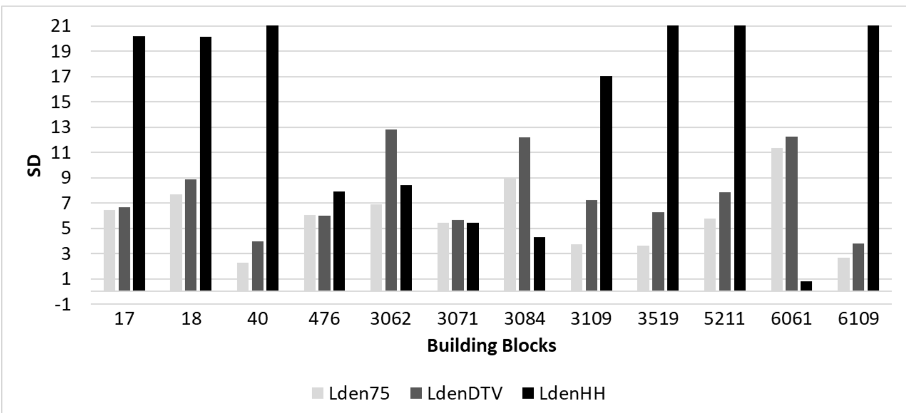

Fig. 30: Standard deviation of L_{den} within the exemplary building blocks

In some BBs there are buildings with similar (e.g. BBs 3071, regarding all three scenarios) and in some with high differences of L_{den} (e.g. BBs =18, regarding all three scenarios, but highest for the L_{den}HH). The highest deviation on building level are recorded for the L_{den}HH Scenario. This can also be attributed to the reasons mentioned above.

But since the classification where carried out at the building block level and the main question in this section is whether classification shows significant difference regarding the exposure level, the L_{den} values of the single buildings where aggregated for the respective BB. As can be seen in the Fig. 31, the different levels of exposure, depending on the scenarios are on that level visually even more evident.

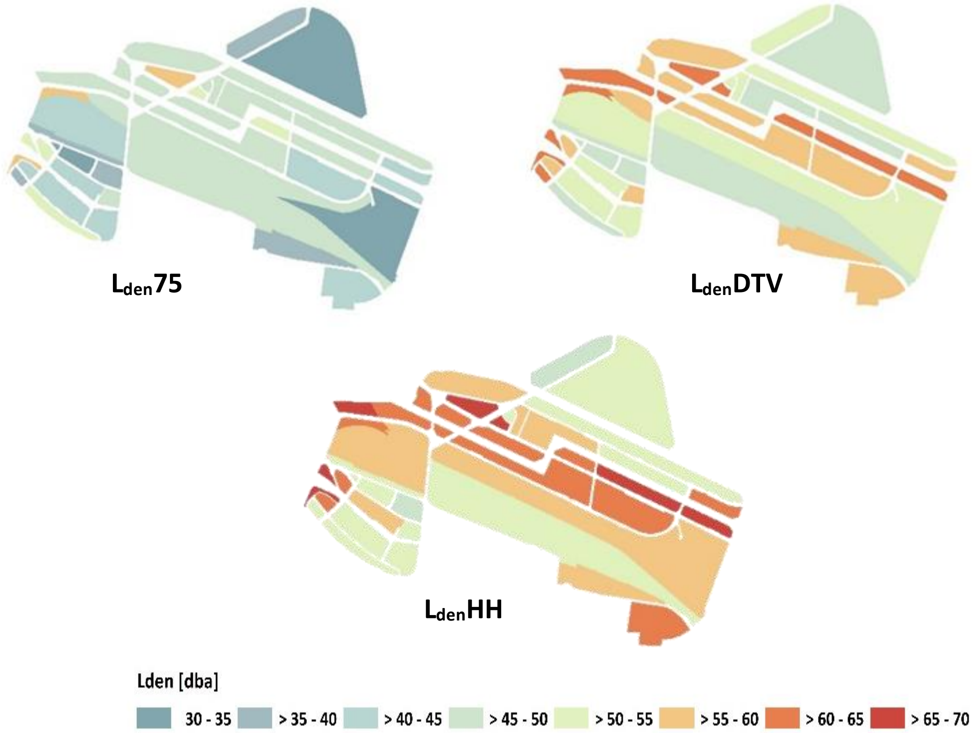

Fig. 31: Sound exposure on building block level

Having calculated both, the classifications and the scenarios, it was possible to investigate the sub-question: ***"1.4 Do the noise levels of the sound propagation scenario differ significantly between the classes of the obtained generalized maps?"*** The first step was a basic analysis of the SD of the sound exposure level regarding the classification. This was done exemplary for each approach on basis of the classification with the initial parameter set, followed by a variance analysis by the means of a Kruskal Wallis test for all combinations of classifications and scenarios in question.

5.5 Variance Analysis of the Urban Sound Sensitive Zones

By comparing the SD with regard to the scenario or with regard to the classification approach. As shown in Fig. 32, and as expected from the first visual comparison, in the section above, the SD within all classes is constantly lower for the L_{den}75 scenario (SD = 6.63 - 7.71) for all three approaches, compared to the other two scenarios.

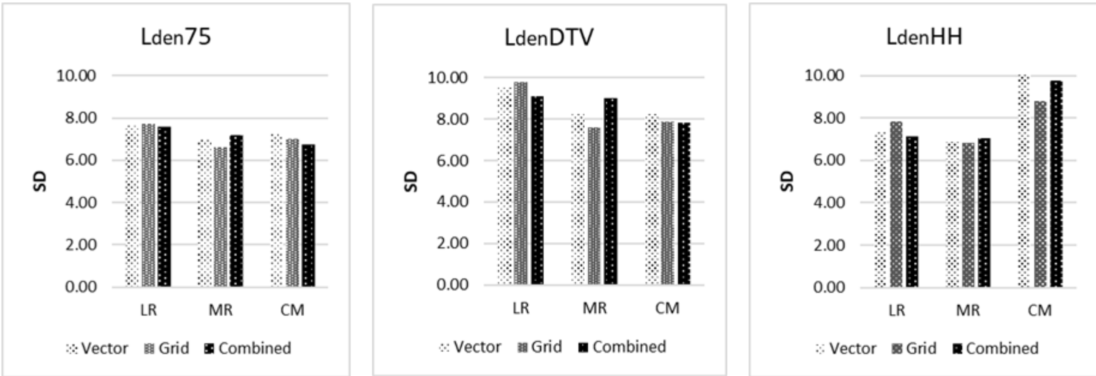

Fig. 32. Comparison of SD between the approaches

For the L_{den}DTV scenario SD ranges between 7.58 and 9.76 and is particularly high for the class LR for all approaches and regarding MR for the Combined approach. Whereas in turn the SD for MR is slightly lower for this scenario regarding the Grid-based approach (SD = 7.58). In the case of class CM, the SD is similar for all approaches.

For the L_{den}HH scenario, especially the deviations within the class CM are high, for all approaches, but highest for the Vector-based (SD = 10.09). In turned the SD is relatively low for MR and medium for LR, it looks like the high variance of the values which was already reflected on building level seems to be concentrated on building block level, for the BBs which are classified as CM.

If the deviation of the L_{den} values within the classes is not compared within the scenarios, but within the approaches, then it becomes apparent, that the Vector-based approach goes along with low SD for the L_{den}75 scenario for all three classes, but in turn the SD is higher regarding the L_{den}DTV scenario. Regarding the L_{den}HH scenario, the values in the classes LR and MR are more unevenly distributed, especially there is a high SD for the CM class.

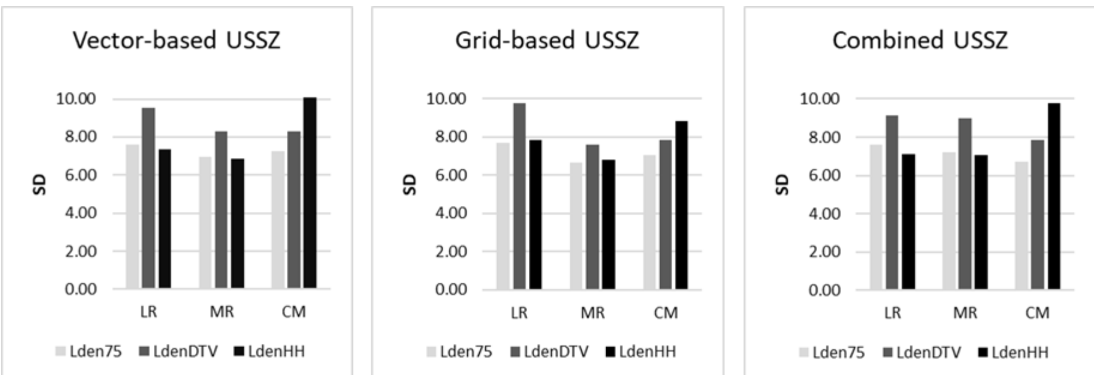

Fig. 33: Comparison of SD between the scenarios

The Grid-based approach seems to lead to smaller deviations, especially in the case of MR and CM, with the exception of the L_{den}DTV scenario and the class LR, where the SD is suggestively higher than for the other classes and scenarios. Just for this class and this scenario the Combined approach leads to slightly lower deviation(SD = 7.12). Overall, the deviations here are similar to those in the Vecortor-based approach, only slightly lower.

Despite the high SD of the L_{den}HH scenario in the CM class, a look at the averaged values for all BBs shows that the L_{den}HH scenario has the smallest differences between over all means of classes for all approaches. For the L_{den}DTV scenario, however, these are highest across all approaches.

Tab. 29: Mean of L_{den} for the classes of the USSZ

	Vector-based			Grid-based			Combined		
	L_{den}75	L_{den}DTV	L_{den}HH	L_{den}75	L_{den}DTV	L_{den}HH	L_{den}75	L_{den}DTV	L_{den}HH
LR	39.38	47.37	50.66	39.59	47.77	51.35	39.23	47.11	50.45
MR	42.10	51.22	52.91	42.61	51.95	52.04	41.93	51.08	52.80
CM	44.00	54.44	52.84	44.36	54.70	53.88	44.35	54.87	53.29

This suggests that the L_{den}HH scenario, due to the consideration of all influencing variables, does not allow conclusions to be drawn about the relationship between the structure of the building and the sound exposure. In the opposite, all classification seems to represent the different exposure levels of the L_{den}DTV best, which not only reflects the influence of the urban structure, but also considered the traffic volume.

But to finally answer this question: "***1.4 Do the noise levels of the sound propagation scenarios differ significantly between the classes of the obtained generalized maps?"*** a Kruskal Wallis test was performed for all classification of three approaches and the three different sound propagation scenarios. The hypothesis, which was examined, is therefore for all classifications and each sound scenario as following:

Hypothesis:
"*The mean values of the sound exposure of the different USSZ differ significantly"*
Null hypothesis:
"The mean values of the sound exposure of the different USSZ do not differ significantly"

First, the results for the Vector and Grid-based approach are presented and discussed, before the presentation and discussion of the Combined approach follows based on the resulting of the first two approaches.

The result of the Kruskal Wallis test for both approaches showed, that for none of the runs with the initial parameter sets the Null Hypotheses can be rejected. Both classification approaches seem to lead to a significant difference between all classes for all three sound exposure scenarios. But as already expected, the differences between the mean values of the L_{den}HH scenario showed slightly lower significance for both approaches (Vector-based: Sig. = 0.001, Grid-based: Sig. = 0.032). Nevertheless, as described in section 4.5 Variance Analysis, the Kruskal Wallis test only provides an answer to the question of whether the classes generally differ with regard to the mean, but not between which and whether there is a significant difference between all classes. A pairwise comparison was performed to eliminate a type I error.

The results of the pairwise comparison showed that this error occurs for both approaches regarding the L_{den}HH scenario for the runs based on the initial parameter set. Regarding the Vector-based approach for this scenario there is no significant difference between the classes CM and MR at all, as can be seen in Tab. 30.

Tab. 30: Pairwise Comparisons of USSZ - L_{den}HH - Vector- and Grid-based approach

Vector-based					
Sample 1-2	**Test Statistic**	**Std. Error**	**Std. Test Statistic**	**Sig.**	**Adj. Sig.[a]**
LR-MR	42.486	24.490	1.735	0.083	0.248
LR-CM	-62.770	17.335	-3.621	0.000	0.001
MR-CM	-20.284	24.885	-0.815	**0.415**	**1.000**
Grid-based					
Sample 1-2	**Test Statistic**	**Std. Error**	**Std. Test Statistic**	**Sig.**	**Adj. Sig.[a]**
LR-MR	-13.207	17.556	-0.752	**0.452**	**1.000**
LR-CM	68.830	26.208	2.626	0.009	0.026
MR-CM	55.623	27.598	2.015	**0.044**	**0.132**
Each row tests the null hypothesis that the Sample 1 and Sample 2 distributions are the same. Asymptotic significances (2-sided tests) are displayed. The significance level is ,05.					

In the case of the Grid-based approach, this is true likewise for the LR and MR. Thus, for both classifications and the L_{den}HH scenario the null hypothesis cannot be rejected any longer.

Regarding the L_{den}75 scenario the pairwise comparison for the classification based on the initial parameter sets, showed, that both approaches achieve significant results for the difference between the classes LR and MR as well as for the classes LR and CM. But the significance between MR and CM is somewhat weaker, especially for the Vector-based approach (Vector-based: Adj.Sig. = 0.048; Grid-based: Adj.Sig. = 0.014).

Tab. 31: Pairwise Comparisons of USSZ - L_{den}75 - Vector- and Grid-based approach

Vector-based					
Sample 1-2	**Test Statistic**	**Std. Error**	**Std. Test Statistic**	**Sig.**	**Adj. Sig.[a]**
LR-MR	-84.720	17.343	-4.885	0.000	0.000
LR-CM	145.930	24.899	5.861	0.000	0.000
MR-CM	61.210	25.389	2.411	0.016	**0.048**
Grid-based					
Sample 1-2	**Test Statistic**	**Std. Error**	**Std. Test Statistic**	**Sig.**	**Adj. Sig.[a]**
LR-MR	-81.009	17.671	-4.584	0.000	0.000
LR-CM	160.223	26.543	6.036	0.000	0.000
MR-CM	79.214	28.052	2.824	0.005	**0.014**
Each row tests the null hypothesis that the Sample 1 and Sample 2 distributions are the same. Asymptotic significances (2-sided tests) are displayed. The significance level is ,05.					

For the L_{den}DTV scenario, slightly better results are achieved. The pairwise comparison, with the exception of the Vector-based approach for LR and CM (Adj.Sig. = 0.008), showed highly significant differences between all classes. Even if the results of the various random samples differ slightly, a trend can be identified, that the L_{den}DTV is reflected best. This suggest that the relationship between traffic intensity and permitted speed is mapped too. But the question is, if this stays that way, in the case of the reduction of the input parameter.

The parameter reduction in the case of the Vector-based approach did not affect the overall significance regarding all three scenarios. The same applies for the Grid-based approach regarding the $L_{den}75$ and $L_{den}DTV$ scenarios, but in contrast for the $L_{den}HH$ scenario, the Sig. rises slightly. Due to the input parameter reduction Grid-based approach went up to 0.057. The pairwise comparison for the $L_{den}HH$ scenario thus shows no significance difference between the classes even for all reduced classifications. Thus, the hypothesis regarding the $L_{den}HH$ scenario cannot be rejected for any classification.

Regarding the $L_{den}75$ scenarios significant differences can be demonstrated for LR-MR and LR-CM on the basis of the reduced sample for both approaches. But the difference between MR and CR, while still significant (e.g. reduction 3: Adj.Sig. = 0.044), are on a lower level across all the classifications. Therefore, the difficulties in distinguishing between MR and CR that arose during the classification process, seem to be reflected in the differences of sound exposure level as well. The same applies for the Grid-based approach, but on a weaker level (reduction 1: Adj.Sig. = 0.052).

For the $L_{den}DTV$ scenario, however, slightly better results are achieved. But likewise, to the $L_{den}75$ scenario, the pairwise comparison showed a weaker result for the distinction between MR and CM (reduction 1 Adj.Sig. = 0.006). This is true although for the Grid-based approach (reduction 1 Adj.Sig. = 0.004). The reduction runs showed, however, that especially with respect to CM and MR the classification quality is slightly reduced. The question is therefore, can a result be achieved with less than 21 parameters by means of the Combined approach, which corresponds to the two initial runs of the Vector and the Grid-based approach?

In the case of the Combined approach, the result of the Kruskal Wallis test initially suggests likewise that there are significant differences between the classes at a significance level of 0.00. But likewise, as for the other two approaches, the pairwise comparison shows, as can be seen in Tab. 32 something different. Again, the null hypothesis must be accepted for the $L_{den}HH$ model. The best result is obtained for the $L_{den}DTV$ scenario. In addition, however, the $L_{den}75$ scenario is reproduced almost as well.

Overall, the Combined approach achieves the best results. Regarding the $L_{den}75$ scenario differences can be demonstrated for LR-MR and LR-CM on the basis of the reduced sample for all approaches regarding all three scenarios. But the difference between MR and CR, while still significant, are on a lower level across all the classifications. Therefore, the difficulties in distinguishing between MR and CR that arose during the classification process, seem to be reflected in the differences of sound exposure level as well. Since all classifications as well as the two scenarios, $L_{den}75$ and $L_{den}DTV$ in contrast to $L_{den}HH$, consider predominantly urban structural parameters, it can be assumed, that classifications seem to allow statements to be made about the exposure caused by the urban structure.

Tab. 32: Pairwise Comparisons of USSZ – Combined approach

$L_{den}75$					
Sample 1-2	**Test Statistic**	**Std. Error**	**Std. Test Statistic**	**Sig.**	**Adj. Sig.[a]**
LR-MR	-80.030	17.488	-4.576	0.000	0.000
LR-CM	154.163	23.872	6.458	0.000	0.000
MR-CM	74.133	24.047	3.083	0.002	0.006
L_{den}DTV					
Sample 1-2	**Test Statistic**	**Std. Error**	**Std. Test Statistic**	**Sig.**	**Adj. Sig.[a]**
LR-MR	-102.109	17.488	-5.839	0.000	0.000
LR-CM	197.497	23.872	8.273	0.000	0.000
MR-CM	95.389	24.047	3.967	0.000	0.000
L_{den}HH					
Sample 1-2	**Test Statistic**	**Std. Error**	**Std. Test Statistic**	**Sig.**	**Adj. Sig.[a]**
LR-MR	-60.899	17.515	-3.477	0.001	0.002
LR-CM	79.214	23.459	3.377	0.001	0.002
MR-CM	18.316	23.590	0.776	0.438	1.000
Each row tests the null hypothesis that the Sample 1 and Sample 2 distributions are the same. Asymptotic significances (2-sided tests) are displayed. The significance level is ,05.					

That the results for the L_{den}DTV which are slightly better suggests that the relationship between traffic intensity and permitted speed, is mapped too.

Even if the results of the various random samples differ slightly, a trend can be identified. The answer to the question: ***"1.4 Do the average noise levels of the propagation scenarios differ significantly between the classes of the generalized maps?*"** is positive for all three approaches for the two scenarios. However, this does not answer the question of how strong differences between the classes actually are. In order to be able to answer the question: ***"1.5 Which classifying approach is most appropriate to represent which propagation scenario?"*** the effect size was calculated. The results and thus the final USSZ are presented in the following.

The highest effect size for the classification of each approach are presented in Tab. 33. All of them are in the middle range for three class. If comparing the two classifications based on Vector or Grid-based approaches. The effect size for the L_{den}DTV scenario is above that for the $L_{den}75$ scenario. Thus, it becomes clear that both approaches are better suited to draw conclusions about the sound exposure, which can be attributed to building development and the associated traffic volume.

Tab. 33: Effect Size L_{den}

USSZ	**Vector-based Classification**		**Gird-based Classification**		**Combined Classification**	
	$L_{den}75$/R-2	**L_{den}DTV/ R-1**	**$L_{den}75$**	**L_{den}DTV**	**$L_{den}75$**	**L_{den}DTV**
LR-MR	0.181	0.234	0.174	0.190	0.177	**0.225**
LR-CM	0.269	0.337	0.275	0.336	0.297	**0.381**
MR-CM	0.121	0.150	0.137	0.186	0.146	**0.187**

Overall, however, the Combined classification has the strongest effect for regarding scenarios. Only the LR classes seem to be slightly better delineated on the basis of the Vector-based approach.

The fact that the L_{den}DTV scenario is better represented by the classifications confirms the findings presented in the State of Research that the traffic volume also varies depending on the type of area. This is consistent with the statements made by, for example Häußermann and Siebel, that density cannot be used as an explanation, neither for the spatial distribution of stressors nor for the spatial distribution of social groups. But when analysing the influence of cities on environmental stressors, density often plays a crucial role. In this context, it should be noted that density and size are not social categories, but that the existing urban structures themselves are consequences of social and political processes and structures. In this way, road networks, traffic systems and building structures do not develop independently of each other. It can be assumed that both the road network and the density of development will increase towards the city centre or subcentres, and that this will not only increase the influence of the development, but also increase the traffic intensity. Since, as can be seen in Tab. 33, the effect sizes for the Combined approach is the strongest, it can be assumed that this approach takes these facts into account to the greatest extent.

Thus, the answer to the first research question***: "1. Does a generalized map based on surface parameters reflect the noise sensitivity of urban areas?"*** is that it is possible to generate a generalized structure map based on geometric and density surface parameter, that represents the noise sensitivity of the differently characterised urban areas. But the effect size is only on medium level between the classes CM and LR and on a lower level for LR and MR and MR and CM.

Since the following question is whether it is possible to draw conclusions about health variables from the classification, and since the traffic volume plays a not negligible role in the actual exposure, the Combined approach, which provides the best results for the L_{den}DTV scenario, but also for the differentiation between Lowrise and MR classes for the L_{den}75 scenario, was used for further calculations and validations.

5.6 Heath related Variables

In order to address the second research question: ***"2. What conclusions about adverse health effects can be drawn from the final generalized map?",*** it was first examined to what extent the USSZ classes in the final classification enables conclusions about the actual sound exposure. For this purpose, measurements the L_{den}DTV and L_dDTV single point results (SP) where compared. The results are presented and discussed in sub-section 5.6.*1 Measuring Noise Exposure*. In the second sub-section, 5.6.2 *Modelled Noise Annoyance*, the results and discussion of the Kruskal Wallis test for the $\%Ha$ in accordance with the END of the L_{den}DTV scenario is presented, before it is examined if the $\%HA$ correspond to the surveyed self-reported $TRNA$ in sub-section 5.6.3 *Surveyed Noise Annoyance****.*** Finally, the second main research question is answered in 5.7 *Adverse Health Effects*.

5.6.1 Measuring Noise Exposure

In order to answer the sub-question: ***"2.1 Does the final sound propagation scenario allow statements about the effective sound exposure?"***, the L_{den}DTV scenario was validated by examining whether the measured values approximate the point-exact L_dDTV values, calculated as described in sub-section 4.6.1. As can be seen in Tab. 34, the point values of the L_{den}DTV scenario correlate with the L_{aeq}, while the correlation with the L_d is slightly higher. This result can be considered as good, particularly for a small sample size (n = 12).

Tab. 34: Correlation of measured and modelled sound exposure

			LdenDTV SP	LdDTV SP
L_{aeq}	Pearson Correlation	Corr. Coeff.	0.806**	0.857**
		Sig. (2-tailed)	0.000	0.000
		N	12	12
**Correlation is significant at the 0.01 level (2-tailed).				

However, it must be acknowledged that as displayed in Fig. 33 , the scenarios values deviate rather strongly from the measured values. Reasons for this high difference can be attributed to the locations where the measurement took place. As the locations had to be well-suited for the survey and since the socio-economic aspect played a significant role here, care was taken to ensure that socio-economic variability was well represented at city level. However, regarding the measurements, the selection of the locations cannot be considered as ideal, especially in inner courtyards where there is background noise which is amplified by multiple reflections and that has a considerable influence on the measurement level. Additionally, it is impossible to eliminate background noise that cannot be attributed to traffic.

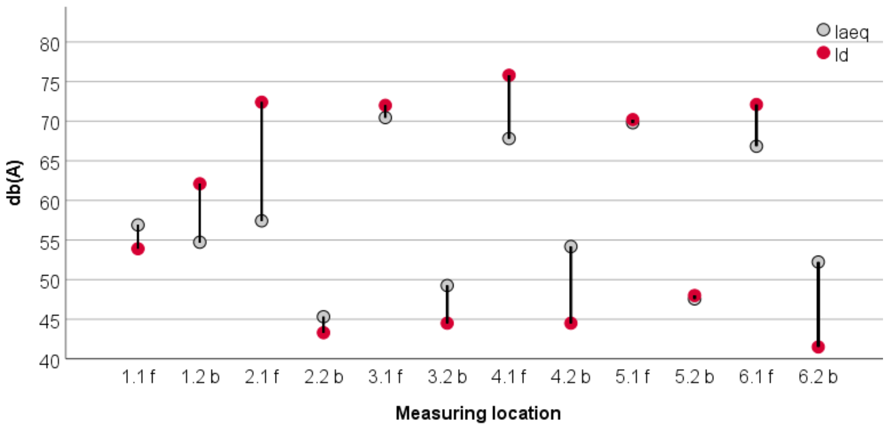

Fig. 34: Composite diagram

Thus, the reason for choosing *Kaltenbergen* (e.g. 1.2 b) was that this area is characterized by a particularly low socio-economic status and is located directly on the highway. The close location to the highway is from a measurement and modelling point of view, extremely unfavourable. The measuring point behind the house is in the immediate vicinity of the highway, which causes the high Ld. But nowadays there is a noise barrier, which was not considered separately in the scenario. This explains why the measured value is below the calculated L_d.

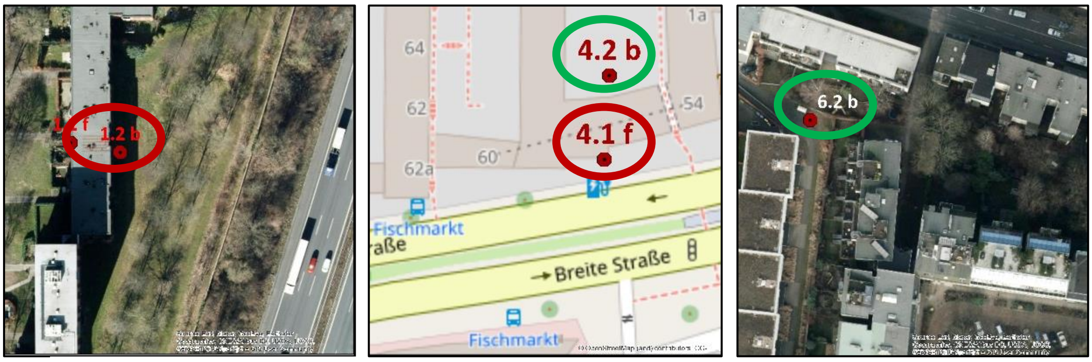

Fig. 35: Measuring points with highly deviation from the scenario values

The second measuring location which has a particularly strong deviation is *Breite Straße* (4.1 f). *Breite Straße* is one of the main roads en-route to the harbour. Thus, in the immediate vicinity there is not only a main road but also a shipyard and parts of the container port. Therefore, it can be excluded that the measurement level was increased by harbour noise. Moreover, it was placed right next to a bus stop, which additionally influenced the measuring level. In contrast to this, measurement point 4.2 b in the inner courtyard at the same location shows a downward deviation. This could confirm that the increased measurement in the case of 4.1 f is not due to an increased traffic volume, but to the above-mentioned noise sources.

The highest downward deviation is found for the location *Streesemannstraße* (6.2 b). As can be seen in Fig. 35, there is a strip of greenery here that has dense foliage in summer. This can act as a sound screen. However, as described in sub-section 2.2.2, vegetation is not considered in the calculation.

Despite the unfavourable measuring points and the associated deviations, the research question ***2.1 Does the sound propagation scenario adequately represent the actual sound exposure?*** can be answered positively. The high and significant correlation showed that both the L_d or the L_{den}DTV scenarios represent the measurable exposure well. Thus, it will be analysed next whether the corresponding $\%HA$ differs significantly between the tree final USSZ.

5.6.2 Modelled Noise Annoyance

To investigate correlations between the modeled scenario values and the data collected through the survey, the investigation by means of the Kruskal Wallis test was carried out for the buildings that are located in the survey areas. Since the class size varies greatly, approximately 285 houses were selected from each class for which L_{den}DTV was available. This served the purpose, as mentioned in section 4.6.2, to avoid that the high number of buildings (10,181 for the SAs survey) cause a significant result. Furthermore, this time, instead of using the exposure levels, the $\%HA$ was considered.

As the overall mean for the $\%HA$ regarding the USSZ (Tab. 35) already differs this could be a first hint, as the USSZ not only represents the different exposure levels, but likewise the absolute risk of being annoyed.

Tab. 35: Average %HA for the USSZ

USSZ	%HA
LR	0.085
MR	0.066
CM	0.123

The Kruskal Wallis test shows that this is true for the distribution of L_{den}DTV $\%HA$. The Null Hypotheses: *"The distribution of %HA is the same across categories of USSZ"* can be rejected. Furthermore, even though the adjusted significance level is not constant across all three classes 0.00, (Adj. Sig LR and MR 0.07), the pairwise comparison (Tab. 36) confirmed this result.

Tab. 36: Pairwise comparison of USSZ - %HA

% HA $_{Lden}$DTV					
Sample 1-2	**Test Statistic**	**Std. Error**	**Std. Test Statistic**	**Sig.**	**Adj. Sig.[a]**
LR-MR	61.949	20.425	3.033	0.002	0.007
LR-CM	177.274	20.685	8.570	0.000	0.000
MR-CM	239.223	20.425	11.712	0.000	0.000
Each row tests the null hypothesis that the Sample 1 and Sample 2 distributions are the same. Asymptotic significances (2-sided tests) are displayed. The significance level is ,05.					

This difference is also reflected in the effect size shown in Tab. 37. In terms of $\%HA$, the differences between the USSZs are even more evident than the differences regarding exposure level.

Tab. 37: Effect Size %HA

LR-MR	0.125
LR-CM	0.354
MR-CM	0.491

Thus, it can be deduced from the USSZ that the absolute risk of being highly annoyed differs between the classes. Particularly the BBs classified as CM show a higher absolute risk of being annoyed than the other two classes. However, even though the $\%HA$ is lower in LR and MR, there is still a considerable difference which is significant between the two classes. Thus, the answer to the sub-question: ***"2.2 Does the %HA of the final scenario in accordance to the END differ significantly between the classes of the final generalized map?"*** is likewise positive.

Since the L_{den}DTV scenario on which the $\%HA$ is calculated only considers the traffic volume and the average speed, and it therefore does not fully correspond to the END, the next step was to see whether this model allows statements about the actual suffered annoyance. Therefore the $TRNA$ was compared against the $\%HA$.

5.6.3 Surveyed Noise Annoyance

In this section the results of the survey will be outlined first, before the results of the comparison of the $\%HA$ and the $\%TRNA$, on which the answer to the sub-question that is addressed in this sub-section: ***"2.3 Does the relative number of self-reported $\%TRNA$ correspond to the $\%HA$ calculated in accordance to the END?"***, are presented.

In total, 1,081 surveys were returned, giving a response rate of 16,24%. This is below the response rates of similar surveys and can be explained by the absence of a reminder due to a lack of resources. The variation of the response rate across the survey areas was high (response rates varied from 3.1 % to 43.5 %). In general, the highest response rates are achieved in areas of people with a high socio-economic status and the lowest rates match those with a low socio-economic status (rho = 0.34, significant at the 0.01 level). The distribution of the age structure is on average 10 years above the values for Hamburg; but since it was a condition of participation to be over 18, this was to be expected. The median income structure is in line with the Hamburg average and the proportion of women is somewhat higher, which is not unusual for postal surveys.

As can be seen from Tab. 38 there were 992 valid answers for the question: *"To what extent do you feel annoyed in your apartment/house by road traffic noise?"* In order to see how strongly the responses correspond to the calculated sound exposure, this was divided into the usual 5 dB(A) intervals. Then, it was first explored which sound level class had which response frequency for which answer category. This result can be seen in the table below.

Tab. 38: No. of answers per sound level class

TRNA	Sound level classes L_{den}DTV							Total
	≤ 40	40 - 45	45 - 50	50 - 55	55 - 60	60 - 65	≥ 70	
very much = 1	3	15	30	23	62	58	0	191
quite = 2	2	21	43	34	39	44	2	185
Somewhat = 3	17	52	87	47	67	43	4	317
and not at all = 4	15	78	93	46	34	30	3	299
Total	37	166	253	150	202	175	9	**992**

What was surprising is that out of the nine respondents living in areas affected by dB(A) > 70, no one selected answer = 1. However, as explained in section 2.2, in addition to the physical sound intensity, psychological factors also have an influence on whether a noise is perceived as an annoyance. The focus area to which these responses can be assigned are near to the harbour area and next to a main road leading to the inner city and the harbour. People who move there might assume that the noise exposure will be higher than elsewhere, therefore they may feel less annoyed because they are expecting it. Conversely, this can also be applied to the area where despite the low exposure < 40dB(A), answer 1 was given three times and answer 2 was given twice. This survey area is located directly next to a green space and consists of small side streets and cul-de-sacs; here the residents might have expected a lower sound exposure than acutely received.

Since the $\%HA$ indicates the absolute risk of being annoyed in percentage, the of responses 1 of all responses per level class had to be calculated to be able to compare the two indicators. Additionally, as explained in section 2.2, level classes 45dB(A) ≤ L_{den} ≥ 75dB(A) should be excluded. The answers that are falling in to these sound level classes where therefore not considered in the comparison.

As can be seen in Tab. 39 the $\%HA$ is lower than the $\%TRNA$. The $\%HA$, based on the calculation guidelines in accordance with END, seems to underestimate the absolute risk of being annoyed, in comparison to the self-reported $\%TRNA$.

Tab. 39: Comparison of %TRNA and % HA

Sound level class	%TRNA	%HA	%TRNA - %HA
45-50	0.12	0.08	0.04
50-55	0.15	0.10	0.06
55-60	0.31	0.13	0.18
60-65	0.33	0.18	0.16

However, the trend of being more annoyed with the rising sound level is constant for all four variables. The final answer to the sub-question: ***"2.3 Does the relative number of self-reported $\%TRNA$ correspond to the $\%HA$ calculated in accordance to the END?"*** is therefore that the $\%TRNA$ is higher than the $\%HA$, but the overall trend is the same.

However, since significant differences between the classes of the USSZ exist for the %HA, the question is whether these differences also occur for the $TRNA$.

For the sample of investigated buildings. The results so far suggest that based on the Combining approach the BBs are classified in such a way that they differ with regard to the sound exposure calculated by means of the L_{den}DTV scenario between the three classes LR, MR and CM significantly. The largest effect size was found between the classes LR and CM, the difference between MR and CM were in contrast relatively less pronounced, with an effect size of 0.187.

A somewhat different picture emerged for the significant differences of the USSZ with regard to the absolute risk of being highly annoyed expressed in $\%HA$. Overall, the effect sizes were somewhat stronger. This is highest in the MR and CM classes, but LR and CM also differed on an intermediate level. This indicates that while the classification is already suitable for making statements about the average exposure of the BBs, they are additionally appropriate to represent the differences of the $\%HA$. With regard to the USSZ. However, as pointed out earlier, with regard to the investigated sample, $\%H$A seems to underestimates self-assessed traffic related noise annoyance. Therefore, the question arose whether the USSZ might be more suitable than $\%TRNA$. For this purpose, the percentage of category 1 responses per all responses per USSZ was calculated. As can be seen inTab. 40, the differences indicated by the previous analyses are also reflected for the $\%TRNA$.

Tab. 40: Average %TRNA and %HA for USSZ

	%TRNA	%HA
LR	0.23	0.085
MR	0.21	0.066
CM	0.28	0.123

Thus, in the buildings of the sample categorized as CM, 28% of all responses in this class were strongly annoyed. for the LR and MR classes, it was 23% and 21%, respectively.

Since according to the EU guidelines, a value of %HA>10 is considered critical, the results of the examination of the sample of houses in which surveys were carried out suggest that the USSZ are also suitable for representing the absolute risk of being annoyed by traffic noise. At this level of investigation, this would be the case for the CM category. Thus, it can be finally examined whether this result can also be confirmed for the entire survey areas.

5.7 Adverse Health Effects

Based on the results presented and discussed above, the question "***2. What conclusions about adverse health effects can be drawn from the final generalized map?"*** will be answered in this section. For this purpose, a Kruskal Wallis test and the pairwise comparison were carried out for the %HA L_{den}DTV at building block level and the effect size was calculated.

Again, the null hypothesis can be rejected at a significance level of 0.000. This result is confirmed by the pairwise comparison. All classes differ with regard to %HA at a significance level of Adj.Sig = 0.000. The effect size is also highest here between CM and LR with 0.399. For LR and MR it is still 0.231, whereas at this level between MR and CM it is relatively small at 0.198.

If one looks at the average L_{den}DTV values and the average %HA for the BBs with the different USSZ, it can be seen (Tab. 41) that the values of %HA again exceeded = 10% for CM.

Tab. 41: Average %TRNA and %HA per USSZ all BB

	L_{den}DTV	**%HA BB**
LR	47.11	0.08
MR	51.16	0.10
CM	55.09	0.13

In addition, the L_{den}DTV for this class is above the 53 dB. As was shown in section 2.2.1 in the case of an average noise exposure 53db, the GDG strongly recommends *"reducing noise levels produced by road as road traffic noise above this level is associated with adverse health effects"* (WHO, 2018, p. 16). Thus, the second research question of this thesis: "***2. What conclusions about adverse health effects can be drawn from the final generalized map?"*** can now be answered.

The USSZs classified in this thesis on the basis of surface parameters are also suitable for determining the spatial distribution of adverse health effects. However, the effect sizes between the MR and LR classes are relatively small. The result is clearer for the CM class. not only is the effect size higher, especially between CM and LR. in addition, the mean load of the LdenDTV and the %HA is above the recommended limits.

6 Conclusion

In the *State of Research,* it was asserted that human health and wellbeing are influenced by personal characteristics but also by the human environment. As the UN expects that by 2050 about 75 % of the world's population will live in or around cities, urban space and its liveable design are becoming more and more important. However, due to increased urbanization and the associated increase in traffic volume, urban agglomerations do not only have to deal with air, but also with noise pollution. As stated in the *Conceptual Modelling Approach to Health-Related Urban Well-Being* introduced in 2017 by Szombathely et al., it is important to understand the interrelations between urban morphology and noise exposure on the highest resolution possible, to estimate the resulting adverse health effect of environmental stressors.

The confrontation with high, but also with continuous sound exposure, can be the cause of various diseases, e.g. cardiovascular and respiratory, as well as high annoyance. Even though the WHO's estimate of DALYs is lower than for other illnesses, recent studies have shown that annoyance can be the precursor to more serious illnesses. As the overall health burden is high for annoyance, this assessment of the population for those affected by annoyance is of outstanding importance. As a result, there are EU wide guidelines and laws that specify regulations. The calculation of the absolute risk of being annoyed by noise depends, among other things, on the sound level. These are included in various sound forecasting programmes.

As the calculation of the L_{den} is complex, these programmes are usually computationally intensive and restricted by high licensing fees, in recent years, various research fields have dealt with the question of how sound propagation is influenced by urban structures, and how this relationship can be represented in a simplified way. An intensively researched topic is the determination of the exposure level based on the surface parameters of different urban morphological structures. Regarding the different research approaches, a distinction can be made between surface parameters that relate to the building structure or the density of the investigated areas, and of surface parameters that are related to the characteristics of the traffic network. Thus, the question arose whether, based on the findings concerning the correlations of surface parameters and sound exposure, it would be possible to generate an accessible and generalized map that refences the urban sound sensitivity of the different areas. For this purpose, it was necessary to investigate which parameters are suitable for such a classification. In the *Theoretical Considerations* it was shown that the surface parameters used in other research fields that are very similar when dealing with mapping of urban structure maps, are the same ones that often point out the relationship between the urban structure and the exposure level of traffic induced noise.

In the field of building classification, mainly geometric and structural surface parameters are used, which are calculated on the basis of vector data. In the field of LCZ classification, there are density and structure surface parameters based on grid data. Following from this, three different classification approaches were used; a Vector-based, a Grid-based and a

Combined. While all three achieved good results (even with a reduction of the input parameters), the best results were achieved by the Combined approach. It could be shown that a combination of geometric and density parameters is suitable for generating a stable classification of different urban zones using the well-known Random Forest algorithm. Thus, the BBs were classified in to the Lowrise, Midrise and Compact Midrise classes, which differ with regard to surface parameters such as the Height, Volume and density parameters like the Sky View Factor.

In the field of urban sound propagation, often different sound propagation scenarios are used to investigate the interconnection between urban surface parameters and the exposure level. Some are based on EU directives and real-world conditions, while others assume a uniform traffic flow, and others still work with measured data. Additionally, in some studies it has been shown that the traffic volume is also related to surface structure. The question therefore arose whether the classification based on these parameters only represents the influence of the urban structure on the sound propagation or if the associated traffic volume is likewise represented. Three different sound propagation scenarios were therefore used to validate the final USSZ map. The first one was calculated based on uniform traffic volumes and speeds (L_{den}75), the second was based on the modelled traffic volumes and the maximum permitted speeds (L_{den}DTV), while the third was extracted out of the official noise map of the city of Hamburg. By applying a Kruskal Wallis test and the related pairwise comparison it was proven that the Lden differed significantly between the resulting USSZ for the L_{den}75 and the L_{den}DTV scenario. For the L_{den}DTV the significance level is Adj. Sig. is 0.00 between all three classes. That the L_{den}DTV is represented best by the USSZ could be confirmed by the resulting effect size, which is at a medium level for the classes LR and MR (0.381). Consequently, the first question that was addressed in this thesis: ***"1. Does a generalized map based on surface parameters reflect the noise sensitivity of urban area***?" was answered that such a classification is possible. That the L_{den}DTV is represented best by the USSZ leads to the assumption that the classification based on the Combined approach not only considers the influence of the urban surface, but likewise the related traffic volume as well as the maximum speeds allowed.

Based on the answers to this first question, the second research question, which addresses the possibilities to draw conclusions about noise induced adverse health effects are based on the generalized maps was be looked at. To be able to do so, it was first necessary to check whether the L_{den}DTV scenario approximated the real exposure level. The comparison of point exact calculations and measuring results showed a correlation of 0.848 with a significance level of 0.001. Especially in view of the relatively small sample size of n = 12, this can be proven to be a strong correlation. It was pointed out, that there are high deviations between the modeled and measured values at some measurement locations, but this can be attributed to influences resulting from the selection and setting of the measurement locations. Thus, despite these discrepancies, it can be assumed that the L_{den}DTV represents the actual exposure reasonably well.

Next, it was analyzed whether the $\%HA$ differs significantly between the classes of the USSZ. Since it is important to have the lowest possible resolution, especially in the case of socio-economic questions affecting people, the analysis of variance was carried out on building level for a sample of the buildings within the areas in which the survey was carried out. In addition, in accordance with the WHO recommendations, only buildings with $45 \leq L_{den} \geq 75$ dB(A) where included. Here, too, the result was positive. The significant level between the classes LR and MR is somewhat lower with Adj. Sig = 0.007, but the resulting effect sizes are higher than in the case of the L_{den}DTV. In particular, MR and CM, but also LR and CM, differ at a medium level with 0.491 and 0.354. Only for the classes LR and MR the effect size is somewhat weaker (0.125).

It was then clarified whether the curve of the $\%HA$, based on the L_{den}DTV scenario calculated in accordance with the END, adequately reflects the actual annoyance for Hamburg's population. The answers to the question *"To what extent do you feel annoyed in your apartment/house by road traffic noise?"* was looked at. It was referred to as *Traffic Related Noise Annoyance* ($TRNA$), which were taken from a UrbMod project-wide survey. It was then examined whether the percentage of $\%HA$ and the $\%TRNA$ in respective sound level class are corresponded. It became clear that although both indicators have an upward trend with increasing sound level class, the $\%HA$ is below the $\%TRNA$ for all classes. This deviation increases with increasing level class. Therefore, based on the data available, it can be assumed that the $\%HA$ underestimated the annoyance of the residents after the END.

The Kruskal Wallis for the $\%HA$ already suggested that the USSZ map represents the difference of adverse health effects of road noise quite well. However, since the $\%TRNA$ is above the $\%HA$, it was then examined how high the difference of mean of people who felt highly exposed between the final classes is. Here, the previous results could be confirmed again. In the LR class it was 23%, in the MR class 21% and in the CM 28%, who felt highly annoyed by traffic noise.

Finally, it was examined whether the results of the analysis at house level and for the focus areas are also reflected in the classification at building block level. Again, the null hypothesis could be rejected at a significance level of 0.000. This result is confirmed by the pairwise comparison. The effect size is also highest here between CM and LR with 0.399. As the average values of $\%HA$ for the CM class exceeds 10% and the L_{den}DTV > 53 dB it can be assumed that based on data of this research regions that have a higher risk of adverse health effects due to traffic noise can be located.

Thus, the second question of this research ***2. What conclusions about adverse health effects can be drawn from the final generalized map?*** can also be answered positively. The classification based on structure and density surface parameters not only reflects the differences in noise exposure, it also represses the different risk of falling into the $\%HA$ category, which could be confirmed at an even higher level for the $\%TRNA$ by real world data. Both is highest for the Building Blocks classified as CM.

What cannot be concluded form this map is the personal risk of being taken ill for the individual person living in the CM class. As was shown in the State of Research in the subsection on Noise induced Health Effects, and is also considered in the *Conceptual Modelling Approach to Health-Related Urban Well-Being* introduced in 2017 by Szombathely et al. is, that in addition to the level of noise exposure, other personal factors such as age, health and personal attitude, also play a role in the question of whether the noise is perceived as an annoyance or not. In addition, it was shown that due to the risk of ecological fallacy, especially when analyzing such personal factors, aggregates should be avoided. For this reason, the noise maps with the higher resolution, which are calculated on the basis of the END, are much better suited here.

However, the USSZ map was very good at identifying so-called hotspots. In combination with the knowledge of where particularly vulnerable groups live in the city, it is possible to identify quickly and with little effort where it is particularly important to take measures to reduce traffic noise.

7 ANNEX

Annex Directory

Annex: List of Figures

Annex: List of Tables

Annex 1: Physical Principles of Sound Propagation

Noise is an evaluative term as mentioned in section 2.2, it cannot be measured physically. However, sound itself, which is dep(SINAMBARI, 2017)ending on the intensity and psychological condition of the receiver and the corresponding negative valuation perceived as noise, has a physical component which therefore is a measurable quantity (MOORE, 2014). The physical rules of sound propagation and the influence of urban conditions and structures on the propagation path are explained in this chapter first. This is followed by an overview of the related directives and norms. Since the propagation properties of sound, especially in urban areas, are very diverse and complex, and a multitude of numerical and empirical approaches exist, only those included in the ISO, 1993 and ISO, 1999 and those which are of importance for noise pollution caused by road traffic in urban areas are considered in more detail.

The term sound describes the mechanical vibration of an elastic medium which can be in any state of aggregation (solid, liquid, gaseous). The sound pressure is thus the compression and relaxation of the air (DIN, 2009; SCHÖNHOLTZ, 2013). Sound pressure propagates in waves, which can differ in their amplitude $(\hat{x})$ and frequency (f). The amplitude measures the expansion of the sound wave and is the part that humans perceive as loudness. The frequency represents the number of oscillations per second measured in Hertz (Hz). The higher the frequency, the higher the tone (KUTTRUFF, 2007).

If one frequency dominates, it can be identified as a tone, if several frequencies overlap, in the positive sense it can create a sound, in the negative sense it can be perceived as noise (WILLEMS et al., 2006). Acoustic sound physically comprises all signals that can be perceived by the human ear and that can be acoustically recognized. This is, as illustrated in Fig. 36, usually the case if the amplitude of the sound pressure is between 20 µ Pa and 200 Pa and the frequency ranges between 0 and 125 kHz (hearing threshold) and 20 kHz (upper hearing threshold) (KUTTRUFF, 2007; LIN & ABDULLA, 2015; WILLEMS ET AL., 2006).

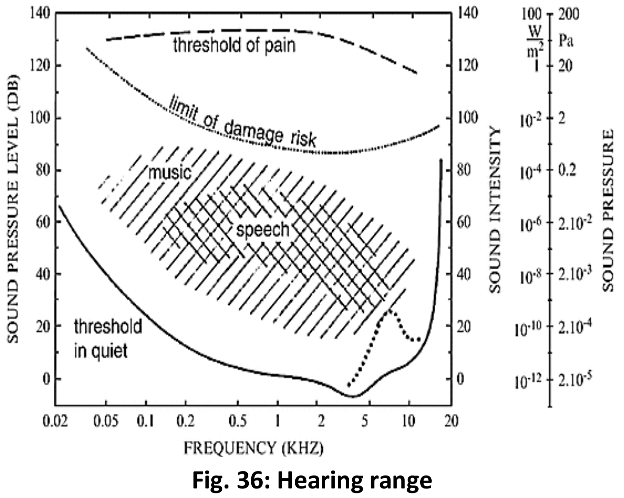

Fig. 36: Hearing range
Source: LIN & ABDULLA , 2015, p.15.

When scaling the sound pressure, the perception scale of the human ear is considered by relating the measured sound pressure to the threshold of human hearing, the quietest sound pressures the human ear can appreciate. To adjust the scale of the sound levels to the loudness scale, the ratio must be transferred to a logarithmic scaling. The result is the sound pressure level L_p measured in decibels (dB):

[44] $$L_p = 20\,log\left(\frac{p}{p_0}\right) dB$$

$$for\ given:$$
$$p = The\ Root\ Mean\ Square\ Sound\ Pressure$$
$$p_0 = The\ Reference\ Sound\ Pressure = 20\mu Pa\ = Human\ Hearing\ Threshold$$

Comparing different tones, it becomes apparent that the human ear perceives a different loudness depending on the frequency of each tone. This is called apparent loudness, and it can be measured in phon. The phon of a given tone corresponds to the sound pressure level of a tone at 1,000 Hz which is perceived as having the same loudness. If, for example, the same loudness is to be produced as at 1.000 Hz and 50 dB, at 63 Hz it must be generated 73 dB in order to be perceived at the same loudness (ROSSING, 2014).

Annex 1.1.: Sound Level Statistics

When several sound sources interact, there can be an increase in sound impact. In particular, if referred to multiple sources which produce incoherent sound (noise), it can be assumed that their interaction creates an increase of sound pressure. Since the levels in decibels are not measured in a linear scale, they cannot simply be added. The different sound pressure levels must therefore be summed up energetically according to the following equation (WILLEMS et al., 2006):

[45] $$L_p = 10lg \sum_i 10^{0.1L_i}$$

$$for\ given:$$
$$L_i = Single\ Sound\ Pressure\ Level$$

This applies to the subtraction of sound pressure levels as well (WILLEMS et al., 2006):

[46] $$L_p = 10lg[10^{0.1L_i} - 10^{0.1L_i}]$$

Few noises are constant over time, the sound pressure level rather change continually. In order to make statements about the sound pressure level within a certain observation period T and to be able to compare sound pressure levels from different sources, there are various statistical parameters which can be calculated from the measured values. The averaging process is analogous to the energetic sound pressure level addition, whereby $\sum_i 10^{0.1L_i}$ must be divided by the total number of time periods (or sources) before they are scaled logarithmically (WILLEMS et al., 2006):

[47] $$L_{eq} = 10lg(\frac{1}{T}\int_0^T 10^{0.1L(t)dt})$$

$$for\ given:$$
$$T = \sum_{i=1}^{n} T_i$$

If each time period T_i has the same length, the determination of the equivalent continuous sound level is simplified to an L_m (WILLEMS et al., 2006):

[48] $L_m = 10lg\left[\frac{1}{n}\sum_i^n 10^{0.1L_i}\right]$

When sound propagates a reduction of the sound pressure occurs due to various factors. As for the human ear, it is not the emission (directly at the sound source) but the immission (at the point of the receiver) level that is relevant, the physical propagation laws and how this are affected due to urban settings is therefore essential.

Annex 1.2: Propagation

Each medium has its characteristic acoustic impedance, which is indicated by the ratio of sound pressure p and velocity v. Acoustic impedance describes therefore resistance which is set against the propagating sound waves:

[49] $\xi = \frac{p}{v} = \varrho * c$

Due to the fact that, in the case of gases, the sound pressure amplitude is proportional to the (average) gas density, the speed of sound and the sound velocity, impedance can be converted to the term $\varrho * c$, where ϱ is the density and c is the speed. Consequently, the propagation speed is dependent on the density of the relevant medium (KUTTRUFF, 2007). The characteristic acoustic impedance of air in standard conditions is approximately 400 [kg/(m^2·s)]. For the propagation in the free atmosphere, as temperature rises, air expands and reduces its density, this means that the speed of sound increases with increasing temperatures and vice versa. When assuming a temperature value of 0°, the speed of sound is $c_{sound} \approx 331\,\frac{m}{s}$. If the temperature differs, the corresponding term is added or subtracted as shown below:

[50] $c_{sound} = \left(331 + 0{,}6\,\frac{Temp}{C°}\right)\frac{m}{s}$

In the lower atmosphere (at approx. 15°) sound pressure waves propagate with $c_{sound} \approx 340\,\frac{m}{s}$ (HENN et al., 2008).

As mentioned earlier, in order to determine the noise exposure of residents, however, it is not the emission level L_w at the source but the immission level L_p at the receiver point that is of interest. In general, a distinction can be made between point, line and surface sound sources. Since all common calculation methods are based on the addition of point sources as an approximation, only these procedures are explained in more detail.

Two main mechanisms of sound pressure level reduction can be found: a geometric one, related to the expansion of the area impacted by a sound wave, and attenuation, due to the internal mechanical friction between particles moved by sound waves.

In the theoretical ideal case sound propagates equally in all directions into an undisturbed, homogeneous and loss-free space, a spherical wave field builds up around the source. On the way out from a sound source, sound waves therefore spread out over an increasing spherical surface. This causes the so-called energy dilution, which is expressed by the sound level reduction by distance (A_{div}) (VEIT, 2005). The sound pressure level L_p at a distance d is reduced by (HENN et al., 2008):

[51] $$A_{div} = 10\,lg\left(4\,\pi\frac{d^2}{d_0^2}\right)\,dB$$

$$for\ given:$$
$$d = Distance\ between\ Source\ and\ Receiver$$
$$d_0 = Reference\ Distance = 1m$$

The second essential attenuation effect in free atmosphere is the so-called internal friction loss, expressed by the air absorption measure A_{atm} (HENN et al., 2008). Air absorption is only noticeable from a propagation distance of $d > 200\,m$. Mathematically this is determined by the attenuation coefficient: in $/km$ (NYBORG & MINTZER, 1955):

[52] $$A_{atm} = \alpha_L * d/1.000$$
$$for\ given:$$
$$\alpha_L = \alpha_{class} + \alpha_{mol}$$

α_{class} includes parameters such as viscosity, thermal conductivity, diffusion (of hydrogen and nitrogen molecules) and radiation (of heat). α_{mol} describes the intermolecular influences. For the audible frequency range α_{mol} has the greater influence. As α_{mol} depends strongly on the moisture content of the air at any given frequency it is also called the moisture loss factor (NYBORG & MINTZER, 1955). As can be seen from Tab. 42, the attenuation coefficient is strongly dependent on frequency, humidity and temperature (ATTENBOROUGH et al., 2007; HENN et al., 2008).

Tab. 42: Air attenuation coefficient as a function of temperature and humidity[13]
Source: ISO, 1996

Temperature [° C]	Rel. Humidity [%]	Atmospheric Attenuation Coefficient α_L [dB/km]							
		Nominal Mid-band-Frequency [Hz]							
		63	**125**	**250**	**500**	**1000**	**2000**	**4000**	**8000**
10	70	0.1	0.4	1.0	1.9	3.7	9.7	32.8	117.0
20	70	0.1	0.3	1.1	2.8	5.0	9.0	22.9	76.6
30	70	0.1	0.3	1.0	3.1	7.4	12.7	23.1	59.3
15	20	0.3	0.6	1.2	2.7	8.2	28.2	88.8	202.0
15	50	0.1	0.5	1.2	2.2	4.2	10.8	36.2	129.0
15	80	0.1	0.3	1.1	2.4	4.1	8.3	23.7	82.8

These undisturbed propagation conditions, in which only the attenuation and the air absorption have to be considered to determine the sound pressure at any place of immission, not always corresponds to the reality. Additional influences such as diffraction as a result of meteorological influences, reflections at boundary surfaces (e.g. soil, buildings, forest etc.), vegetation, and shielding effect of obstacles etc. have to be considered (RUDNICK, 1947;

[13] The air attenuation coefficient has been derived from various recognized theories and has been investigated and proven in wide number of laboratory experiments. However, there are deviations from experiments and calculations especially in the high frequency ranges and at high absolute humidity. Which variables are included in the calculations can be read at Nyborg and Mintzer (1955)

ZÜRCHER & FRANK, 2018). When sound waves hit the interface of two media, reflection, absorption, dissipation and transmission can occur (DEGA, 2006; ZÜRCHER & FRANK, 2018).

Sound energy is divided into three components: in the case of buildings the largest part is mostly reflected (red arrow in Fig. 37). Another sound component passes the new surface and is either converted into heat (absorption) or transferred through the boundary surface (transmission) (PIERCE, 2014). For non-absorbing media the transmitted part of the sound will be diffracted (blue arrow in Fig. 37).

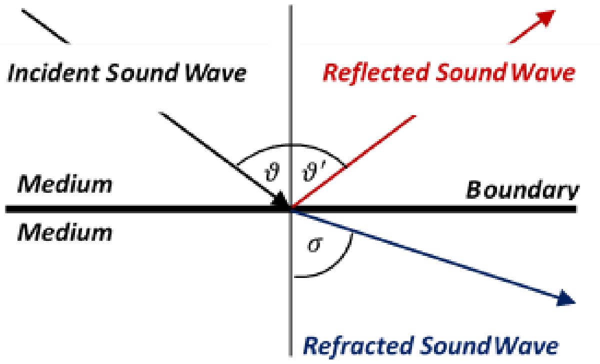

Fig. 37: Refraction and reflection of sound waves at the interface of two media
Modified after ATTENBOROUGH, 2007, p.26.

The direction is depending on ratio of the propagation velocity of both media and the angle of incidence of the wave fronts as shown in the equation below:

[53] $$\sin\sigma = \frac{c_2}{c_1} * \sin\vartheta$$

$for\ given:$
$c_1 = Propagation\ Velocity\ in\ Medium\ 1$
$\vartheta = Angle\ of\ Incidence$
$c_2 = Propagation\ Velocity\ in\ Medium\ 2$
$\sigma = Angle\ of\ Refraction$

The transmitted sound waves are therefore refracted away from the normal direction if $c_2 > c_1$, and if $c_1 > c_2$ towards the normal direction. It must be assumed that the boundary surface is larger than the wave length (ATTENBOROUGH et al., 2007).

An omni-directional sound propagation is indicated by the reference angle 4π. If the sound radiates into a limited angular space, the level reduction due to divergence described early will not have its full effect. The difference can be expressed by the so-called directivity indexD_Ω:

[54] $$D_\Omega = 10lg\frac{4\pi}{\Omega}$$

In the special case of radiation directly in front of or above a total reflecting surface, the propagation occurs in the half space, which is expressed by the half spherical directivity index:

[55] $$D_\Omega = 10lg(2) = 3db = \Omega_{half-space} = 2\pi$$

If a loss-free reflection is assumed and the different height of the source h_S and receiver h_R as well as the absorption coefficient α are taken in to account D_Ω can be calculated as follows (Henn et al., 2008; Rudnick, 1947):

[56] $$D_\Omega = 10lg\left[1 + (1-\alpha)\frac{d_p^2+(h_S-h_R)^2}{d_p^2+(h_S+h_R)^2}\right] dB$$

$for\ given:$

$\alpha = Absorption\ Coefficient\ of\ the\ Reflecting\ Surface$

This reflection process itself can be illustrated by means of an image source. As can be seen from Fig. 38, in case of the sound source S_0 radiating above or in front of a reflecting surface with $h_S < d$, both the direct sound and the sound from the reflection-induced image source S_1 arrive at R (PIERCE, 2014; SINAMBARI et al., 2014; TRAUTWEIN, KREIBIG, & HÜTTERMANN, 2014).

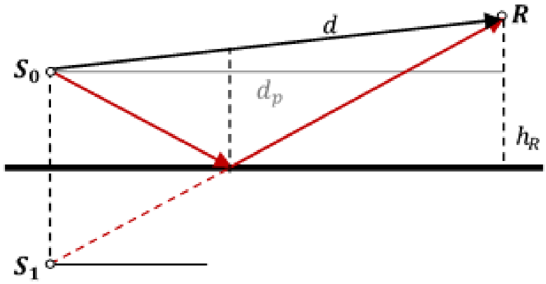

Fig. 38: Sound radiation in front of reflecting surfaces
Modified after SINAMBARI et al., 2014, p. 218.

The sound pressure level L_w for the real source S_0 and the sound pressure level and L_{w,S_1} for the image S_1source is considered separately. $L_{w,S_1}$is calculated as follows (ISO, 1996):

[57] $$L_{w,S_1} = L_w + 10\ lg(\rho)\ dB + D_\Omega$$

$for\ given:$

$\rho = Degree\ of\ Reflection$

In the event of a vertical incidence the reflection and absorption coefficients can be expressed by means of the respective acoustic impedances:

[58] $$\rho = \left(\frac{\xi_2-\xi_1}{\xi_2+\xi_1}\right)^2 = Degree\ of\ Reflection$$

[59] $$\alpha = 1 - \rho = \frac{2\xi_2}{\xi_1+\xi_2} = Degree\ of\ Absorption$$

The more the two materials differ in their propagation velocity, the greater is the reflected share at the same angle of incidence (TRAUTWEIN et al., 2014).

How the propagation is affected through structures and processes in urban space is explained in the following using selected examples relevant to road traffic noise.

Annex 1.3: Influence of Urban Settings

Meteorological condition in urban areas can differ from those of a rural surrounding. In the urban boundary layer, near the ground, turbulent currents are of minor importance, whereas wind speed and temperature gradients are relatively large. Considering the influence of temperature on sound propagation it becomes clear that especially weather conditions with a large temperature gradient near the ground have an effect on the sound propagation (ATTENBOROUGH et al., 2007; DUCKWORTH & SANDBERG, 1954).

Diffraction of the sound waves occurs due to the variable density of the air layers in dependence of their temperature. This effect is shown in Fig. 39. If, as can been on the left side, the temperature gradient is positive with increasing altitude, the sound rays are diffracted towards the ground. If, as can be seen on the right side, the absolute temperature decreases with increasing altitude, this causes a diffraction of the sound rays away from the ground, creating a so-called sound shadow zone (DRAHOS & DRAHOS, 2012; ZIEMANN, 2002).

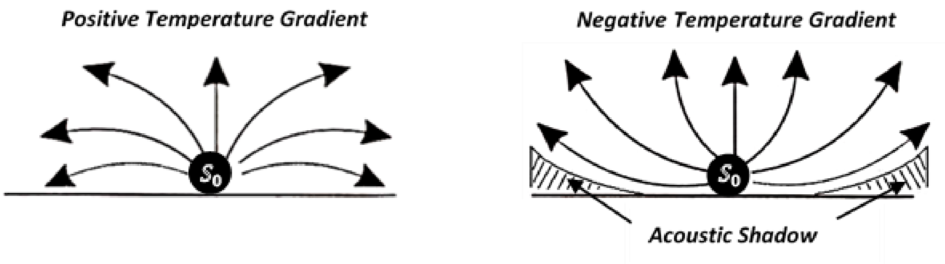

Fig. 39: Sound propagation as a function of the temperature gradient
Modified after DRAHOS & DRAHOS, n.p.

The influence of the wind on sound propagation depends on the relative angle of sound propagation and wind vectors and can be separated into its vertical and horizontal components. On the horizontal axis sound and wind speed add up depending on the direction. Sound propagation speed increases therefore in wind direction and vice versa. If the vertical wind gradient is positive with increasing height, as can be seen Fig. 40 there is a downward refraction. If, on the other hand, wind gradient is negative, an upward refraction occurs (DRAHOS & DRAHOS, 2012; VDI, 1988; ZIEMANN, 2002). Since higher roughness in urban areas results in an increase in wind speed in higher altitude, the propagation speed increases with increasing height in mid-wind direction and a downward refraction occurs. This is referred to as a condition favourable to sound propagation (VDI, 1988).

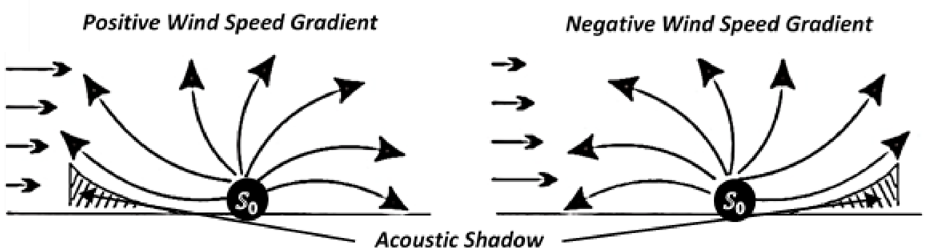

Fig. 40: Sound propagation as a function of the wind speed gradient
Modified after DRAHOS & DRAHOS, n.p.

Next to the meteorological effect, ground and surface effects can occur. Ground with or without vegetation can absorb and/or reflect sound waves, depending on its condition. Soil properties and thus their acoustic impedance[14] must therefore be known. In addition, if

[14] The method for calculating the soil effect for different soils can be read at VYKOUPIL (1982) and ATTENBOROUGH, et al. (2007).

the sound source is particularly close to the ground, the reflected wave can be phase-shifted by almost half a wavelength and thus the direct wave arriving at the receiver can result to be almost eliminated by destructive interference (Nyborg & Mintzer, 1955; Vykoupil, 1982; Ziemann, 2002).

Due to meteorological diffraction and reflection on the ground, sound can reach the receiver on three types of paths. Direct (Path no.1), reflected (path no.2) or refracted (path no.3), as illustrated in Fig 41. Path no.2 can either increase or decrease the sound level, or is absorbed, depending on the acoustic impedance of the ground. Propagation path no.3, which is usually generated by refraction due to the above described positive temperature and wind gradient and propagation in the mid-wind direction, becomes relevant when paths no.1 and no.2 are blocked. This could be caused by obstacles such as vegetation, screening or buildings and other constructions (HANNAH & HUNT, 2006; VDI, 1988).

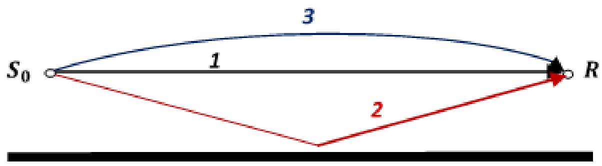

Fig. 41: Outdoor sound propagation near the ground
Modified after HANNAH & HUNT,2006, P.24.

If sound passes e.g. through forest or higher bushes, scattering and absorption cause attenuation, which depends on the type and density of the vegetation. The effect only occurs if the vegetation is so dense that propagation along the direct path is completely blocked.

Only in this case it leads to a level reduction at the receiver due to the longer path travelled (HENN et al., 2008).

Obstacles such as houses, walls and barriers play a much greater role in urban space. They can attenuate and/or reflect sound in different ways due to their position, size and acoustic properties. The effect of single diffraction is illustrated in Fig. 42 using the example of a thin barrier (PIERCE, 2014).

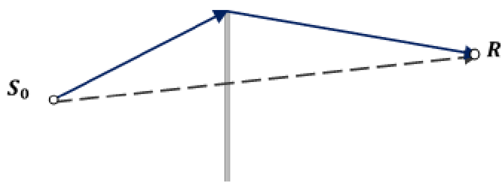

Fig. 42: Diffraction of sound by a thin barrier
Modified after ISO 9613-2:1996-12, p. 9.

Due to the diffraction effect of waves at edges, sound energy can reach the zone of the sound shadow. This is only relevant as long as the transmission loss through the barrier is high. The exact calculation of the obstacle effect is usually not possible. Therefore, empirical approximations are used. This is often done by using the concept of Fresnel numbers and results in (HANNAH & HUNT, 2006; PIERCE, 2014):

[60] $$A_{bar} = -10lg\frac{1}{(D'/d_p)^2+(D'/d_p)}$$

$for\ given:$

$$D' = d_{s+}d_r$$

Shielding’s normally have a finite length and sound is therefore usually also diffracted at the edges (and possibly at the bottom edge). Each diffracted ray at the edges is associated with a specific shielding dimension$A_{bar,i}$ as shown in the figure below:

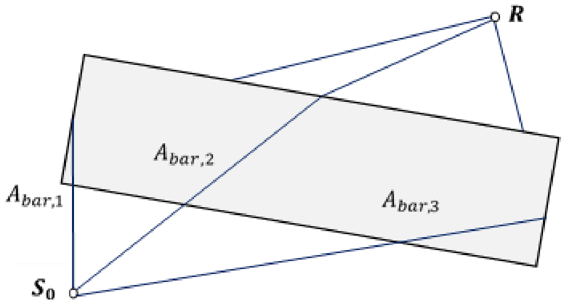

Fig. 43: Refraction on a barrier a finite length
Modified after ISO 9613-2:1996-12, p. 9.

By the interaction of the three illustrated rays a total intensity L_p at R is obtained by:

$$[61] \quad L_p = L_w - 10lg\left[10^{-\frac{A_{bar,1}}{10}} + 10^{-\frac{A_{bar,2}}{10}} + 10^{-\frac{A_{bar,3}}{10}}\right] dB$$

Obstacles and barriers also have an influence on the ground effect, which may have to be taken into account (HANNAH & HUNT, 2006).

In the case of traffic noise, multiple reflections occur due to urban constructions. The sound level increase caused in this way is explained by using the example of a street that passes through two closed facades as shown in Fig. 44 (ATTENBOROUGH et al., 2007; HENN et al., 2008).

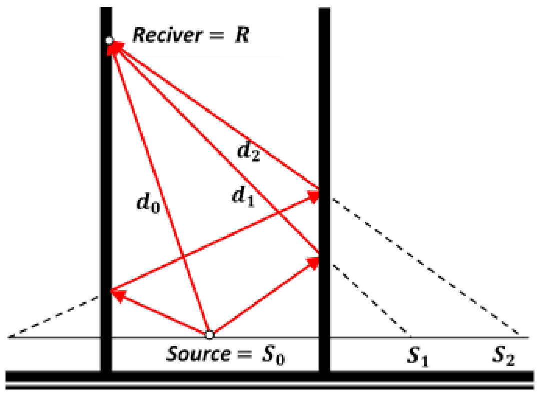

Fig. 44: Multiple reflection in a street canyon
Modified after ATTENBOROUGH, 2007, p. 419.

Without reflection the sound pressure level at the receiver point is calculated as shown earlier the reflections, it changes to:

$$[62] \quad A_{div} = 10\,lg\left(4\,\pi\frac{d^2}{d_0^2}\right)\,dB$$

$for\ given:$
$d = Distance\ between\ Source\ and\ Receiver$
$d_0 = Reference\ Distance = 1m$

Considering the reflections, it changes to:

[63] $L_p = lg \sum 10^{\frac{L_i}{10}}$

$for\ given$:

$L_i = L_{w,S_1}$

$for\ given$:

$L_{w,S_1} = L_w + 10\ lg(\rho)\ dB + D_\Omega$

$for\ given$:

$\rho = Degree\ of\ Reflection$

$$D_\Omega = 10lg\left[1 + (1-\alpha)\frac{d_p^2 + (h_S - h_R)^2}{d_p^2 + (h_S + h_R)^2}\right]$$

$for\ given$:

$\alpha = Absorption\ Coefficient\ of\ the\ Reflecting\ Surface$

Considering all possible reflections, the sound pressure level can theoretically increase by 8 dB. The actual increase, mainly due to the ever present losses at the reflecting surfaces, is always below that value (ATTENBOROUGH et al., 2007; HENN et al., 2008; SINAMBARI et al., 2014).

The physical laws described above are generally only examples of possible numerical solutions. Since there are often different calculation paths for these complex phenomena, general calculation rules have been subsumed in ISO, 1993 and ISO, 1999. Various directives and sound modelling approaches were issued on the basis of the ISO standards.

Annex 2: Tables

Tab. 43: Hypothesis Test Summary - Vector-based approach

	Null Hypothesis	**Test**	**Sig.**	**Decision**
Initial parameter set				
1	The distribution of L_{den}**75** is the same across categories USSZ	Independent-Samples Kruskal-Wallis Test	0.000	Reject the null hypothesis.
2	The distribution of L_{den}**DTV** is the same across categories USSZ	Independent-Samples Kruskal-Wallis Test	0.000	Reject the null hypothesis.
3	The distribution of L_{den}**HH** is the same across categories USSZ	Independent-Samples Kruskal-Wallis Test	0.001	Reject the null hypothesis.
Reduction 1				
	Null Hypothesis	**Test**	**Sig.**	**Decision**
1	The distribution of L_{den}**75** is the same across categories USSZ	Independent-Samples Kruskal-Wallis Test	0.000	Reject the null hypothesis.
2	The distribution of L_{den}**DTV** is the same across categories USSZ	Independent-Samples Kruskal-Wallis Test	0.000	Reject the null hypothesis.
3	The distribution of L_{den}**HH** is the same across categories USSZ	Independent-Samples Kruskal-Wallis Test	0.002	Reject the null hypothesis.
Reduction 2				
	Null Hypothesis	**Test**	**Sig.**	**Decision**
1	The distribution of L_{den}**75** is the same across categories USSZ	Independent-Samples Kruskal-Wallis Test	0.000	Reject the null hypothesis.
2	The distribution of L_{den}**DTV** is the same across categories USSZ	Independent-Samples Kruskal-Wallis Test	0.000	Reject the null hypothesis.
3	The distribution of L_{den}**HH** is the same across categories USSZ	Independent-Samples Kruskal-Wallis Test	0.001	Reject the null hypothesis.
Reduction 3				
	Null Hypothesis	**Test**	**Sig.**	**Decision**
1	The distribution of L_{den}**75** is the same across categories USSZ	Independent-Samples Kruskal-Wallis Test	0.000	Reject the null hypothesis.
2	The distribution of L_{den}**DTV** is the same across categories USSZ	Independent-Samples Kruskal-Wallis Test	0.000	Reject the null hypothesis.
3	The distribution of L_{den}**HH** is the same across categories USSZ	Independent-Samples Kruskal-Wallis Test	0.001	Reject the null hypothesis.
Asymptotic significances are displayed. The significance level is ,05.				

Tab. 44: Pairwise Comparisons of USSZ - Vector- based approach

Sample 1 - 2	**Test Statistic**	**Std. Error**	**Std. Test Statistic**	**Sig.**	**Adj. Sig.[a]**
L_{den}**75**					
LR-MR	-84.720	17.343	-4.885	0.000	0.000
LR-CM	145.930	24.899	5.861	0.000	0.000
MR-CM	61.210	25.389	2.411	0.016	0.048
L_{den}**DTV**					
Sample 1 - 2	**Test Statistic**	**Std. Error**	**Std. Test Statistic**	**Sig.**	**Adj. Sig.[a]**
LR-MR	-105.909	17.343	-6.107	0.000	0.000
LR-CM	182.227	24.899	7.319	0.000	0.000
MR-CM	76.317	25.389	3.006	0.003	0.008
L_{den}**HH**					
Sample 1 - 2	**Test Statistic**	**Std. Error**	**Std. Test Statistic**	**Sig.**	**Adj. Sig.[a]**
LR-MR	42.486	24.490	1.735	0.083	0.248
LR-CM	-62.770	17.335	-3.621	0.000	0.001
MR-CM	-20.284	24.885	-0.815	0.415	1.000
Each row tests the null hypothesis that the Sample 1 and Sample 2 distributions are the same. Asymptotic significances (2-sided tests) are displayed. The significance level is ,05.					

Tab. 45: Pairwise Comparisons of USSZ - reduction 1 - Vector-based approach

$L_{den}75$					
Sample 1 - 2	**Test Statistic**	**Std. Error**	**Std. Test Statistic**	**Sig.**	**Adj. Sig.**[a]
LR-MR	-87.217	17.320	-5.036	0.000	0.000
LR-CM	144.164	25.008	5.765	0.000	0.000
MR-CM	56.947	25.450	2.238	0.025	0.076
L_{den}DTV					
Sample 1 - 2	**Test Statistic**	**Std. Error**	**Std. Test Statistic**	**Sig.**	**Adj. Sig.**[a]
LR-MR	-106.491	17.320	-6.149	0.000	0.000
LR-CM	184.950	25.008	7.396	0.000	0.000
MR-CM	78.459	25.450	3.083	0.002	0.006
L_{den}HH					
Sample 1 - 2	**Test Statistic**	**Std. Error**	**Std. Test Statistic**	**Sig.**	**Adj. Sig.**[a]
LR-MR	40.150	24.586	1.633	0.102	0.307
LR-CM	-60.112	17.317	-3.471	0.001	0.002
MR-CM	-19.962	24.951	-0.800	0.424	1.000
Each row tests the null hypothesis that the Sample 1 and Sample 2 distributions are the same. Asymptotic significances (2-sided tests) are displayed. The significance level is ,05.					

Tab. 46: Pairwise Comparisons of USSZ - reduction 2 - Vector-based approach

$L_{den}75$					
Sample 1 - 2	**Test Statistic**	**Std. Error**	**Std. Test Statistic**	**Sig.**	**Adj. Sig.**[a]
LR-MR	-82.504	17.505	-4.713	0.000	0.000
LR-CM	143.914	24.027	5.990	0.000	0.000
MR-CM	61.410	24.665	2.490	0.013	0.038
L_{den}DTV					
Sample 1 - 2	**Test Statistic**	**Std. Error**	**Std. Test Statistic**	**Sig.**	**Adj. Sig.**[a]
LR-MR	-105.902	17.505	-6.050	0.000	0.000
LR-CM	178.936	24.027	7.447	0.000	0.000
MR-CM	73.034	24.665	2.961	0.003	0.009
L_{den}HH					
Sample 1 - 2	**Test Statistic**	**Std. Error**	**Std. Test Statistic**	**Sig.**	**Adj. Sig.**[a]
LR-MR	57.220	23.674	2.417	0.016	0.047
LR-CM	-58.819	17.493	-3.362	0.001	0.002
MR-CM	-1.598	24.212	-0.066	0.947	1.000
Each row tests the null hypothesis that the Sample 1 and Sample 2 distributions are the same. Asymptotic significances (2-sided tests) are displayed. The significance level is ,05.					

Tab. 47: Pairwise Comparisons of USSZ - reduction 3 - Vector-based approach

$L_{den}75$					
Sample 1 - 2	**Test Statistic**	**Std. Error**	**Std. Test Statistic**	**Sig.**	**Adj. Sig.**[a]
LR-MR	-81.581	17.581	-4.640	0.000	0.000
LR-CM	140.653	23.598	5.960	0.000	0.000
MR-CM	59.072	24.239	2.437	0.015	0.044
L_{den}DTV					
Sample 1 - 2	**Test Statistic**	**Std. Error**	**Std. Test Statistic**	**Sig.**	**Adj. Sig.**[a]
LR-MR	-100.770	17.581	-5.732	0.000	0.000
LR-CM	180.685	23.598	7.657	0.000	0.000
MR-CM	79.914	24.239	3.297	0.001	0.003
L_{den}HH					
Sample 1 - 2	**Test Statistic**	**Std. Error**	**Std. Test Statistic**	**Sig.**	**Adj. Sig.**[a]
LR-MR	-58.225	17.559	-3.316	0.001	0.003
LR-CM	58.637	23.336	2.513	0.012	0.036
MR-CM	0.413	23.880	0.017	0.986	1.000
Each row tests the null hypothesis that the Sample 1 and Sample 2 distributions are the same. Asymptotic significances (2-sided tests) are displayed. The significance level is ,05.					

Tab. 48: Hypothesis Test Summary - Gird-based approach

	Null Hypothesis	Test	Sig.	Decision
Initial parameter set				
	Null Hypothesis	**Test**	**Sig.**	**Decision**
1	The distribution of $\mathbf{L_{den}75}$ is the same across categories USSZ	Independent-Samples Kruskal-Wallis Test	.000	Reject the null hypothesis.
2	The distribution of $\mathbf{L_{den}DTV}$ is the same across categories USSZ	Independent-Samples Kruskal-Wallis Test	.000	Reject the null hypothesis.
3	The distribution of $\mathbf{L_{den}HH}$ is the same across categories USSZ	Independent-Samples Kruskal-Wallis Test	.032	Reject the null hypothesis.
Reduction 1				
	Null Hypothesis	**Test**	**Sig.**	**Decision**
1	The distribution of $\mathbf{L_{den}75}$ is the same across categories USSZ	Independent-Samples Kruskal-Wallis Test	.000	Reject the null hypothesis.
2	The distribution of $\mathbf{L_{den}DTV}$ is the same across categories USSZ	Independent-Samples Kruskal-Wallis Test	.000	Reject the null hypothesis.
3	The distribution of $\mathbf{L_{den}HH}$ is the same across categories USSZ	Independent-Samples Kruskal-Wallis Test	.057	Reject the null hypothesis.
Asymptotic significances are displayed. The significance level is ,05.				

Tab. 49: Pairwise Comparisons of USSZ - Grid-based approach

Sample 1 - 2	Test Statistic	Std. Error	Std. Test Statistic	Sig.	Adj. Sig.[a]
$\mathbf{L_{den}75}$					
LR-MR	-81.009	17.671	-4.584	0.000	0.000
LR-CM	160.223	26.543	6.036	0.000	0.000
MR-CM	79.214	28.052	2.824	0.005	0.014
$\mathbf{L_{den}DTV}$					
Sample 1 - 2	**Test Statistic**	**Std. Error**	**Std. Test Statistic**	**Sig.**	**Adj. Sig.[a]**
LR-MR	-88.069	17.671	-4.984	0.000	0.000
LR-CM	195.910	26.543	7.381	0.000	0.000
MR-CM	107.840	28.052	3.844	0.000	0.000
$\mathbf{L_{den}HH}$					
Sample 1 - 2	**Test Statistic**	**Std. Error**	**Std. Test Statistic**	**Sig.**	**Adj. Sig.[a]**
LR-MR	-13.207	17.556	-0.752	0.452	1.000
LR-CM	68.830	26.208	2.626	0.009	0.026
MR-CM	55.623	27.598	2.015	0.044	0.132
Each row tests the null hypothesis that the Sample 1 and Sample 2 distributions are the same. Asymptotic significances (2-sided tests) are displayed. The significance level is ,05.					

Tab. 50: Pairwise Comparisons of USSZ - reduction 1 - Grid-based approach

Sample 1 - 2	Test Statistic	Std. Error	Std. Test Statistic	Sig.	Adj. Sig.[a]
$\mathbf{L_{den}75}$					
LR-MR	-81.677	17.643	-4.629	0.000	0.000
LR-CM	147.733	26.312	5.615	0.000	0.000
MR-CM	66.055	27.768	2.379	0.017	0.052
$\mathbf{L_{den}DTV}$					
Sample 1 - 2	**Test Statistic**	**Std. Error**	**Std. Test Statistic**	**Sig.**	**Adj. Sig.[a]**
LR-MR	-90.556	17.643	-5.133	0.000	0.000
LR-CM	179.230	26.312	6.812	0.000	0.000
MR-CM	88.674	27.768	3.193	0.001	0.004
Each row tests the null hypothesis that the Sample 1 and Sample 2 distributions are the same. Asymptotic significances (2-sided tests) are displayed. The significance level is ,05.					

Tab. 51: Hypothesis Test Summary - Combined approach

Initial parameter set				
	Null Hypothesis	**Test**	**Sig.**	**Decision**
1	The distribution of **L_{den}75** is the same across categories USSZ	Independent-Samples Kruskal-Wallis Test	.000	Reject the null hypothesis.
2	The distribution of **L_{den}DTV** is the same across categories USSZ	Independent-Samples Kruskal-Wallis Test	.000	Reject the null hypothesis.
3	The distribution of **L_{den}HH** is the same across categories USSZ	Independent-Samples Kruskal-Wallis Test	.000	Reject the null hypothesis.
Reduction 2				
Asymptotic significances are displayed. The significance level is ,05.				

Tab. 52: Pairwise Comparisons of USSZ - Combined

L_{den}75					
Sample 1 - 2	**Test Statistic**	**Std. Error**	**Std. Test Statistic**	**Sig.**	**Adj. Sig.**[a]
LR-MR	-80.030	17.488	-4.576	0.000	0.000
LR-CM	154.163	23.872	6.458	0.000	0.000
MR-CM	74.133	24.047	3.083	0.002	0.006
L_{den}DTV					
Sample 1 - 2	**Test Statistic**	**Std. Error**	**Std. Test Statistic**	**Sig.**	**Adj. Sig.**[a]
LR-MR	-102.109	17.488	-5.839	0.000	0.000
LR-CM	197.497	23.872	8.273	0.000	0.000
MR-CM	95.389	24.047	3.967	0.000	0.000
L_{den}HH					
Sample 1 - 2	**Test Statistic**	**Std. Error**	**Std. Test Statistic**	**Sig.**	**Adj. Sig.**[a]
LR-MR	-60.899	17.515	-3.477	0.001	0.002
LR-CM	79.214	23.459	3.377	0.001	0.002
MR-CM	18.316	23.590	0.776	0.438	1.000
Each row tests the null hypothesis that the Sample 1 and Sample 2 distributions are the same. Asymptotic significances (2-sided tests) are displayed. The significance level is ,05.					

Tab. 53: Effect Size L_{den} - Vector-based approach

USSZ	**L_{den}75**			
	Initial	**Reduction 1**	**Reduction 2**	**Reduction 3**
LR-MR	0.186	0.192	0.181	0.179
LR-CM	0.267	0.263	0.269	0.268
MR-CM	0.117	0.109	0.121	0.118
USSZ	**L_{den}DTV**			
	Initial	**Reduction 1**	**Reduction 2**	**Reduction 3**
LR-MR	0.232	0.234	0.221	0.221
LR-CM	0.333	0.337	0.344	0.344
MR-CM	0.146	0.150	0.160	0.160

Tab. 54: Effect Size L_{den} - Gird-based approach

USSZ	**L_{den}75**	
	Initial	**Reduction 1**
LR-MR	0.174	0.174
LR-CM	0.275	0.243
MR-CM	0.137	0.127

Annex 3: Maps

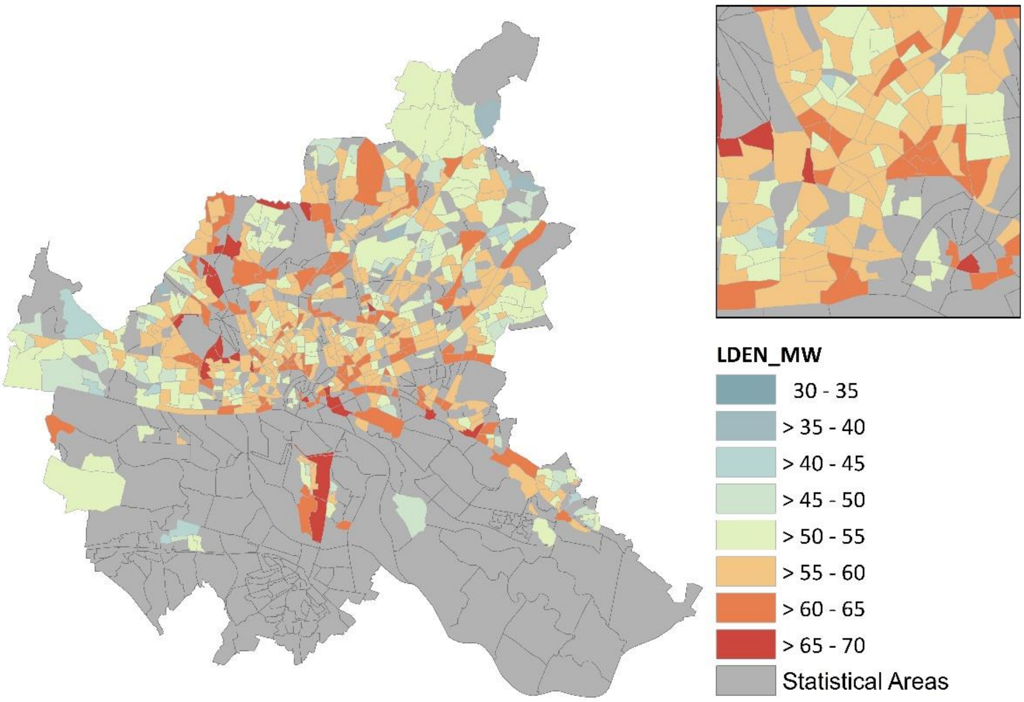

Fig. 45: LdenHH SAs
Illustration based on data of BSU, 2012 and STATISTIKAMT NORD, 2015.

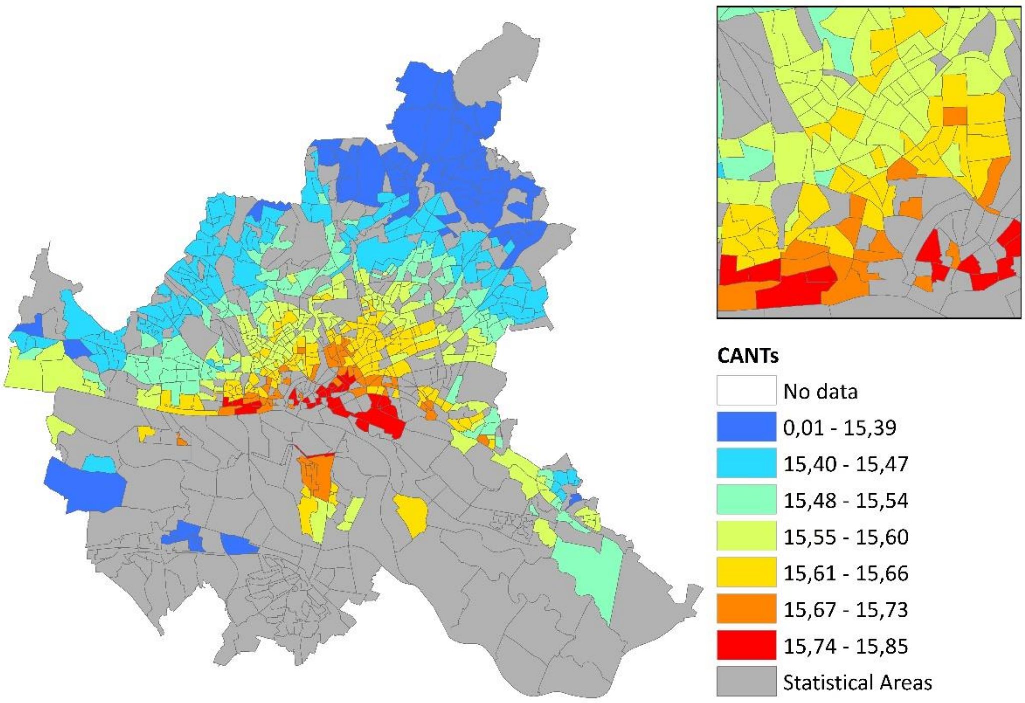

Fig. 46: Climatologically average night temperature in summer SAs
Illustration based on data of BOETTCHER, 2017 and STATISTIKAMT NORD, 2015.

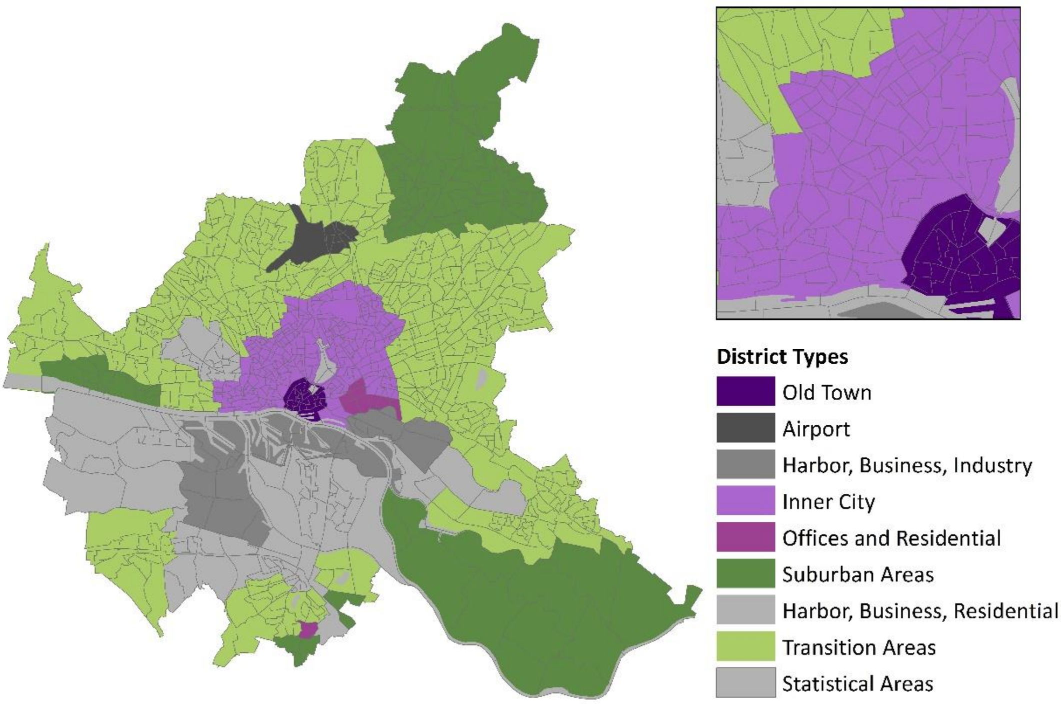

Fig. 47: District Types SAs
Illustration based on data of SZOMBATHELY et al., 2017 and STATISTIKAMT NORD, 2015.

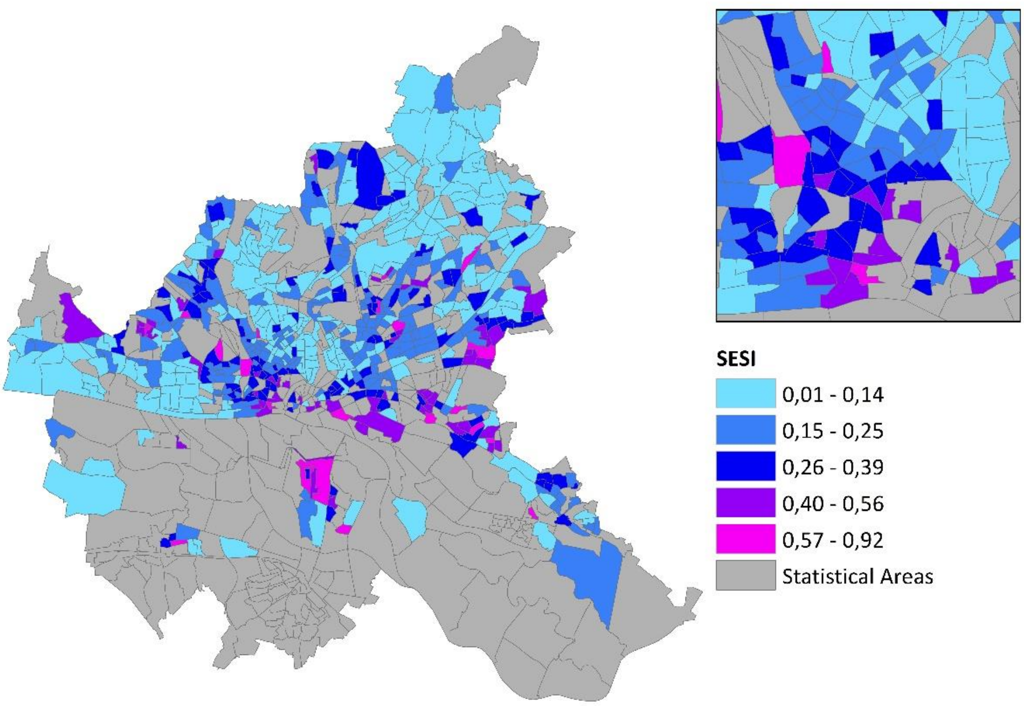

Fig. 48: Socio economic status index SAs
Illustration based on data of GEWOS, 2018 and STATISTIKAMT NORD, 2015.

REFERENCES

REFERENCES

Angel, S., Parent, J., & Civico, D. (2010). Ten compactness properties of circles: measuring shape in geography. *The Canadian Geographer / Le Géographe Canadien, 54(4),* 441–461. https://doi.org/10.1111/j.1541-0064.2009.00304.

Anjos, C.S., Lacerda, M.G., Andrade, L.D., & Salles, R.N. (2017). Classification of urban environments using feature extraction and random forest. 2017 IEEE International Geoscience and Remote Sensing Symposium (IGARSS), 1205-1208.

Albrecht, M. (2019). Generating a structural map of urban zones noise sensitivity using the concept of Local Climate Zones mapping. In Institute of Noise Control Engineering (Chair), *Conference Proceeindings:InterNoise 19,* Madrid

Arnds, D., Böhner, J., & Bechtel, B. (2017*).* Spatio-temporal variance and meteorological drivers of the urban heat island in a European city. *Theoretical and Applied Climatology, 128(1-2),* 43–61. https://doi.org/10.1007/s00704-015-1687-4

Arnfield, A. J. (2003). Two decades of urban climate research: a review of turbulence, exchanges of energy and water, and the urban heat island. *International Journal of Climatology, 23(1),* 1–26. https://doi.org/10.1002/joc.859

Attenborough, K., Li, K. M., & Horoshenkov, K. (2007). *Predicting outdoor sound*. London, New York: Taylor & Francis.

Babisch, W. (2002). The Noise/Stress Concept, Risk Assessment and Research Needs. *Noise & Health*, 4(16), 1–11. PMID: 12537836.

Babisch, W., Wolf, K., Petz, M., Heinrich, J., Cyrys, J., & Peters, A. (2014). Associations between Traffic Noise, Particulate Air Pollution, Hypertension, and Isolated Systolic Hypertension in Adults: The KORA Study*. Environmental Health Perspectives, 122(5),* 492–498. https://doi.org/10.1289/ehp.1306981

Babisch, W., Wölke, G., Heinrich, J., & Straff, W. (2014). Road traffic noise and hypertension - accounting for the location of rooms. *Environmental Research*, 133, 380–387. https://doi.org/10.1016/j.envres.2014.05.007

Backhaus, K., Erichson, B., Plinke, W., & Weiber, R. (2011). *Multivariate Analysemethoden: Eine anwendungsorientierte Einführung*; (13., überarbeitete Auflage). Springer-Lehrbuch. Berlin, Dordrecht, London, New York: Springer.

Backhaus, K., Erichson, B., Plinke, W., & Weiber, R. (2016). *Multivariate Analysemethoden.* Berlin, Heidelberg: Springer Berlin Heidelberg. https://doi.org/10.1007/978-3-662-46076-4

Bahrenberg, G., Giese, E., Mevenkamp, N., & Nipper, J. (2010). *Statistische Methoden in der Geographie* (5., vollst. neubearb. und korrigierte Aufl.). Studienbücher der Geographie. Stuttgart: Borntraeger.

Bai, X., Nath, I., Capon, A., Hasan, N., & Jaron, D. (2012). Health and wellbeing in the changing urban environment: Complex challenges, scientific responses, and the way forward.

Current Opinion in Environmental Sustainability, 4(4), 465–472. https://doi.org/10.1016/j.cosust.2012.09.009

Ballas, D. (2013). What makes a ‘happy city’? *Cities*, 32, S39-S50. https://doi.org/10.1016/j.cities.2013.04.009

Bechtel, B., Alexander, P. J., Beck, C., Böhner, J., Brousse, O., Ching, J., . . . Xu, Y. (2019). Generating WUDAPT Level 0 data – Current status of production and evaluation. *Urban Climate, 27,* 24–45. https://doi.org/10.1016/j.uclim.2018.10.001

Bechtel, B., Alexander, P., Böhner, J., Ching, J., Conrad, O., Feddema, J., . . . Stewart, I. (2015). Mapping Local Climate Zones for a Worldwide Database of the Form and Function of Cities. *ISPRS International Journal of Geo-Information, 4(1),* 199–219. https://doi.org/10.3390/ijgi4010199

Bechtel, B., & Daneke, C. (2012). Classification of Local Climate Zones Based on Multiple Earth Observation Data. *IEEE Journal of Selected Topics in Applied Earth Observations and Remote Sensing, 5(4),* 1191–1202. https://doi.org/10.1109/JSTARS.2012.2189873

Bechtel, B., & Schmidt, K. (2011). Floristic mapping data as a proxy for the mean Urban heat Island. *Climate Research, 49(1),* 45–58. https://doi.org/10.3354/cr01009

Beutel, M. E., Brähler, E., Ernst, M., Klein, E., Reiner, I., Wiltink, J., . . . Tibubos, A. N. (2020). Noise annoyance predicts symptoms of depression, anxiety and sleep disturbance 5 years later. *Findings from the Gutenberg Health Study. European Journal of Public Health, 30(3),* 516–521. https://doi.org/10.1093/eurpub/ckaa015

BMLFUW (2009). *Handbuch Umgebungslärm: Minderung und Ruhevorsorge*. Wien.

BMZ (2014). *Perspektiven der Urbanisierung – Städte nachhaltig gestalten* (No. 3).

Boettcher, M. (2017). *Selected climate mitigation and adaptation measures and their impact Selected climate mitigation and adaptation measures and their impact on the climate of the region of Hamburg* (Dissertation). Universität Hamburg.

Bouzir, T. A. K., & Zemmouri, N. (2017). Effect of urban morphology on road noise distribution. *Energy Procedia, 119*, 376–385. Elsevier. https://doi.org/10.1016/j.egypro.2017.07.121

Braun, B., Oßenbrügge, J., & Schulz, C. (2018). Environmental economic geography and environmental inequality: challenges and new research prospects. *Zeitschrift Für Wirtschaftsgeographie, 62(2),* 120–134. https://doi.org/10.1515/zfw-2018-0001

Breiman, L. (2001). Random Forest. *Machine Learning, 45(1),* 5–32. https://doi.org/10.1023/A:1010933404324

Brüel & Kjær Sound & Vibration Measurement A/S (Ed.). Powerful and intuitive environmental noise calculation and mapping: Predictor-LimA™ [Special issue]. Nærum: Brüel & Kjær Sound & Vibration Measurement A/S: Brüel & Kjær Sound & Vibration Measurement A/S.

BSU (2007). *Räumliches Leitbild Entwurf: Wachsende Stadt - Grüne Metropole am Wasser*. Hamburg.

BSU (2012). Strategische Lärmkarte Straßenverkehr Lden. Retrieved from http://www.hamburg.de/contentblob/3476512/data/lden-strasse-2012.pdf

BUE (2017). Lärmkarten Hamburg. Retrieved from https://www.hamburg.de/laermkarten/

Bundesministerium (2006, May 22). *Bekanntmachung der Vorläufigen Berechnungsverfahren für den Umgebungslärm nach § 5 Abs. 1 der Verordnung über die Lärmkartierung (34. BImSchV).* (Richtlinie, 34. BImSchV).

Ching, J., Mills, G., Bechtel, B., See, L., Feddema, J., Wang, X., . . . Theeuwes, N. (2018). WUDAPT: An Urban Weather, Climate, and Environmental Modeling Infrastructure for the Anthropocene. *Bulletin of the American Meteorological Society, 99(9),* 1907–1924. https://doi.org/10.1175/BAMS-D-16-0236.1

Cohen, B. H. (2008). Explaining psychological statistics. Hoboken, N.J: John Wiley.

Conrad, O., Bechtel, B., Bock, M., Dietrich, H., Fischer, E., Gerlitz, L., . . . Böhner, J. (2015). System for Automated Geoscientific Analyses (SAGA) v. 2.1.4. *Geoscientific Model Development, 8(7),* 1991–2007. https://doi.org/10.5194/gmd-8-1991-2015

Conrad, O. (2020). SAGA GIS (Version 7.6.0b) [Computer software]. SAGA GIS: SAGA GIS.

DataKustik GmbH (Ed.) (2018). Cadna/A: Einführung [Special issue]. Gilching.

DataKustik GmbH (2019). Cadna/A (Version MR 2) [Computer software]. DataKustik GmbH: DataKustik GmbH.

DEGA (2006). *Akustische Wellen und Felder: DEGA-Empfehlung 101*. Berlin.

DIN (2009-12). *Akustik - Begriffe*. (DIN, 1320:2009-12). Berlin: Beuth Verlag GmbH: Beuth Verlag GmbH.

Drahos, M., & Drahos, R. (2012). *Influence of meteorological conditions on propagation of sound*. Proprad.

Dratva, J., Zemp, E., Felber Dietrich, D., Bridevaux, P.-O., Rochat, T., Schindler, C., & Gerbase, M. W. (2010). Impact of road traffic noise annoyance on health-related quality of life: Results from a population-based study. Quality of Life Research: *An International Journal of Quality of Life Aspects of Treatment, Care and* Rehabilitation, 19(1), 37–46. https://doi.org/10.1007/s11136-009-9571-2

Duckworth, F.S. and Sandberg, J.S. (1954) The Effect of Cities upon Horizontal and Vertical Temperature Gradients. *Bulletin of American Meteorological Society, 35,* 198-207.

Dinno, A. (2015). Nonparametric Pairwise Multiple Comparisons in Independent Groups using Dunn's Test. *The Stata Journal: Promoting Communications on Statistics and Stata, 15(1),* 292–300. https://doi.org/10.1177/1536867X1501500117

Dugord, P.-A., Lauf, S., Schuster, C., & Kleinschmit, B. (2014). Land use patterns, temperature distribution, and potential heat stress risk – The case study Berlin, Germany. Computers, *Environment and Urban Systems, 48*, 86–98. https://doi.org/10.1016/j.compenvurbsys.2014.07.005

Duhme H, Weiland SK, Keil U, Kraemer B, Schmid M, Stender M, Chambless L. The association between self-reported symptoms of asthma and allergic rhinitis and self-reported traffic density on street of residence in adolescents. *Epidemiology. 1996 Nov;7(6),* 578-82. doi: 10.1097/00001648-199611000-00003. PMID: 8899382.

EEA (2009). *Ensuring quality of life in Europe's cities and towns: Tackling the environmental challenges by European and global change.* Luxembourg: Office for Official Publications of the European Communities.

EEA (2014). *Noise in Europe 2014* (EEA report). Luxembourg: Publications Office.

Erhorn-Kluttig, H., Jank, R., Schrempf, L., Duetz, A., Rumpel, F., Schrade, J., . . . Schmidt, D. (2011). *Energetische Quartiersplanung: Methoden - Technologien - Praxisbeispiele; [im Rahmen des Begleitforschungsprojektes der Förderinitiative "Energieeffiziente Stadt (EnEff:Stadt)" des Bundesministeriums für Wirtschaft und Technologie (BMWi). Stuttgart*: Fraunhofer-IRB-Verl.

Eriksson, C., Pershagen, G., & Nilsson, M. (2018). *Biological Mechanisms Related To Cardiovascular And Metabolic Effects By Environmental Noise*. Copenhagen.

END, Directive 2002/49/EC 1 (2002). Directive relating to the assessment and management of environmental Noise. L 189/12.

European Commission (Ed.). *Grünbuch der Europäischen Kommission vom 4. November 1996 über die künftige Lärmschutzpolitik:* DE/11/96/03030100.P00 (EN). Brüssel.

Evans, R. G., & Stoddart, G. L. (1990). Producing health, consuming health care. *Social Science & Medicine (1982), 31(12),* 1347–1363.

Eze, I. C., Foraster, M., Schaffner, E., Vienneau, D., Pieren, R., Imboden, M., . . . Probst-Hensch, N. (2020). Incidence of depression in relation to transportation noise exposure and noise annoyance in the SAPALDIA study. *Environment* International, 144, 106014. https://doi.org/10.1016/j.envint.2020.106014

Follmer, Robert & Gruschwitz, Dana (2019): *Mobilität in Deutschland - MiD Kurzreport. Ausgabe 4.0.* Studie von infas, DLR, IVT und infas 360 im Auftrag des Bundesministers für Verkehr und digitale Infrastruktur. (FE-Nr. 70.904/15). Bonn, Berlin. www.mobilitaet-in-deutschland.de

Franck, U., Krüger, M., Schwarz, N., Grossmann, K., Röder, S., & Schlink, U. (2013). Heat stress in urban areas: Indoor and outdoor temperatures in different urban structure types and subjectively reported well-being during a heat wave in the city of Leipzig. *Meteorologische Zeitschrift, 22(2),* 167–177. https://doi.org/10.1127/0941-2948/2013/0384

Fürst, P., & Kühne, R. (2010). *Strasenverkehrslärm: Eine Hilfestellung für Betroffene*. Berlin.

Füssel, H.-M. (2005). *Vulnerability in Climate Change Research: A Comprehensive Conceptual Framework.* (Working Paper), Breslauer.

Galea, S., Freudenberg, N., & Vlahov, D. (2005). Cities and population health. *Social Science & Medicine (1982), 60(5),* 1017–1033. https://doi.org/10.1016/j.socscimed.2004.06.036

Gamba, Lisini, P. E., Liu, P., Du, P., & Lin, H. (2012). Urban climate zone detection and discrimination using object-based analysis of VHR scenes: *Proceedings of the 4th GEOBIA*. Rio de Janeiro.

Garg, N., & Maji, S. (2014). A critical review of principal traffic noise models: Strategies and implications. *Environmental Impact Assessment Review, 46,* 68–81. https://doi.org/10.1016/j.eiar.2014.02.001

Gehl, J. (2012). *Leben zwischen Häusern*. Berlin: Jovis Verlag.

UN General Assembly (1972, October 15). *Declaration of the United Nations Conference on the Human Environment: Stockholm Declaration 1972*. Stockholm. Retrieved from UN General Assembly website: https://www.refworld.org/docid/3b00f1c840

Gertz, C., & Maaß, J. (2015). *Auswirkungen von steigenden Energiepreisen auf die Mobilität und Landnutzung in der Metropolregion Hamburg*. Harburger Berichte zur Verkehrsplanung und Logistik Band 13. (Harburger Berichte zur Verkehrsplanung und Logistik, Bd. 13). Münster: Monsenstein und Vannerdat.

GEWOS (2018). *Sozialmonitoring Integrierte Stadtteilentwicklung 2017: Karten- und Tabellenband.* Hamburg.

Giunta, M. B., Suriano, M. T., Souza, C. L. de, & Viviani, E. (2015). The role of traffic flow and the Floor Space Index (FSI) in predicting environmental noise. *Conference Proceedings CUPUM, 143.* Cambridge.

Golmohammadi, R., Darvishi, E., Shafiee Motlagh, M., & Faradmal, J. (2021). Role of individual and personality traits in occupational noise-induced psychological effects. *Applied Acoustics, 173,* 107699. https://doi.org/10.1016/j.apacoust.2020.107699

Gregory, D., & Urry, J. (1985). Social relations and spatial structures. *Critical human geography.* Basingstoke, Hampshire: Macmillan.

Grouven, U., Bender, R., Ziegler, A., & Lange, S. (2007). Der Kappa-Koeffizient [The kappa coefficient]. *Deutsche medizinische Wochenschrift* (1946), 132 Suppl 1, e65-8. https://doi.org/10.1055/s-2007-959046

Guski, R., Schreckenberg, D., & Schuemer, R. (2017). Who Environmental Noise Guidelines for the European Region: A Systematic Review on Environmental Noise and Annoyance. *International Journal of Environmental Research and Public Health, 14(12).* https://doi.org/10.3390/ijerph14121539

Hägerstrand, T. (1970). What about people in Regional Science? *Papers of the Regional Science Association, 24(1), 6–21*. https://doi.org/10.1007/BF01936872

Hägerstrand, T (1974). The impact of transport on the quality of life. Lund: Lunds universitets kulturgeografiska institution

Han, J.-Y., Baik, J.-J., & Lee, H. (2014). Urban impacts on precipitation*. Asia-Pacific Journal of Atmospheric* Sciences, 50(1), 17–30. https://doi.org/10.1007/s13143-014-0016-7

Hancock, T. (1985). The mandala of health: A model of the human ecosystem. *Family & Community Health, 8(3),* 1–10. https://doi.org/10.1097/00003727-198511000-00002

Hannah, L., & Hunt, M. (2006). Ground, Terrain and Structure Effects on Sound Propagation: The fourth in a series of articles taken from a paper entitled “Factors Affecting Outdoor Sound Propagation“. *New Zealand Acoustics, 3(20),* 22–30.

Hao, Y., Kang, J., Krijnders, D., & Wörtche, H. (2013). On the Relationship between Traffic Noise Resistance and Urban Morphology in Low-Density Residential Areas. *Acta Acustica United with Acustica, 101(3),* 510–519. https://doi.org/10.3813/AAA.918848

Hastie, T., Tibshirani, R., & Friedman, J. H. (2009). The elements of statistical learning: Data mining, inference, and prediction (Second edition). *Springer series in statistics*. New York: Springer.

Häußermann, H., & Siebel, W. (1978). *Thesen zur Soziologie der Stadt*. *Leviathan, 6(4),* 484–500. Retrieved from http://www.jstor.org/stable/23983057

Hecht, R. (2014). *Automatische Klassifizierung von Gebäudegrundrissen: Ein Beitrag zur kleinräumigen Beschreibung der Siedlungsstruktur*. Zugl.: Dresden, Techn. Univ., Diss., 2013. IÖR-Schriften: Vol. 63. Berlin: Rhombos-Verl. Retrieved from http://d-nb.info/1058946455/34

Henn, H., Sinambari, G. R. [Gh. Reza], & Fallen, M. (2008). *Ingenieurakustik: Physikalische Grundlagen und Anwendungsbeispiele.* Wiesbaden: Springer Vieweg. https://doi.org/10.1007/978-3-8348-9537-0

Héritier, H., Vienneau, D., Frei, P., Eze, I. C., Brink, M., Probst-Hensch, N., & Röösli, M. (2014). The association between road traffic noise exposure, annoyance and health-related quality of life (HRQOL). *International Journal of Environmental Research and Public Health, 11(12)*, 12652–12667. https://doi.org/10.3390/ijerph111212652

Hoffmann, P. [Peter], Fischereit, J., Heitmann, S., Schlünzen, K., & Gasser, I. (2018). Modeling Exposure to Heat Stress with a Simple Urban Model. *Urban Science, 2(1),* 9. https://doi.org/10.3390/urbansci2010009

Hoffmann, P. [Peter], Krueger, O., & Schlünzen, K. H. [K. Heinke] (2012). A statistical model for the urban heat island and its application to a climate change scenario. *International Journal of Climatology, 32(8),* 1238–1248. https://doi.org/10.1002/joc.2348

Hu, J., Ghamisi, P., & Zhu, X. (2018). Feature Extraction and Selection of Sentinel-1 Dual-Pol Data for Global-Scale Local Climate Zone Classification. *ISPRS International Journal of Geo-Information, 7(9),* 379. https://doi.org/10.3390/ijgi7090379

Hunter, M. R., & Askarinejad, A. (2015). Designer's approach for scene selection in tests of preference and restoration along a continuum of natural to manmade environments. *Frontiers in Psychology, 6,* 1228. https://doi.org/10.3389/fpsyg.2015.01228

Hupeng, W., Kang, J., & Hong, J. (2019). Effects of urban street spatial parameters on sound propagation. *Environment and Planning B: Urban Analytics and City Science, 46(2),* 341–358. https://doi.org/10.1177/2399808317714799

Ising, H., Lange-Asschenfeldt, H., Lieber, G. F., Weinhold, H., & Eilts, M. (2003). Respiratory and dermatological diseases in children with long-term exposure to road traffic immissions. *Noise & Health, 5(19)*, 41–50. Retrieved from http://www.ncbi.nlm.nih.gov/pubmed/12804211

ISO (1993-06). *Acoustics - Attenuation of sound during propagation outdoors.* (ISO, 9613-1:1993-06). Geneva.

ISO (1996-12). *Acoustics - Attenuation of sound during propagation outdoo*rs. (ISO, 9613-2:1996-12). Berlin: Beuth Verlag GmbH: Beuth Verlag GmbH.

ISO (1999-10). *Akustik - Dämpfung des Schalls bei der Ausbreitung im Freien.* (ISO, 9613-2:1999-10). Berlin: Beuth Verlag GmbH: Beuth Verlag GmbH.

ISO (2017-7). *Acoustics - Description, measurement and assessment of environmental noise*. (ISO, 1996-2:2017-07). Geneva.

Jakovljevic, B., Paunovic, K., & Belojevic, G. (2009). Road-traffic noise and factors influencing noise annoyance in an urban population. *Environment International*, *35(3),* 552–556. https://doi.org/10.1016/j.envint.2008.10.001

Jarup, L., Babisch, W., Houthuijs, D., Pershagen, G. [Goran], Katsouyanni, K., Cadum, E., . . . Vigna-Taglianti, F. (2008). Hypertension and exposure to noise near airports: The HYENA study. *Environmental Health* Perspectives, 116(3), 329–333. https://doi.org/10.1289/ehp.10775

Jürgens, C., & Kasper, B. (2006). *Alltagsmobilität, Raum und Lebensstile. In K. J. Beckmann (Ed.), StadtLeben - Wohnen, Mobilität und Lebensstil: Neue Perspektiven für Raum- und Verkehrsentwicklung* (1st ed., pp. 125–141). Wiesbaden, Germany: VS, Verl. für Sozialwiss.

Kang, J. (2001). Sound Propagation in Interconnected Urban Streets: A Parametric Study. *Environment and Planning B: Planning and Design, 28(2),* 281–294. https://doi.org/10.1068/b2680

Kaveckis, G. (2017). *Modeling future populations vulnerability to heat waves in Greater Hamburg* (Dissertation). Universität Hamburg, Hamburg.

Kaveckis, G., & Bechtel, B. [Benjamin] (2014). Land Use Based Urban Vulnerability to Climate Change Assessment. In D. Cygas & T. Tollazzi (Eds.), *9th ICEE: Selected papers: [proceedings] (p. 268).* Vilnius, Lithuania: Vilnius Gediminas Technical University Press Technika [etc.]. https://doi.org/10.3846/enviro.2014.122

Kheirbek, I., Ito, K., Neitzel, R., Kim, J., Johnson, S., Ross, Z., . . . Matte, T. (2014). Spatial variation in environmental noise and air pollution in New York City. Journal of Urban Health: *Bulletin of the New York Academy of Medicine, 91(3),* 415–431. https://doi.org/10.1007/s11524-013-9857-0

King, G., Roland-Mieszkowski, M., Jason, T., & Rainham, D. G. (2012). Noise levels associated with urban land use. Journal of Urban Health: *Bulletin of the New York Academy of Medicine, 89(6),* 1017–1030. https://doi.org/10.1007/s11524-012-9721-7

Knieling, J. (2010). *Leitbilder nachhaltiger Raum- und Siedlungsentwicklung in Großstadtregionen: Reflektionen am Beispiel von Hamburg, Hanoi und Helsinki.: „Stadt der Zukunft –Zukunft der Stadt. Probleme und Perspektiven nachhaltiger städtischer Transportsysteme im deutsch-vietnamesischen interdisziplinären Dialog*. Hanoi.

Köthe, U. (2017). VIGRA Homepage: Machine Learning. random forest classifier with various tree building strategies. Retrieved from http://ukoethe.github.io/vigra/

Krefis, A., Albrecht, M., Kis, A., Jagodzinski, A., Augustin, M., & Augustin, J. (2017a Hägerstrand). Associations of Noise and Socioeconomic and -Demographic Status on Cardiovascular and Respiratory Diseases on Borough Level in a Large German City State. *Urban* Science, 1(3), 27. https://doi.org/10.3390/urbansci1030027

Krefis, A., Augustin, M., Schlünzen, K. [Katharina], Oßenbrügge, J., & Augustin, J. (2018). How Does the Urban Environment Affect Health and Well-Being? A Systematic Review. *Urban Science, 2(1),* 21. https://doi.org/10.3390/urbansci2010021

Krefis, A. C., Albrecht, M., Kis, A., Langenbruch, A., Augustin, M., & Augustin, J. (2017b). Multivariate Analysis of Noise, Socioeconomic and Sociodemographic Factors and Their Association with Depression on Borough Level in the City State of Hamburg, Germany. *Journal of Depression and Therapy, 1(4)*, 1–14. https://doi.org/10.14302/issn.2476-1710.jdt-17-1564

Kuttruff, H. (2007). Acoustics: An introduction. London: Taylor & Francis. Retrieved from http://site.ebrary.com/lib/alltitles/docDetail.action?docID=10155663Kruskal, W. H., & Wallis, W. A. (1952). Use of Ranks in One-Criterion Variance Analysis. *Journal of the American Statistical Association, 47(260),* 583. https://doi.org/10.2307/2280779

Lechner, C., Schnaiter, D., & Bose-O'Reilly, S. (2019). Combined Effects of Aircraft, Rail, and Road Traffic Noise on Total Noise Annoyance—A Cross-Sectional Study in Innsbruck. *International Journal of Environmental Research and Public Health, 16(18).* https://doi.org/10.3390/ijerph16183504

Lelovics, E., Unger, J., Gál, T. [T.], & Gál, C. V. (2014). Design of an urban monitoring network based on Local Climate Zone mapping and temperature pattern modelling. *Climate Research, 60(1),* 51–62. https://doi.org/10.3354/cr01220

LGV Hamburg (2022*). 3D-Stadtmodell LoD2-DE Hamburg*. LGV. Retrieved from https://www.govdata.de/daten/-/details/3d-stadtmodell-lod2-de-hamburg

Lin, M., Lucas, H. C., & Shmueli, G. (2013). Research Commentary —Too Big to Fail: Large Samples and the p -Value Problem. *Information Systems Research, 24(4),* 906–917. https://doi.org/10.1287/isre.2013.0480

Mage, D., Ozolins, G., Peterson, P., Webster, A., Orthofer, R., Vandeweerd, V., & Gwynne, M. (1996). Urban air pollution in megacities of the world. *Atmospheric Environment, 30(5),* 681–686. https://doi.org/10.1016/1352-2310(95)00219-7

McGarigal, K. (2015). *Fragstats*. University of Massachusetts Amherst: University of Massachusetts Amherst.

Mendis, S., & Banerjee, A. (2010). Equity, social determinants and public health programmes. In E. Blas & A. S. Kurup (Eds.), Nonserial Publications. *Equity, social determinants and public health programmes.* Geneva: World Health Organization.

Menze, B. H., Kelm, B. M., Masuch, R., Himmelreich, U., Bachert, P., Petrich, W., & Hamprecht, F. A. (2009). A comparison of random forest and its Gini importance with standard chemometric methods for the feature selection and classification of spectral data. *BMC Bioinformatics, 10, 213.* https://doi.org/10.1186/1471-2105-10-213

Miedema, H. M. [H. M.], & Oudshoorn, C. G. (2001). Annoyance from transportation noise: Relationships with exposure metrics DNL and DENL and their confidence intervals. *Environmental Health Perspectives, 109(4),* 409–416. https://doi.org/10.2307/3454901

Miedema, H. M. [Henk M.E.] (2007). Annoyance Caused by Environmental Noise: Elements for Evidence-Based Noise Policies. *Journal of Social Issues, 63(1), 41–57.* https://doi.org/10.1111/j.1540-4560.2007.00495.x

Moore, B. C. J. (2014). Psychoacoustics. In T. D. Rossing (Ed.), *Springer handbook of acoustics (2nd ed., pp. 475–518)*. Dordrecht: Springer.

Moussiopoulos, N. (Ed.) (2003). *Air Quality in Cities.* Springer.

MWAW (2018). *Lärmfibel: Hinweise für die Bauleitplanung*. Stuttgart

Neun, & Steiniger (Eds.) (2005). Modelling cartographic relations for categorical maps. *Conference Proceedings International Cartographic Conference (ICC 2005).*

Northridge, M. E., Sclar, E. D., & Biswas, M. P. (2003). Sorting out the connections between the built environment and health: A conceptual framework for navigating pathways and planning healthy cities. *Journal of Urban Health, 80(4)*, 556–568. https://doi.org/10.1093/jurban/jtg064

Nyborg, W., & Mintzer, D. (1955). Review of Sound Propagation in the lower Athmosphere. *ADC Technical Report No. 54-602.* Providence. Retrieved from Defense Technical Information Center website: http://www.dtic.mil/docs/citations/AD0067880

OECD (2019). *OECD-Berichte zur Regionalentwicklung: Metropolregion Hamburg, Deutschland.* OECD. https://doi.org/10.1787/6843d6f0-de

Oke, T. R. (1973). City size and the urban heat island. *Atmospheric Environment (1967), 7(8),* 769–779. https://doi.org/10.1016/0004-6981(73)90140-6

Oke, T. R. (1982). The energetic basis of the urban heat island. *Quarterly Journal of the Royal Meteorological Society, 108(455),* 1–24. https://doi.org/10.1002/qj.49710845502

Oke, T. R. (1987). *Boundary Layer Climate*s (2nd ed.). London: Routledge.

Oke, T. R. (1988). Street design and urban canopy layer climate. *Energy and Buildings, 11(1-3),* 103–113. https://doi.org/10.1016/0378-7788(88)90026-6

Oke, T. R., & Fuggle, R. F. (1972). Comparison of urban/rural counter and net radiation at night. *Boundary-Layer Meteorology, 2(3),* 290–308. https://doi.org/10.1007/BF02184771

Oliveira, M., & Silva, L. (2011). The influence of urban form on facades noise levels. WSEAS TRANSACTIONS on ENVIRONMENT and DEVELOPMENT. (7), 125–136.

Oßenbrügge, J., Pohl, T., & Vogelpohl, A. (2009). Entgrenzte Zeitregime und wirtschaftsräumliche Konzentrationen*. Zeitschrift Für Wirtschaftsgeographie, 53(1-2).* https://doi.org/10.1515/zfw.2009.0018

Pearce, N. (2000). The ecological fallacy strikes back. *Journal of Epidemiology and Community Health, 54(5),* 326–327. https://doi.org/10.1136/jech.54.5.326

Pierce, A. D. (2014). Basic Linear Acoustics. In T. D. Rossing (Ed.), *Springer handbook of acoustics* (2nd ed., pp. 29–116). Dordrecht: Springer.

Pohl, T. (2009). Entgrenzte Stadt: Räumliche Fragmentierung und zeitliche Flexibilisierung in der Spätmoderne. *Urban Studies.* Bielefeld: Transcript.

Rasch, B., Friese, M., & Hofmann, W. (2021). *Quantitative Methoden* (5. Auflage). Lehrbuch. Berlin: Springer. https://doi.org/10.1007/978-3-662-63284-0

Ren, C. (2017). *WUDAPT Global Initiative: Census of Global Cities*. Retrieved from http://www.wudapt.org/wp-content/uploads/2017/06/WUDAPT-Briefing-Doc_20170630.pdf

Ren, C., Ng, E., Mills, G., Ching, J., Bechtel, B., See, L. , . . . Aliaga, D.. WUDAPT Global Initiative: Census of Global Cities: Briefing 2017, 2017. Retrieved from http://www.wudapt.org/

Rey Gozalo, G., Suárez, E., Montenegro, A. L., Arenas, J. P., Barrigón Morillas, J. M., & Montes González, D. (2020). *Noise Estimation Using Road and Urban Features. Sustainability, 12(21),* 9217. https://doi.org/10.3390/su12219217

Ross, B. M., & Wolde, T. ten (2001). Noise from traffic as a worldwide policy problem. *Noise Control Engineering Journal, 49(4),* 159. https://doi.org/10.3397/1.2839651

Rossing, T. D. (2014). Introduction to Acoustics. In T. D. Rossing (Ed.), *Springer handbook of acoustics* (2nd ed., pp. 1–10). Dordrecht: Springer.

Ryu, H., Park, I. K., Chun, B. S., & Chang, S. I. (2017). Spatial statistical analysis of the effects of urban form indicators on road-traffic noise exposure of a city in South Korea. *Applied Acoustics, 115,* 93–100. https://doi.org/10.1016/j.apacoust.2016.08.025

Sandri, M., & Zuccolotto, P. (2006). Variable Selection Using Random Forests. In S. Zani, A. Cerioli, & M. R. e. al. (Eds*.), Studies in Classification, Data Analysis, and Knowledge Organization.* Springer-Verlag. https://doi.org/10.1007/3-540-35978-8_30

Schlicht, W. (Ed.) (2017). *essentials. Urban Health*. Wiesbaden: Springer Fachmedien Wiesbaden. https://doi.org/10.1007/978-3-658-18654-8

Schlosberg, D. (2007). *Defining Environmental Justice*. Oxford University Press. https://doi.org/10.1093/acprof:oso/9780199286294.001.0001

Schlünzen, K. H., Hoffmann, P., Rosenhagen, G., & Riecke, W. (2009). Long-term changes and regional differences in temperature and precipitation in the metropolitan area of Hamburg. *International Journal of Climatology, 30(8),* 1121–1136. https://doi.org/10.1002/joc.1968

Schultz, T. J. (1978). Synthesis of Social Surveys on noise annoyance. *Journal of the Acoustical Society of America. (64),* 377–405.

Shanahan, D. F., Lin, B. B., Bush, R., Gaston, K. J., Dean, J. H., Barber, E., & Fuller, R. A. (2015). Toward improved public health outcomes from urban nature. *American Journal of Public Health, 105(3),* 470–477. https://doi.org/10.2105/AJPH.2014.302324

Shannon, J. (2018). *The health effects of environmental noise*. Commonwealth of Australia as represented by the Department of Health.

Sheng, N., & Tang, U. W. [U. Wa] (2011). Spatial analysis of urban form and pedestrian exposure to traffic noise. *International Journal of Environmental Research and Public Health, 8(6),* 1977–1990. https://doi.org/10.3390/ijerph8061977

Shepherd, J. M. (2005). A Review of Current Investigations of Urban-Induced Rainfall and Recommendations for the Future. *Earth Interactions, 9(12),* 1–27. https://doi.org/10.1175/EI156.1

Silva, L. T. [Lígia T], Fernando, F., Rodrigues, D. S., & Campos, A. (2018). Assessing the influence of urban geometry on noise propagation by using the sky view factor. *Journal of Environmental Planning and Management, 60(60),* 1–18. https://doi.org/10.1080/09640568.2017.1319804

Silva, L. T. [Lígia T.], Oliveira, M., & Silva, J. F. (2014). Urban form indicators as proxy on the noise exposure of buildings. *Applied Acoustics, 76,* 366–376. https://doi.org/10.1016/j.apacoust.2013.07.027

Sinambari, G. R., Sentpali, S., & Kunz, F. (2014). *Ingenieurakustik: Physikalische Grundlagen und Anwendungsbeispiele* (5th ed.). SpringerLink. Wiesbaden: Springer Vieweg. Retrieved from http://dx.doi.org/10.1007/978-3-658-05072-6 https://doi.org/10.1007/978-3-658-05072-6

Smits, P. C., Dellepiane, S. G., & Schowengerdt, R. A. (1999). Quality assessment of image classification algorithms for land-cover mapping: A review and a proposal for a cost-based approach. *International Journal of Remote Sensing, 20(8),* 1461–1486. https://doi.org/10.1080/014311699212560

Softnoise GmbH. LimA [Computer software]. Softnoise GmbH: Softnoise GmbH.

SoundPLAN GmbH. SoundPLAN GmbH [Computer software]. SoundPLAN GmbH: SoundPLAN GmbH.

Souza, L. C. L. de, & Giunta, M. B. (2011). Urban indices as environmental noise indicators. *Computers, Environment and Urban Systems, 35(5),* 421–430. https://doi.org/10.1016/j.compenvurbsys.2011.06.001

Staab, J., Schady, A., Weigand, M., Lakes, T., & Taubenböck, H. (2022). Predicting traffic noise using land-use regression-a scalable approach. *Journal of Exposure Science & Environmental Epidemiology, 32(2),* 232–243. https://doi.org/10.1038/s41370-021-00355-z

Stansfeld, S., Clark, C., Smuk, M., Gallacher, J., & Babisch, W. (2021). Road traffic noise, noise sensitivity, noise annoyance, psychological and physical health and mortality. *Environmental Health : A Global Access Science Source, 20(1),* 32. https://doi.org/10.1186/S12940-021-00720-3

Statistikamt Nord (2015). *Faltblatt Mikrozensus 2015*. Retrieved from http://www.statistik-nord.de/fileadmin/Dokumente/Faltbl%C3%A4tter/Faltblatt_Mikrozensus_2015.pdf.

Statistikamt Nord (2016). *Statistisches Jahrbuch Hamburg 2015/2016: Bauen und Wohnen.* Hamburg. fileadmin/Dokumente/Jahrb%C3%BCcher/Hamburg/JB15HH_Gesamt_Internet_korr.pdf

Steele, C. (2001). A critical review of some traffic noise prediction models. *Applied Acoustics, 62(3),* 271–287. https://doi.org/10.1016/S0003-682X(00)00030-X

Stehman, S. V. (2009). Sampling designs for accuracy assessment of land cover. *International Journal of Remote Sensing, 30(20),* 5243–5272. https://doi.org/10.1080/01431160903131000

Steiniger, S., & Weibel, R. (2007). Relations among Map Objects in Cartographic Generalization. *Cartography and Geographic Information Science, 34(3),* 175–197. https://doi.org/10.1559/152304007781697866

Stewart, I. D. (2011). A systematic review and scientific critique of methodology in modern urban heat island literature. *International Journal of Climatology, 31(2),* 200–217. https://doi.org/10.1002/joc.2141

Stewart, I. D., & Oke, T. R. (2012). Local Climate Zones for Urban Temperature Studies. Bulletin of the *American Meteorological Society, 93(12),* 1879–1900. https://doi.org/10.1175/BAMS-D-11-00019.1

S Storper, Michael (2013) Keys to the city: how economics, institutions, social interactions and politics affect regional development. *Princeton University Press*. Princeton, USA.

Story, M., & Congalton, R. G. (1986). Accuracy Assessment: A User's Perspective. *Photogrammetric Engineering and Remote Sensing, 52(3),* 397–399.

Strobl, C., Boulesteix, A.-L., Kneib, T., Augustin, T., & Zeileis, A. (2008). Conditional variable importance for random forests. *BMC Bioinformatics, 9, 307*. https://doi.org/10.1186/1471-2105-9-307

Strobl, C., Malley, J., & Tutz, G. (2009). An Introduction to Recursive Partitioning: Rationale, Application and Characteristics of Classification and Regression Trees, Bagging and Random Forests. *Psychological Methods, 14(4),* 323–348. https://doi.org/10.1037/a0016973

Szombathely, M. von, Albrecht, M., Antanaskovic, D., Augustin, J., Augustin, M., Bechtel, B., . . . Schlünzen, K. (2017). A Conceptual Modeling Approach to Health-Related Urban Well-Being. *Urban Science, 1(2),* 1–18. https://doi.org/10.3390/urbansci1020017

Szombathely, M. von, Albrecht, M., Augustin, J., Bechtel, B. [Benjamin], Dwinger, I., Gaffron, P., . . . Strüver, A. (2018). Relation between Observed and Perceived Traffic Noise and Socio-Economic Status in Urban Blocks of Different Characteristics. Urban Science, 2(1). https://doi.org/10.3390/urbansci2010020

Tang, U. W., & Wang, Z. S. (2007). Influences of urban forms on traffic-induced noise and air pollution: Results from a modelling system*. Environmental Modelling & Software, 22(12),* 1750–1764. https://doi.org/10.1016/j.envsoft.2007.02.003

Thornes, J. E. (2002). IPCC, 2001: Climate change 2001: impacts, adaptation and vulnerability. *International Journal of Climatology, 22(10),* 1285–1286. https://doi.org/10.1002/joc.775

Tong, H., & Kang, J. (2021). Relationship between urban development patterns and noise complaints in England. *Environment and Planning B: Urban Analytics and City Science, 48(6),* 1632–1649. https://doi.org/10.1177/2399808320930247

Turner, B. L., Kasperson, R. E., Matson, P. A., McCarthy, J. J., Corell, R. W., Christensen, L., . . . Schiller, A. (2003). A framework for vulnerability analysis in sustainability science. *Proceedings of the National Academy of Sciences of the United States of America, 100(14),* 8074–8079. https://doi.org/10.1073/pnas.1231335100

UBA (2010a). *Lärmaktionsplanung in Ballungsräumen - Minderungspotentiale am Beispiel Hamburg.* Dessau-Roßlau: UBA.

UBA (2010b). *Lärmwirkungen: Dosis-Wirkungsrelationen*. Dessau-Roßlau: UBA.

UBA (2015). *Umweltbewusstsein in Deutschland 2014: Ergebnisse einer repräsentativen Bevölkerungsumfrage.* Dessau-Roßlau: UBA.

UN (2018). *WORLD CITIES REPORT 2018: Main Report.* Nairobi. Retrieved from http://wcr.unhabitat.org/main-report/

VBUS (2006) V*orläufige Berechnungsmethode für den Umgebungslärm an Straßen.* 58 Bundesanzeiger.

VDI (1988-01). *Schallausbreitung im Freien*. (VDI, 2714). Düsseldorf.

Veit, I. (2005). *Technische Akustik: Grundlagen der physikalischen, physiologischen und Elektroakustik* (6th ed.). Kamprath-Reihe. Würzburg: Vogel.

Wang, B., & Kang, J. (2011). Effects of urban morphology on the traffic noise distribution through noise mapping: A comparative study between UK and China. *Applied Acoustics, 72(8),* 556–568. https://doi.org/10.1016/j.apacoust.2011.01.011

Wang, R., Ren, C., Xu, Y., Lau, K. K.-L., & Shi, Y. (2018). Mapping the local climate zones of urban areas by GIS-based and WUDAPT methods: A case study of Hong Kong. *Urban Climate, 24,* 567–576. https://doi.org/10.1016/j.uclim.2017.10.001

Wardhani, N. W. S., Rochayani, M. Y., Iriany, A., Sulistyono, A. D., & Lestantyo, P. (2019). Cross-validation Metrics for Evaluating Classification Performance on Imbalanced Data. In 2019 *International Conference on Computer, Control, Informatics and its Applications (IC3INA) (pp. 14–18).* IEEE. https://doi.org/10.1109/IC3INA48034.2019.8949568

Weber, N. (2015). *Using landscape metrics to assess traffic noise, air pollution and temperature conditions.* Dissertation. Berlin.

Weber, N., Haase, D., & Franck, U. (2014a). Assessing modelled outdoor traffic-induced noise and air pollution around urban structures using the concept of landscape metrics. *Landscape and Urban Planning, 125, 105–116.* https://doi.org/10.1016/j.landurbplan.2014.02.018

Weber, N., Haase, D., & Franck, U. (2014b). Traffic-induced noise levels in residential urban structures using landscape metrics as indicators. *Ecological Indicators, 45,* 611–621. https://doi.org/10.1016/j.ecolind.2014.05.004

Weng, Q. (Ed.) (2014). *Global urban monitoring and assessment through Earth observation,10.* Boca Raton, FL: CRC Press Taylor & Francis Group.

WHO (1946). *Constitution of the World Health Organization.* American Journal of Public Health and the Nation's Health, 36(11), 1315–1323. https://doi.org/10.2105/ajph.36.11.1315

WHO (2010). *Environmental health inequalities in Europe.* Geneva: World Health Organization.

WHO (2011). *Burden of Disease from Environmental Noise: Quantification of Healthy Life Years Lost in Europe*. Geneva: World Health Organization. Retrieved from http://gbv.eblib.com/patron/FullRecord.aspx?p=1582968

WHO (2018). *Environmental noise guidelines for the European Region*. Copenhagen, Denmark: World Health Organization, Regional Office for Europe.

WHO (2019). *Environmental health inequalities in Europe. Second assessment report.* Retrieved from WHO Regional Office for Europe; WHO-Regionalbüro für Europa; Le Bureau régional de l'OMS pour l'Europe; Всемирная организация здравоохранения; ВОЗ website: https://apps.who.int/iris/bitstream/handle/10665/325176/9789289054157-eng.pdf?sequence=1&isAllowed=y

WHO (2020). *Methods and Data Sources for Global Burden of Disease 2000–2019*. Geneva.

Willems, W., Dinter, S., & Schild, K. (2006). *Vieweg Handbuch Bauphysik Teil 2* (1. Aufl.). Wiesbaden: Vieweg.

Wölfel Meßsysteme. IMMI [Computer software]. Wölfel Meßsysteme: Wölfel Meßsysteme.

Wurm, M., Schmitt, A., & Taubenböck, H. (2016). Building Types' Classification Using Shape-Based Features and Linear Discriminant Functions*. IEEE Journal of Selected Topics in Applied Earth Observations and Remote Sensing, 9(5),* 1901–1912. https://doi.org/10.1109/JSTARS.2015.2465131

Yoo, C., Han, D., Im, J., & Bechtel, B. [Benjamin] (2019). Comparison between convolutional neural networks and random forest for local climate zone classification in mega urban areas using Landsat images*. ISPRS Journal of Photogrammetry and Remote Sensing, 157,* 155–170. https://doi.org/10.1016/j.isprsjprs.2019.09.009

Yu, B., Ma, H., & Kang, J. (2019). A Hybrid Model for Investigating the Effect of Scattering from Building Façade on Sound Propagation in Street Canyons. *Applied Sciences, 9(14),* 2803. https://doi.org/10.3390/app9142803

Zhang, C., & Ma, Y. (2012). *Ensemble Machine Learning: Methods and Applications* (1. Aufl.). s.l.: Springer-Verlag.

Zhou, Z., Kang, J., Zou, Z., & Wang, H. (2017). Analysis of traffic noise distribution and influence factors in Chinese urban residential blocks. *Environment and Planning B: Urban Analytics and City Science, 44(3),* 570–587. https://doi.org/10.1177/0265813516647733

Ziemann, A. (2002). Zum Einfluss vertikaler Gradienten meteorologischer Größen auf die Laufzeit von akustischen Signalen zwischen Schallquellen und Schallempfängern in der bodennahen Atmosphäre. *Wissenschaftliche Mitteilungen aus dem Institut für Meteorologie der Universität Leipzig, 44.* Universität Leipzig, Leipzig.

Eidesstattliche Versicherung | Declaration on Oath

Hiermit erkläre ich an Eides statt, dass ich die vorliegende Dissertationsschrift selbst verfasst und keine anderen als die angegebenen Quellen und Hilfsmittel benutzt habe.

|

I hereby declare upon oath that I have written the present dissertation independently and have not used further resources and aids than those stated.

03.06.2022, Klagenfurt

Ort, den | City, date

Unterschrift | Signature